

AD-A134320



REPORT NO. NADC-81118-60

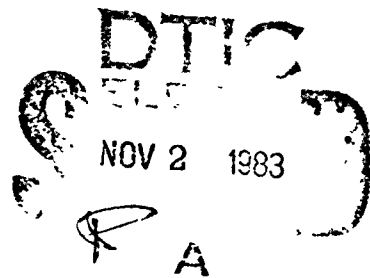


# HELICOPTER FLYING QUALITIES CHARACTERISTICS-CH-46E VOLUME 1

BOEING VERTOL CO.  
Boeing Center, P.O. Box 16858  
Philadelphia, PA 19142

3 OCTOBER 1983

FINAL REPORT  
Program Element No. 62241N  
Work Unit No. 41400



*Approved for Public Release; Distribution Unlimited*

DTIC FILE COPY

Prepared For  
Aircraft & Crew Systems Technology Directorate (Code 6053)  
NAVAL AIR DEVELOPMENT CENTER  
Warminster, PA 18974

83 10 01 003

UNCLASSIFIED

SECURITY CLASSIFICATION OF THIS PAGE (When Data Entered)

REPORT DOCUMENTATION PAGE		READ INSTRUCTIONS BEFORE COMPLETING FORM
1. REPORT NUMBER NADC-81118-60	2. GOVT ACCESSION NO. <b>A134320</b>	3. RECIPIENT'S CATALOG NUMBER
4. TITLE (and Subtitle) Helicopter Flying Qualities Characteristics - CH-46E Volume 1	5. TYPE OF REPORT & PERIOD COVERED Final Report	
	6. PERFORMING ORG. REPORT NUMBER	
7. AUTHOR(s)	8. CONTRACT OR GRANT NUMBER(s)	
9. PERFORMING ORGANIZATION NAME AND ADDRESS Boeing Vertol Co., Div. of the Boeing Co. Boeing Center, P. O. Box 16858 Philadelphia, PA 19142	10. PROGRAM ELEMENT, PROJECT, TASK AREA & WORK UNIT NUMBERS PE 62241N WF 41400	
11. CONTROLLING OFFICE NAME AND ADDRESS Naval Air Development Center Aircraft & Crew Systems Technology Dir. Warminster, PA 18974 (6053)	12. REPORT DATE 3 October 1983	
	13. NUMBER OF PAGES 156	
14. MONITORING AGENCY NAME & ADDRESS (if different from Controlling Office)	15. SECURITY CLASS. (of this report) UNCLASSIFIED	
	15a. DECLASSIFICATION/DOWNGRADING SCHEDULE	
16. DISTRIBUTION STATEMENT (of this Report)  Approved for Public Release; Distribution Unlimited.		
17. DISTRIBUTION STATEMENT (of the abstract entered in Block 20, if different from Report)		
18. SUPPLEMENTARY NOTES		
19. KEY WORDS (Continue on reverse side if necessary and identify by block number)  CH-46E; Helicopter; Flying Qualities		
20. ABSTRACT (Continue on reverse side if necessary and identify by block number)  This document defines the flying qualities characteristics of the CH-46E helicopter. The data are representative of both the metal-bladed and composite-bladed versions. Analytically computed static trim data are presented for a wide range of configurations (gross weight, c.g.) and flight conditions (airspeed, altitude, sideslip, climb, autorotation). Correlation of trim data with available flight test data is provided for validation. (see next page) ←		



## CONTENTS

1.0	INTRODUCTION	1
2.0	DESCRIPTION OF HELICOPTER	2
2.1	GENERAL	2
2.2	BASIC DATA	2
2.2.1	Gross Weight/C.G. Envelope	
2.2.2	Moments of Inertia	
2.2.3	Rotor Parameters	
2.3	OPERATING LIMITATIONS	3
2.3.1	Operational Envelope	
2.3.2	Other Operating Limitations	
3.0	DESCRIPTION OF CONTROL SYSTEM	9
3.1	MECHANICAL CONTROL SYSTEM	9
3.1.1	General	
3.1.2	Control Force Characteristics	
3.1.3	Trim and Stabilization Actuators	
3.2	AUTOMATIC FLIGHT CONTROL SYSTEM	12
3.2.1	General	
3.2.2	Trim Systems	
3.2.3	Stability Augmentation System	
3.2.4	Automatic Trim System	
4.0	TRIM CHARACTERISTICS	33
4.1	TRIM ANALYSIS DATA	33
4.2	CORRELATION WITH FLIGHT TEST	34
5.0	STATIC STABILITY CHARACTERISTICS	53
5.1	LONGITUDINAL STATIC STABILITY	53
5.2	LATERAL-DIRECTIONAL STATIC STABILITY	54
6.0	CONTROL SENSITIVITY	61

CONTENTS  
(continued)

	Page
7.0 TIME HISTORY DATA	65
7.1 GENERAL	65
7.2 DYNAMIC STABILITY	65
7.3 CONTROL RESPONSE	66
7.4 SAS FAILURES	66
7.5 ENGINE FAILURES	67
8.0 TRIM AND STABILITY DATA	101
8.1 GENERAL TRIM AND STABILITY DATA	101
8.2 THREE DEGREE APPROACH PATH DATA	101
9.0 TRIM AND STABILITY ANALYSIS PROGRAM (A-97)	124
9.1 DESCRIPTION OF PROGRAM	124
9.2 INPUT SHEET	125
9.3 FUSELAGE DATA TABLE	125
9.4 AIRFOIL DATA TABLE	126
9.4.1 Format of Airfoil Tables	126
9.4.2 Lift Coefficient	127
9.4.3 Drag Coefficient	129
9.5 OUTPUT DATA	130
10.0 REFERENCES	154

## 1.0 INTRODUCTION

This report presents the stability and control characteristics of the CH-46E helicopter. The data are representative of both the metal-bladed configuration and the composite-bladed configuration. Those minor variations in handling qualities which occur when composite blades are substituted for metal blades are discussed in Reference 1, in which it is concluded that the variations are not significant.

The trim, static stability and control margin data presented herein, as well as the stability and control derivatives, are analytically predicted characteristics obtained from the Boeing Vertol Tandem Rotor Trim and Stability Analysis Program (A-97). Correlation of trim analysis results with available flight test data is presented to validate the analytical predictions.

Time history data relating to dynamic stability, control responses, and SAS and engine failures, are extracted from test records obtained during the CH-46E SLEP II flight test program, conducted at the Boeing Vertol flight test facility at Wilmington, Del., from 20 June to 31 October 1977.

## 2.0 DESCRIPTION OF HELICOPTER

### 2.1 GENERAL

The CH-46E Sea Knight is a tandem-rotor transport helicopter of 20,800 lbs normal gross weight, powered by two T58-GE-16 turboshaft engines. A three-view drawing of the helicopter is presented in Figure 2-1.

The primary mission of the CH-46E is to rapidly deploy up to 25 combat troops and/or supplies from assault landing craft or from established airfields to forward staging areas having limited maintenance and logistic support, under VFR or IFR weather conditions. Alternative uses include medical evacuation, general cargo transportation, and external cargo missions.

### 2.2 BASIC DATA

All configuration data which have a significant impact on the handling characteristics of the CH-46E are set forth in this section, together with the relevant operating limitations of the helicopter.

#### 2.2.1 Gross Weight/C.G. Envelope

The CH-46E center-of-gravity envelope is described in Figure 2-2. This envelope is valid for the helicopter with metal blades and with composite blades.

#### 2.2.2 Moments of Inertia

Estimated moment of inertia data are presented in Table 2-1 for the gross weight and center-of-gravity conditions analyzed in this report.

### 2.2.3 Rotor Parameters

Those rotor parameters which have a significant impact on the handling qualities of the CH-46E are set forth in Table 2-2. Data are presented for the composite blades, with metal blade properties in parenthesis, if different.

## 2.3 OPERATING LIMITATIONS

### 2.3.1 Operational Envelope

The level flight operational envelope for the CH-46E is defined in Figure 2-3. Data were obtained from Reference 2. Below 145 kt IAS, it is permissible to exceed the envelope, provided that:

- CGI limitations are strictly observed
- CGI is operating correctly
- Cyclic trim actuators are operating correctly

### 2.3.2 Other Operating Limitations

From Reference 2, the following operating limitations are also imposed on the helicopter:

Rotor Speed: 94% (248 RPM) minimum steady  
113% (298 RPM) maximum steady  
88% (232 RPM) minimum transient  
125% (330 RPM) maximum transient

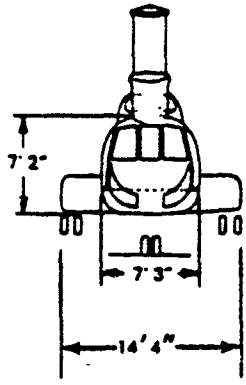
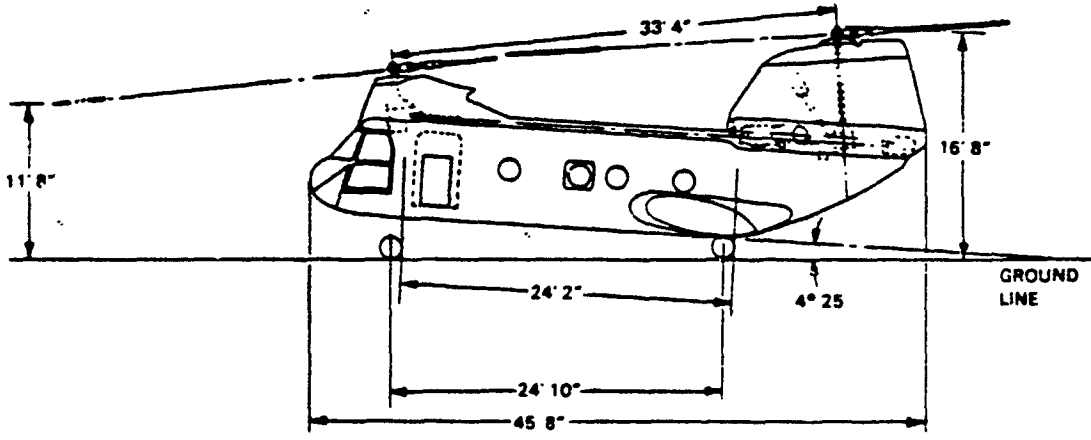
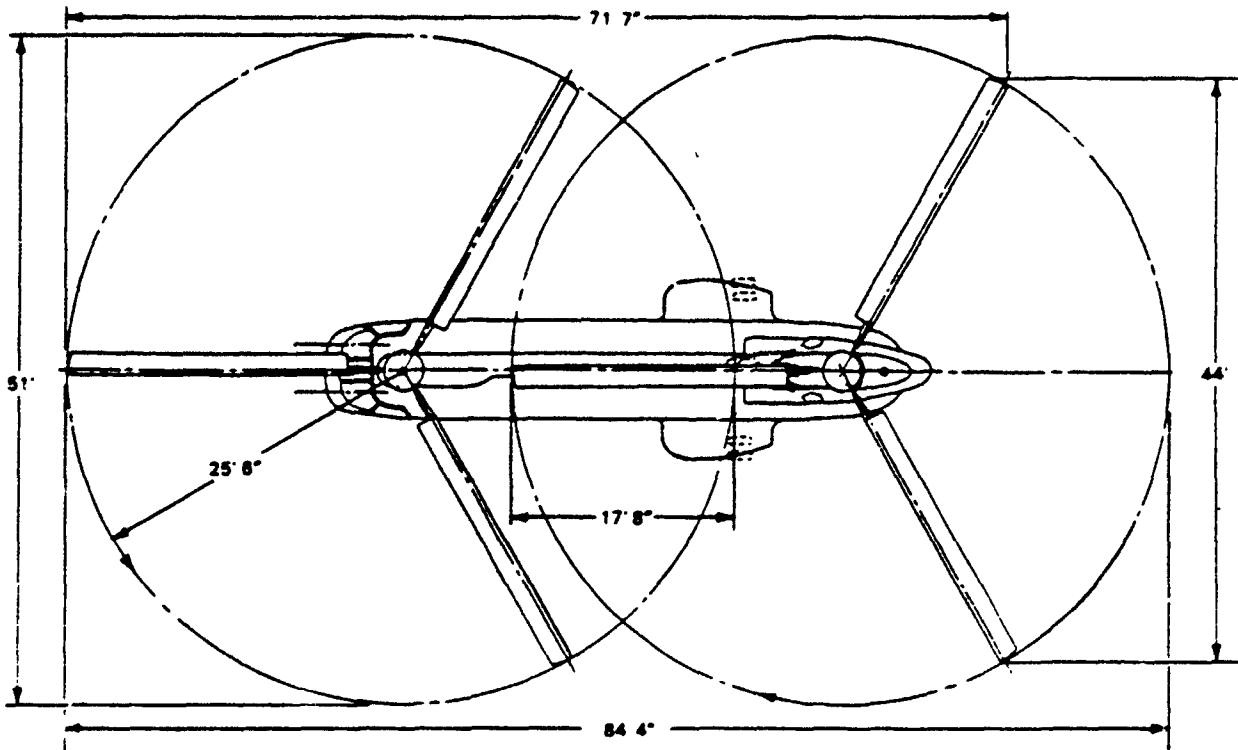
Sideward Flight: 35 knots airspeed

Rearward Flight: 30 knots airspeed

Single SAS Limit Speed: 110 knots IAS

Maneuver Loads: 2.50g max, -0.5g min (20800 lb)  
2.14g max, -0.5g min (24300 lb)

Transmission Limit: 2800 hp maximum continuous



FWD HUB LOC'N:	STA (96.1)	WL (95.0)
AFT HUB LOC'N:	STA (492.4)	WL (150.1)
CG REF LOC'N:	STA (308.0)	WL (0.0)
FWD SHAFT ANGLE:	9.5° FWD	
AFT SHAFT ANGLE:	7.0° FWD	

FIGURE 2-1 HELICOPTER GEOMETRY

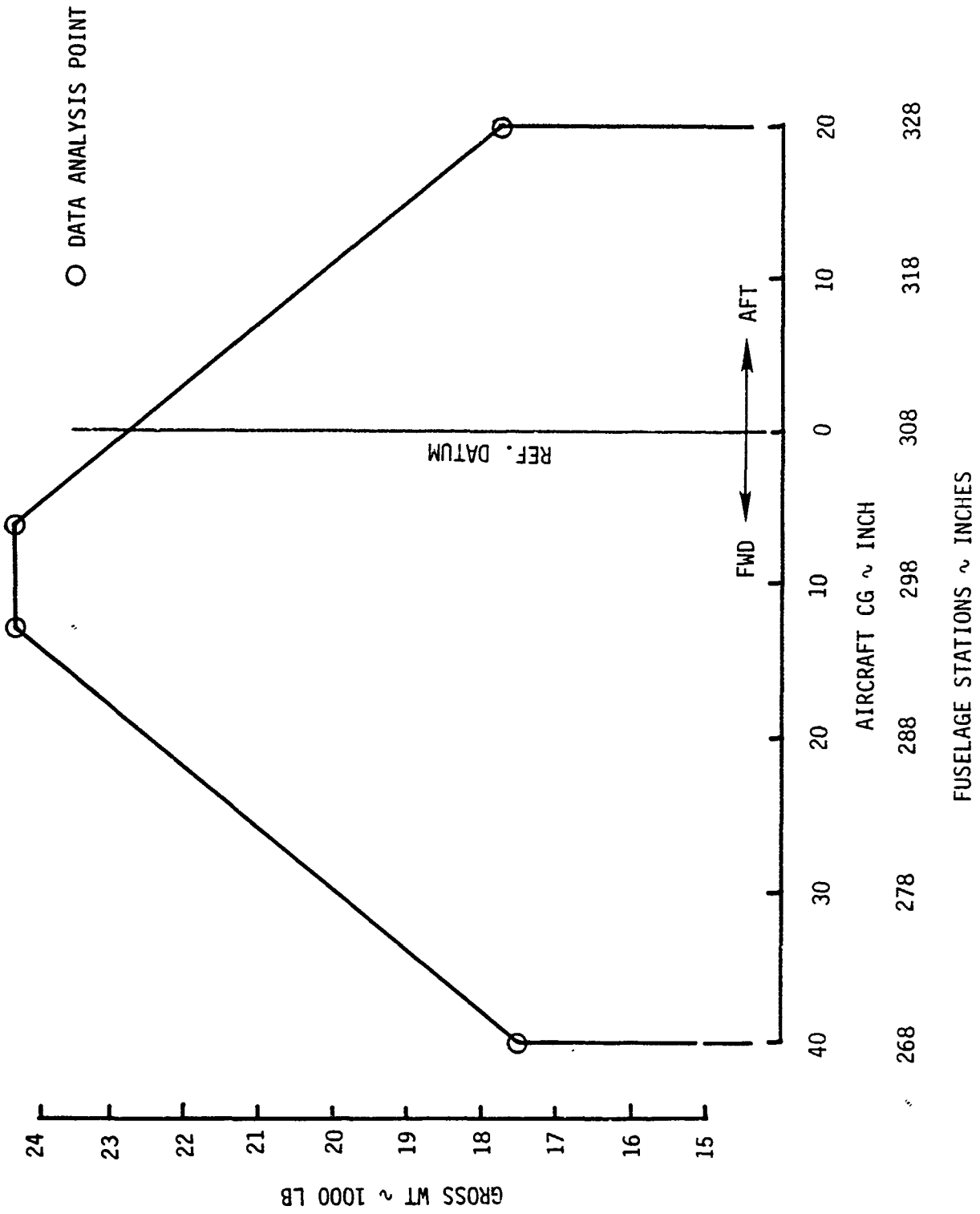


FIGURE 2-2 CENTER OF GRAVITY ENVELOPE

TABLE 2-1  
CH-46E CENTERS OF GRAVITY AND MOMENTS OF INERTIA  
(COMPOSITE ROTOR BLADES)

GROSS WT (LB)	CENTER OF GRAVITY			MOMENTS OF INERTIA (SL FT <sup>2</sup> )				
	(IN.)	STN	WL	I <sub>XX</sub>	I <sub>YY</sub>	I <sub>ZZ</sub>	J <sub>ZX</sub>	
14055	10 fwd	298	42	10773	94227	88090	8817	
17500	20 aft	328	35	14999	109221	103200	8024	
20800	40 fwd	268	35	14999	113935	107953	11338	
	8 aft	316	28	16211	118663	110805	7231	
	27 fwd	281	28	16211	122417	114559	13860	
24300	6 fwd	302	22	17735	115701	106769	10012	
	13 fwd	295	22	17735	116632	107701	11745	

TABLE 2-2  
CH-46E ROTOR GEOMETRY AND PHYSICAL PROPERTIES  
COMPOSITE ROTOR BLADES

Rotor Radius	in.	306	Flap Hinge	in	5.10
Blade Chord	in.	18.75	Flapping Mass	lb	344
Blades/Rotor	-	3	Flap Mass Moment	lb ft	2395 (2430)
Solidity Ratio	-	0.0585	Flap Moment of Inertia	sl ft <sup>2</sup>	1174 (1190)
Blade Twist (CL to tip)	deg	-8.50	CF at Flap Hinge *	lb	60377 (61218)
Root Cutout	in.	67.6	Lag Hinge	in	14.2
Taper Ratio	-	0	Lagging Mass	lb	291
Airfoil	-	V23010-1.58	Lag Mass Moment	lb ft	2155 (2190)
Tab Chord	%	4	Lag Moment of Inertia	sl ft <sup>2</sup>	1067 (1081)
Tab Angle	deg	-3	CF at Lag Hinge *	lb	59386 (60226)

\*At normal operating rotor speed (264 RPM).

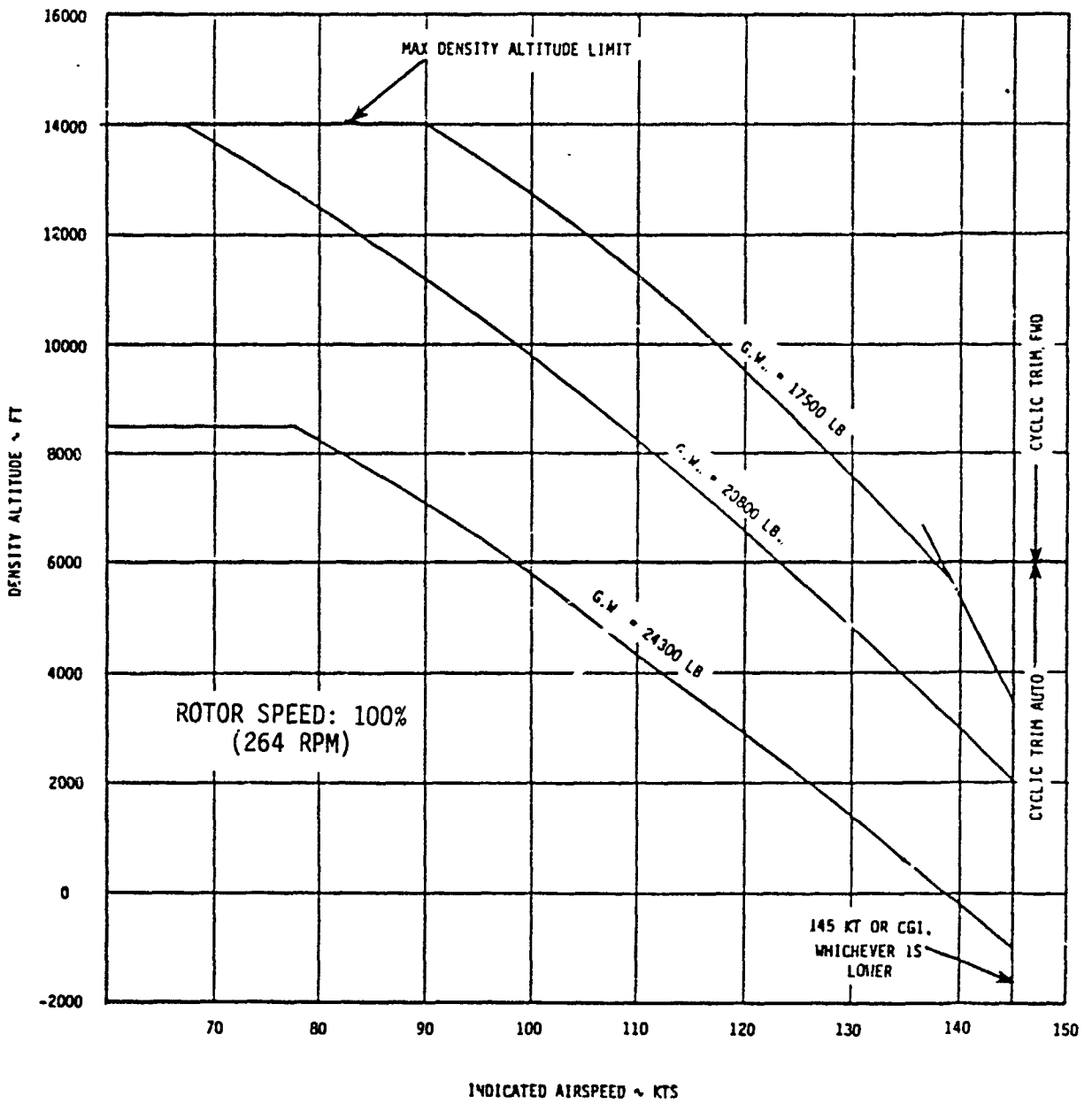


FIGURE 2-3 . AIRSPEED LIMITATIONS

### 3.0 DESCRIPTION OF CONTROL SYSTEM

#### 3.1 MECHANICAL CONTROL SYSTEM

##### 3.1.1 General

The mechanical control system of the CH-46E transmits cockpit control motions through a series of push rods, bellcranks, mix units and cables to the swashplate assembly of each rotor. Swashplate motion acts through the pitch links to generate rotor blade pitch changes proportional to control motion. Forward control stick motion reduces forward rotor collective pitch and increases aft rotor collective pitch, causing a nose down helicopter response. Right control stick motion increases right cyclic pitch on both rotors, resulting in a right roll response. Right pedal motion increases right cyclic pitch on the forward rotor and left cyclic pitch on the aft rotor, causing a nose right helicopter response. Upward motion of the collective lever increases collective pitch equally on both rotors, causing the helicopter to climb. Opposite cockpit control motions cause opposite rotor pitch changes and opposite helicopter responses.

A schematic diagram of the mechanical control system is presented in Figure 3-1. Although originally drawn for the CH-46A, this diagram is applicable to the CH-46E, except for part numbers. The overall kinematic ratio (degrees of blade pitch per inch of control) for each axis of the control system is given in Table 3-1.

##### 3.1.2 Control Force Characteristics

In order to improve the control force characteristics of the helicopter, several functional components are added to the basic mechanical control system.

- Swashplate actuators (two dual hydraulic units per rotor) drive the swashplates in response to cockpit control commands, and completely absorb all aerodynamic and inertial loads fed back from the rotors, during both steady and maneuvering flight.
- Lower boost actuators (one dual hydraulic unit per control system axis) reduce all inherent residual control system forces to zero, so that desired control force characteristics can then be generated for each axis by the centering springs and magnetic brake units.
- Centering springs (one for each control system axis) generate breakout forces and approximately linear force gradients tailored to the requirements of each cockpit control.
- Magnetic brakes (one for each control system axis) allow the control force on each axis to be trimmed to zero at any desired control position.

The control force characteristics for each cockpit control are set forth in Figures 3-2 to 3-9. Although originally prepared for the CH-46A, these characteristics are applicable to the CH-46E as well, except that the control limits shown for the CH-46A are slightly outside the allowable CH-46E limits set forth in Table 3-1.

### 3.1.3 Trim and Stabilization Actuators

In order to implement the trim and stabilization commands of the AFCS (automatic flight control system) discussed in Section 3.2, the following actuators are incorporated in the mechanical control system.

- An electromechanical DCPT (differential collective pitch trim) actuator is incorporated as an extensible link in the longitudinal axis of the control system. This actuator automatically responds to airspeed signals above 30 knots IAS to produce a positive stick position gradient with airspeed. It also responds to manually injected commands from the cockpit trim wheel to adjust longitudinal stick position as desired by the pilot.
  
- Two electromechanical LCT (longitudinal cyclic trim) actuators, one for each rotor, adjust swashplate inclination to control the longitudinal cyclic pitch of the rotors. The actuators automatically respond to airspeed signals above 40 knots IAS to maintain the fuselage pitch attitude within comfortable limits, and to reduce shaft and rotor stresses throughout the speed range.
  
- Three dual hydraulic SAS (stability augmentation system) actuators are incorporated in the control system as extensible links, one in each of the longitudinal, lateral and directional control system axes. These actuators automatically respond to helicopter pitch, roll and yaw rate signals to provide strong rate damping for disturbances in these axes. In addition, at airspeeds above 40 knots IAS, the yaw SAS actuator responds to sideslip signals to provide aerodynamic directional stability, and to roll rate signals to provide turn entry coordination.
  
- Four electromechanical ATS (automatic trim system) actuators are incorporated, one for each control system axis. With ATS on, the actuators drive the cockpit controls thru the centering springs discussed in Section 3.1.2, to provide pitch and roll attitude stability, heading hold, and airspeed and altitude hold. With ATS off, the actuators are locked by their respective magnetic

brakes, and provide control force feel through the centering springs as described in Section 3.1.2.

The authority limits of the SAS and ATS actuators are set forth in Table 3-1.

### 3.2 AUTOMATIC FLIGHT CONTROL SYSTEM

#### 3.2.1 General

The AFCS of the CH-46E consists of two simple speed trim systems, a 3-axis SAS and a 4-axis ATS. Each system consists of one or more sensors which generate signals proportional to helicopter airspeed, attitude, rate, etc., gain and shaping networks which process these signals, and one or more actuators which convert the processed signals into control system inputs.

Figures 3-10 to 3-13 present detailed block diagrams of the complete AFCS, including all gains, shaping, switching, logic, rate and authority limits, etc. The most important features of the system are discussed in the following sections.

#### 3.2.2 Trim Systems

The DCPT system senses airspeed above 30 knots IAS, and processes the resultant signal according to the DCPT schedule shown in Figure 3-14. The processed signal is then input to the DCPT actuator to produce a positive longitudinal stick position gradient with airspeed.

The LCT system senses airspeed above 40 knots IAS, and processes it according to the LCT schedules shown in Figure 3-14. The processed signals are then input to the LCT actuators, one

for each rotor, which adjust longitudinal cyclic pitch to maintain fuselage attitude within comfortable limits and to reduce shaft and rotor stress levels throughout the speed range of the helicopter.

The DCPT and LCT system actuators have low response rates and only moderate authority. A hardover failure in either system presents no handling problems for the pilot, although prolonged high speed flight with an LCT actuator fixed at its low speed position results in high rotor shaft stresses and droop stop pounding due to the large aft flapping angle of the rotor.

### 3.2.3 Stability Augmentation System

The three SAS rate gyros produce signals proportional to the pitch, roll and yaw rate disturbances of the helicopter. After appropriate shaping, these signals are input to the pitch, roll and yaw SAS actuators to produce control inputs which oppose the helicopter motions, thereby providing desirable rate damping characteristics. The yaw SAS sideslip sensors produce a signal approximately proportional to sideslip angle, and process the resultant signal according to the sideslip gain schedule shown in Figure 3-14. This signal is then input to the yaw SAS actuator to produce positive sideslip stability at airspeeds above 30 knots IAS.

The pitch rate signal is shaped by a lag-lead network, so that the pitch SAS provide rate damping and pseudo attitude hold for larger pitch motions of the helicopter, while a washout network prevents pitch SAS actuator bottoming during steady turns at high bank angle. The roll rate signal is processed directly through the roll SAS without shaping. The yaw rate signal is processed through a washout network,

so that short term yaw motions due to turbulence are well damped, but longer term yaw rates associated with intentional steady turns are not opposed by the yaw SAS.

The roll rate signal is also processed into the yaw SAS through a lag network. As the helicopter develops roll rate to enter or exit from a banked turn, this signal overrides the short term damping signal produced by the yaw SAS, thereby producing good control coordination during turn entry and exit at forward speeds. At hover and very low speed, where turns are executed without bank angle, a pedal pickoff signal is processed through a washout network to offset the short term damping of the yaw SAS, so that hover turns can be initiated rapidly without large pedal inputs. This pickoff function is switched off automatically at airspeeds greater than 40 knots.

The SAS actuators have limited authority, but high response rates. A hardover failure in any system can therefore be readily overcome by an offsetting cockpit control input, although the delay time available for doing so may be limited due to the high rate of the failure input and the rapid response of the helicopter.

#### 3.2.4 Automatic Trim System

In contrast to the trim systems and SAS discussed above, which are normally operational throughout the entire flight, the ATS is selected by the pilot for periods of sustained flight at a steady flight condition. The three ATS attitude gyros then produce signals proportional to the pitch, roll and yaw attitude excursions from the trim condition to which they have been referenced. These signals are then processed directly to the pitch, roll and yaw ATS actuators to produce corrective control inputs which return the helicopter to the ori-

ginal trim attitudes and heading. In an analogous manner, the ATS airspeed sensor produces an error signal proportional to airspeed deviation, which is processed to the pitch ATS actuator to return the helicopter to the trim airspeed. Similarly, an altitude hold ATS function, if separately engaged at the pilot's discretion, processes an error signal to the collective ATS actuator to provide altitude hold capability.

The ATS actuators have large authority, but are velocity limited. Since the actuators drive the cockpit controls through the centering springs described in Section 3.1.2, a hardover failure in any ATS axis can be overcome by merely overpowering the centering spring to place the control at the desired position. Since the failure takes place at a slow rate, ample time is available for recovery.

It should be noted that, with ATS engaged, some SAS gain and shaping characteristics are modified so that the two systems will interact harmoniously to provide desirable stability and trim hold characteristics.

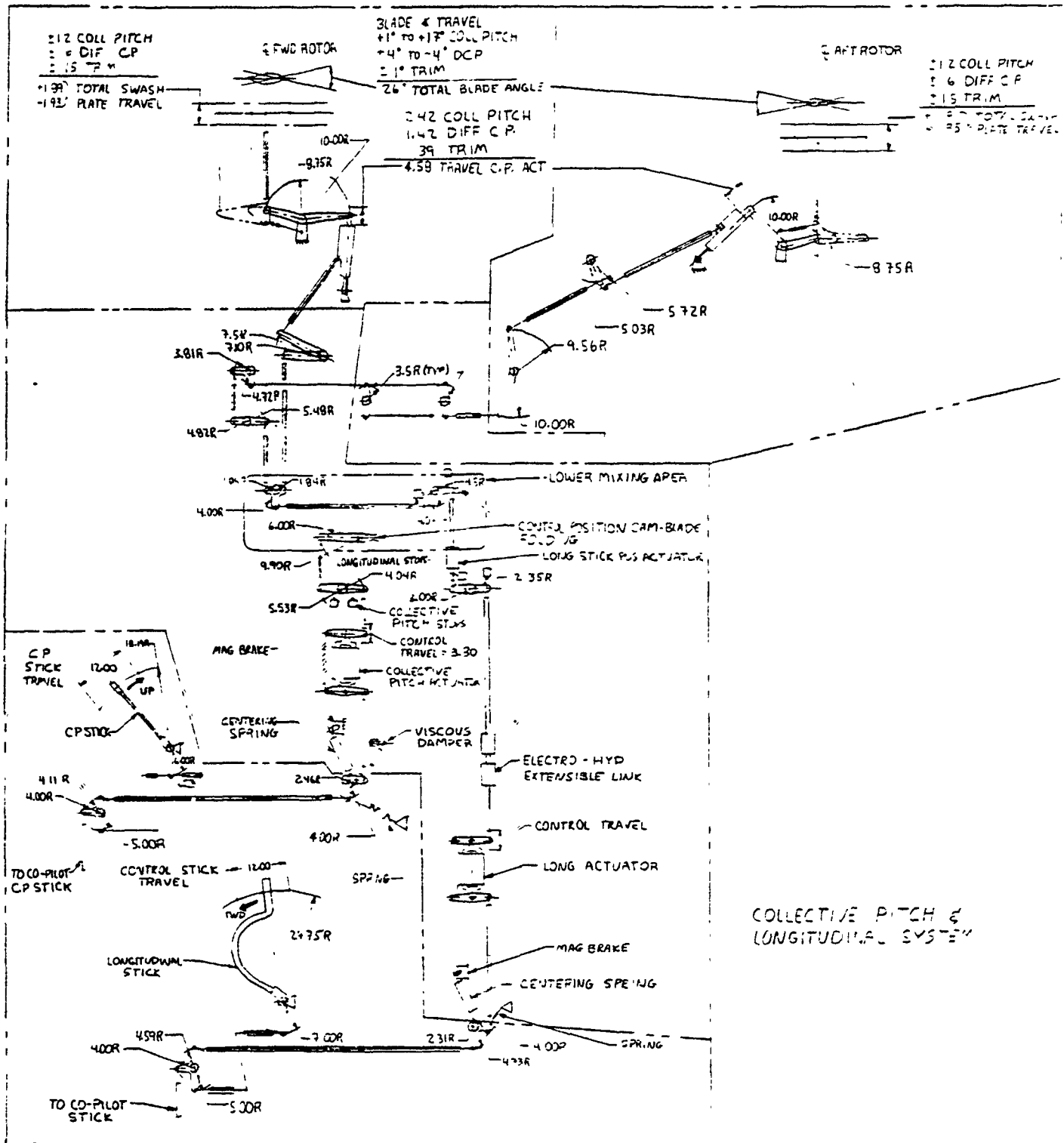


FIGURE 3-1A. CH-46 MECHANICAL CONTROL SYSTEM

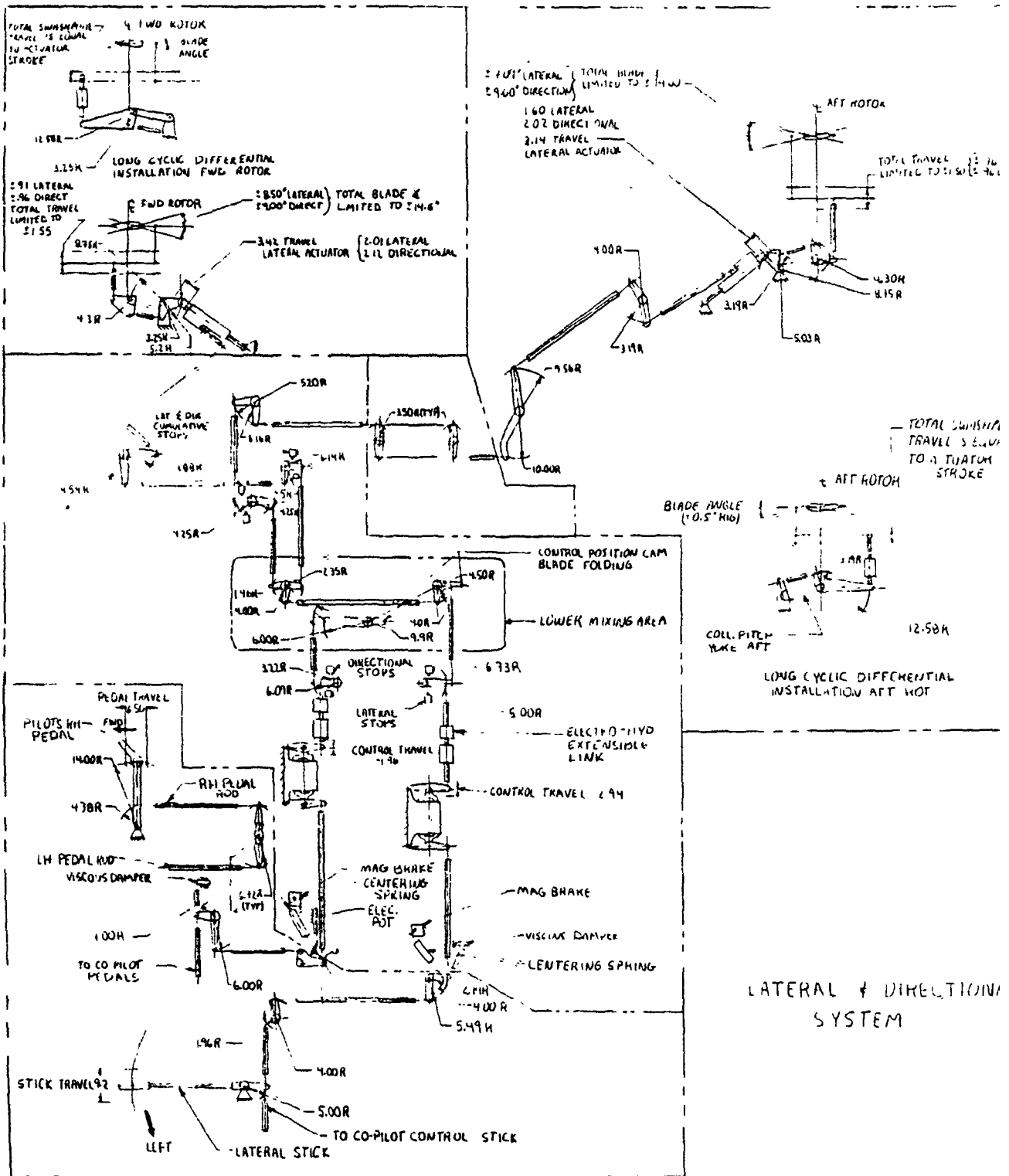


FIGURE 3-1B. CH-46 MECHANICAL CONTROL SYSTEM

CONTROL SOURCE	CONTROL MOTION		SINGLE SAS OR DCPT AUTHORITY				ATS AUTHORITY			ROTOR PITCH RESPONSE	
	RANGE (IN.)	TOL (IN.)	IN. ACT.	EQ. IN. CONT.	% AUTH	DEG. ACT.	EQ. IN. CONT.	% AUTH	FWD ROTOR (DEG)	AFT ROTOR (DEG)	
LONGITUDINAL STICK	6.30 AFT	+ .50	+ .195	+ .90	13	+40	+6.12	87	+4.0	-4.0	
	7.80 FWD	+ .50							-5.0	+5.0	
LATERAL STICK	5.20 LF	+ .50	+ .234	+ .74	14	+40	+3.92	75	-8.5	+7.1**	
	5.20 RT	+ .50							+8.5	-7.1	
DIRECTIONAL PEDAL	3.70 LF	+ .50	+ .340	+1.13	31	+45	+4.14	113	-9.0	-9.0**	
	3.70 RT	+ .50							+9.0	+9.0	
COLLECTIVE LEVER	6.20 DN	+ .50				+45	+6.93	112	+1.0	+1.0	
	6.20 UP	+ .50							+17.0	+17.0	
TRIM WHEEL INTO DCPT ACTUATOR	1.50 AFT		+ .416*	+1.50	21				+1.0	-1.0	
	1.50 FWD								-1.0	+1.0	
AIRSPEED INTO DCPT ACTUATOR	3.00 AFT (150KT)		+ .832*	+3.00	21				+2.0	-2.0	
	0 FWD ( 30KT)								0	0	
AIRSPEED INTO LONG CYCLIC TRIM ACTUATOR	( 65KT)								-2.5	-2.5	
	(120KT)								+2.8	+4.0	
** CUM LAT CYCLIC LIMIT AT ROTOR									+14.5	+14.0	
									-14.5	-14.0	
* CUM DCPT LIMIT AT TRIM ACTUATOR				+3.00					+2.0	-2.0	
				-1.50					-1.0	+1.0	

TABLE 3-1  
CH-46E CONTROL KINEMATICS & AFCS AUTHORITIES

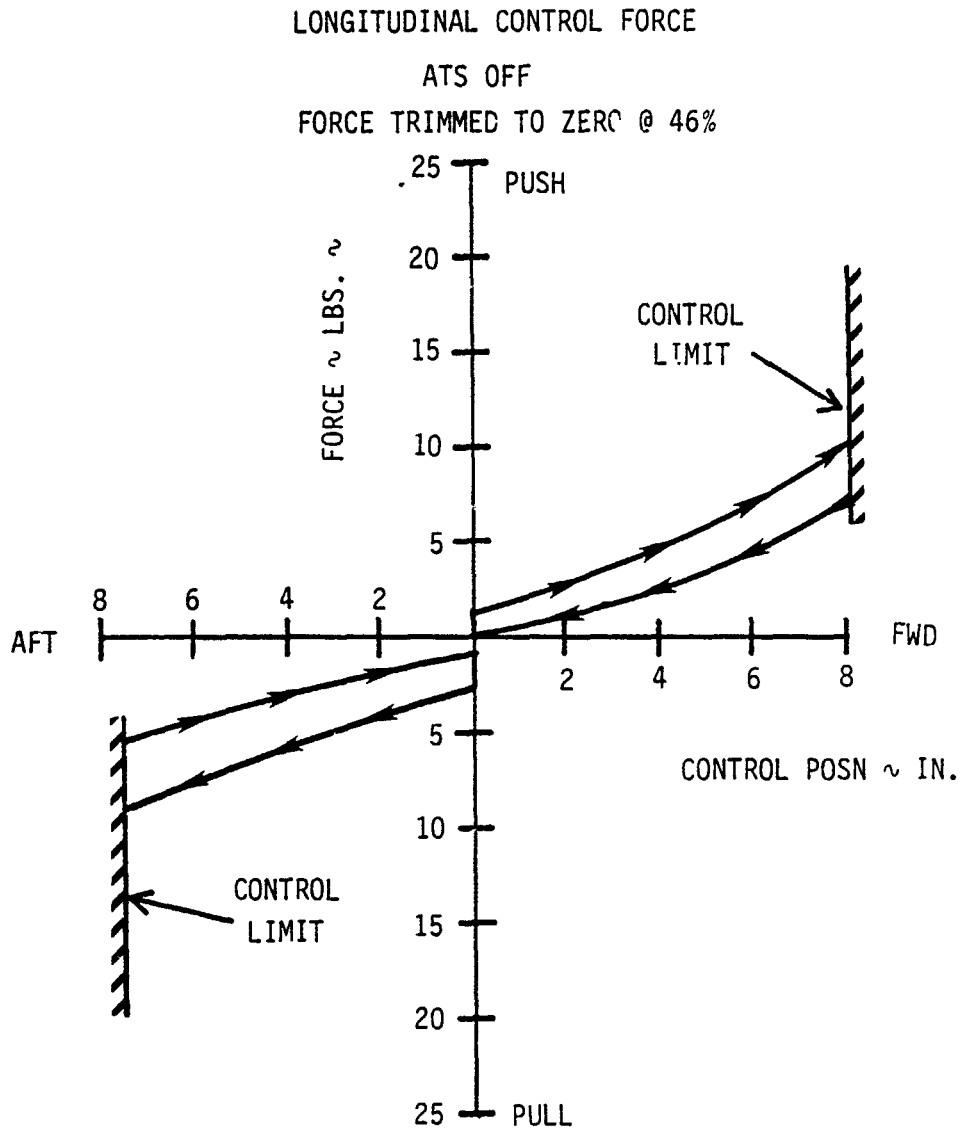


FIGURE 3-2

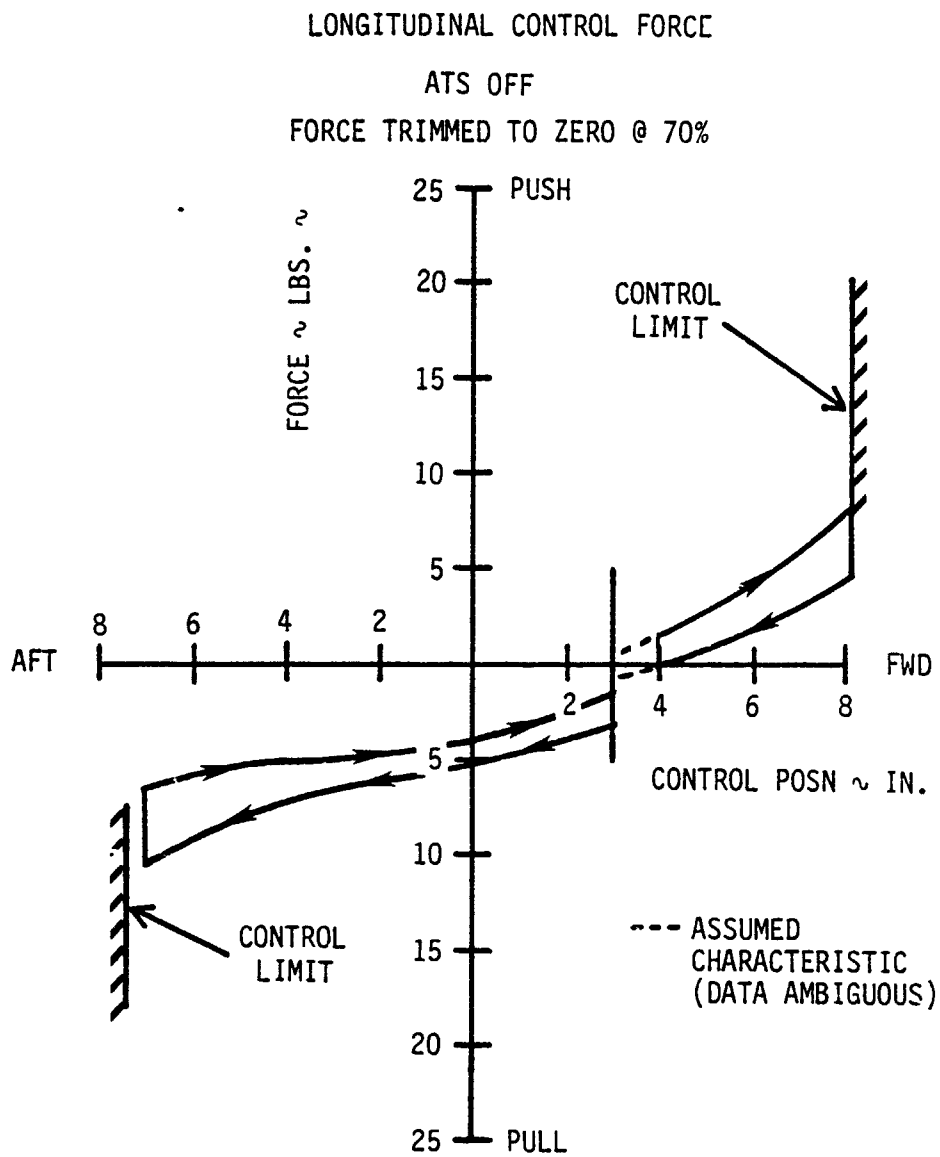


FIGURE 3-3

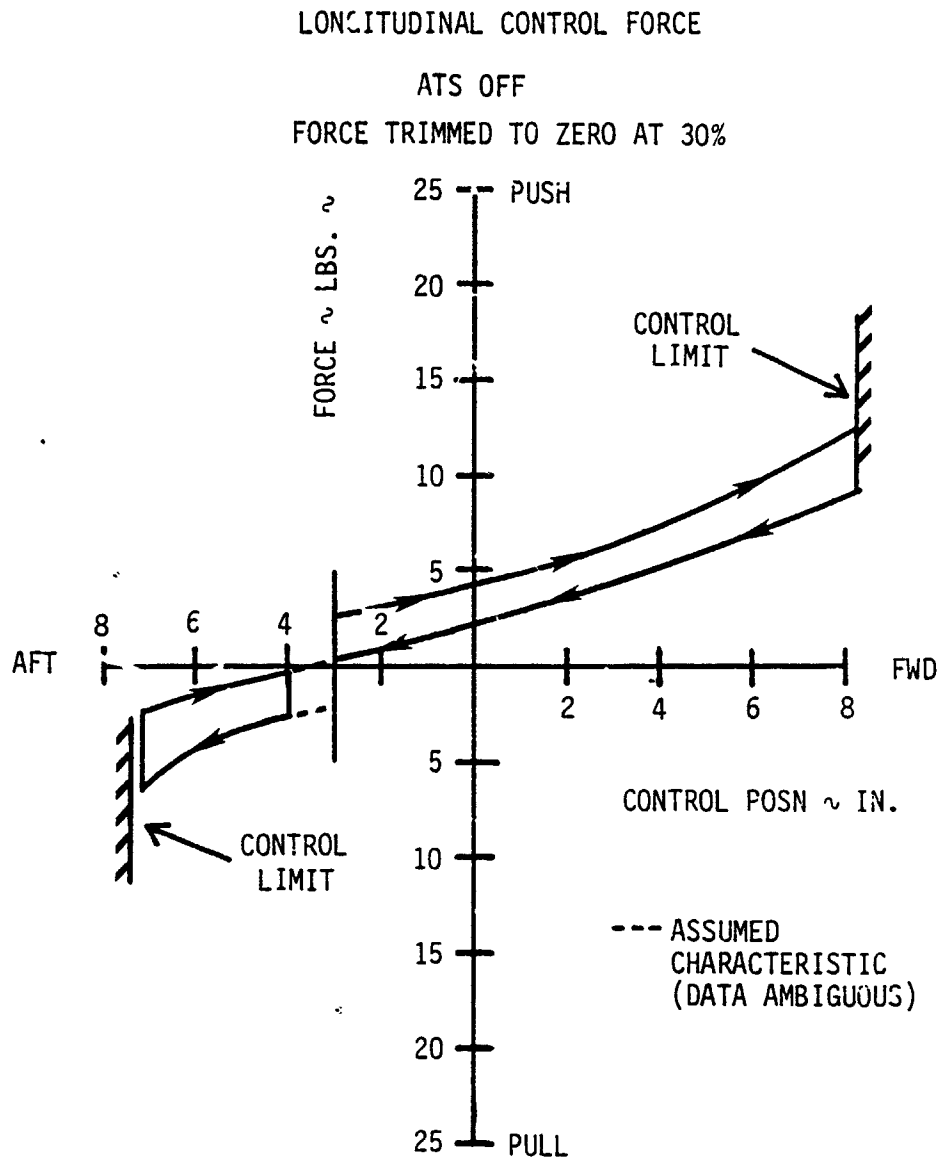


FIGURE 3-4

LONGITUDINAL CONTROL FORCE

ATS ON  
FORCE TRIMMED TO ZERO @ 46%

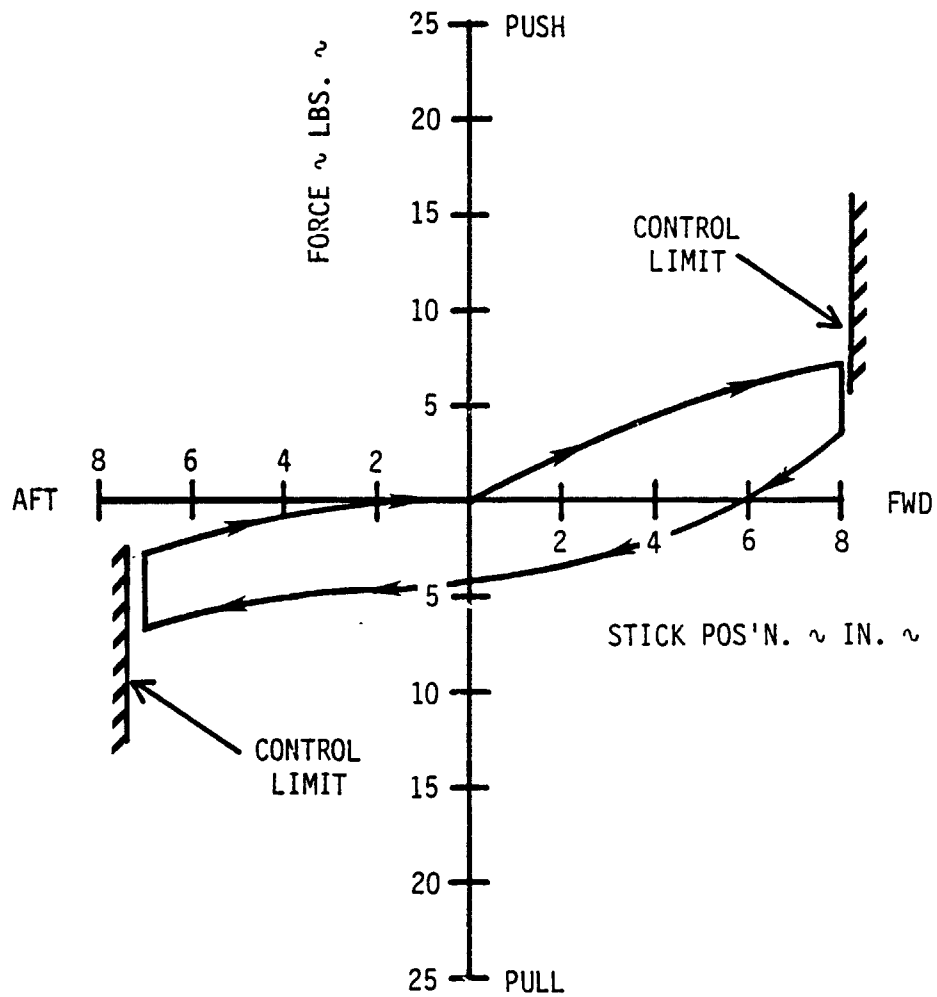


FIGURE 3-5

LONGITUDINAL CONTROL FORCE

ATS ON  
FORCE TRIMMED TO ZERO @ 70%

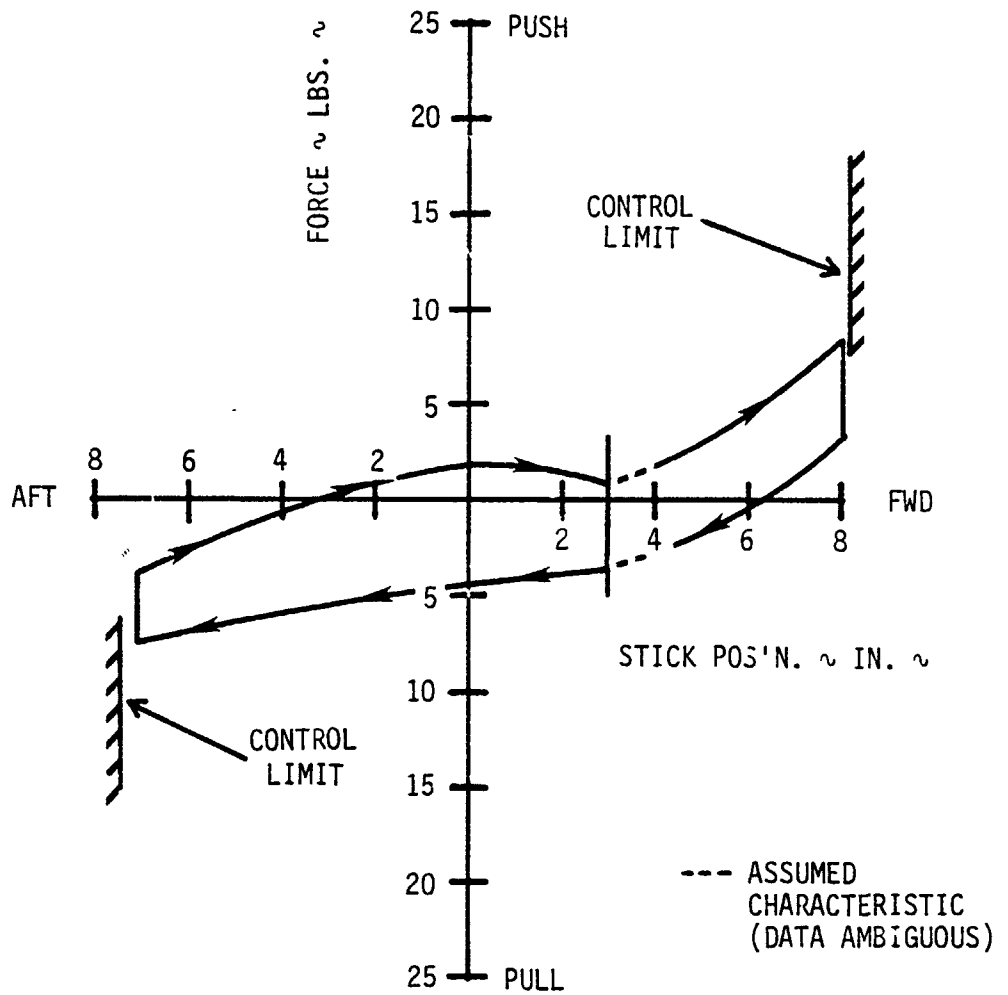


FIGURE 3-6

LONGITUDINAL CONTROL FORCE  
ATS ON  
FORCE TRIMMED TO ZERO @ 30%

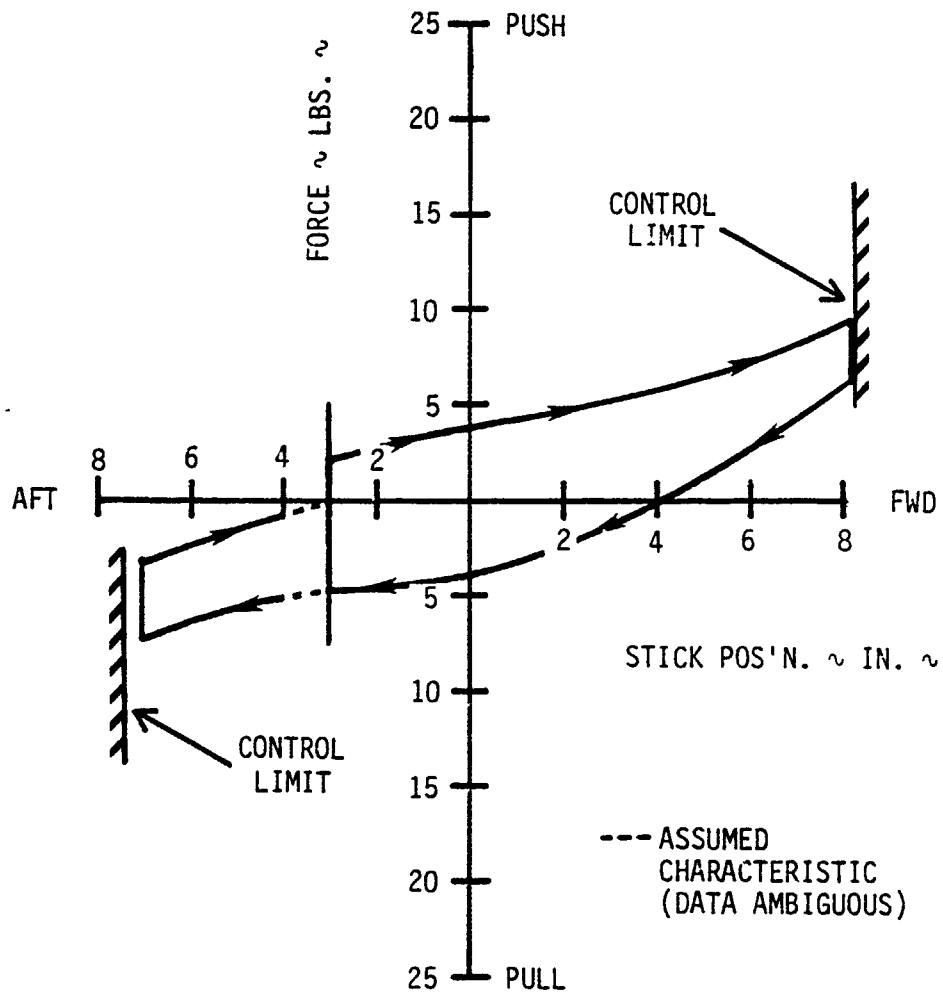
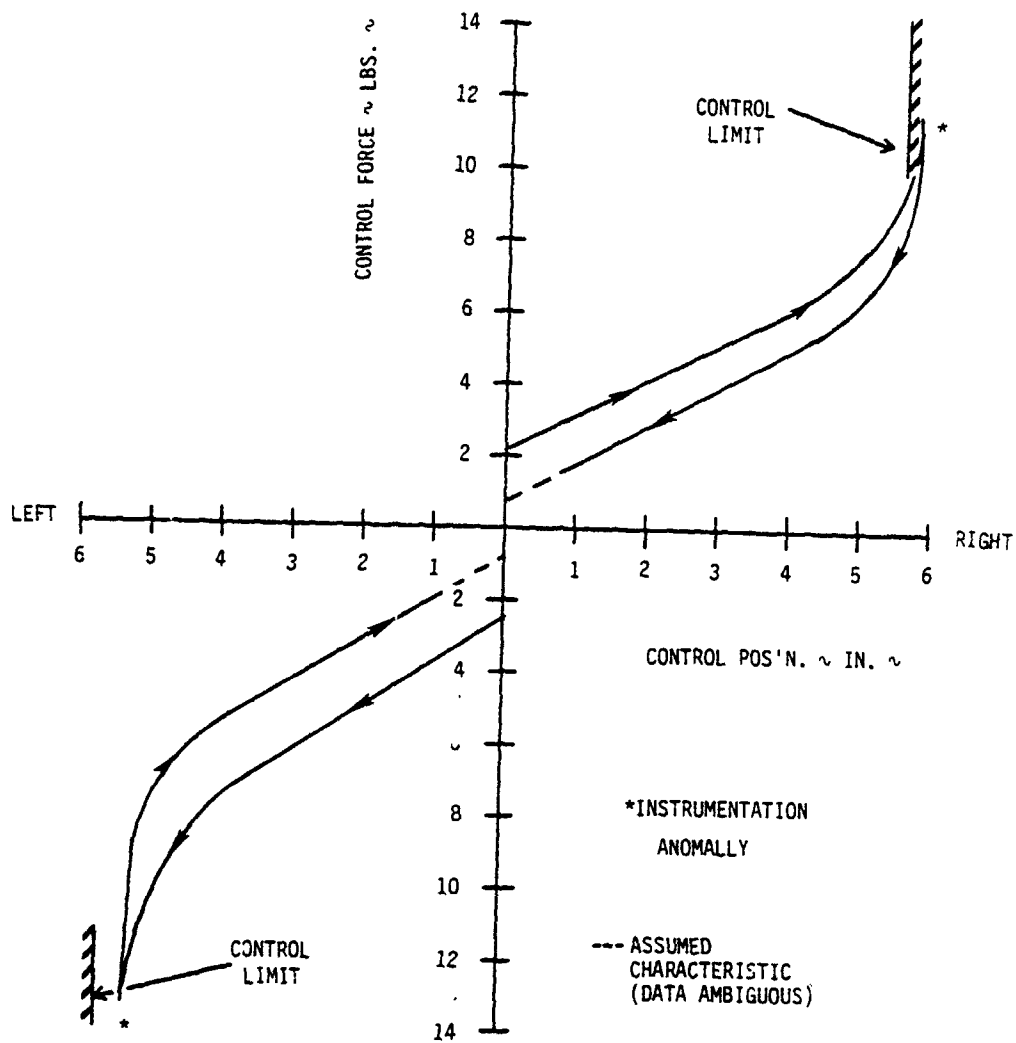


FIGURE 3-7

LATERAL CONTROL FORCE

ATS ON AND OFF



DIRECTIONAL CONTROL FORCE

ATS ON AND OFF

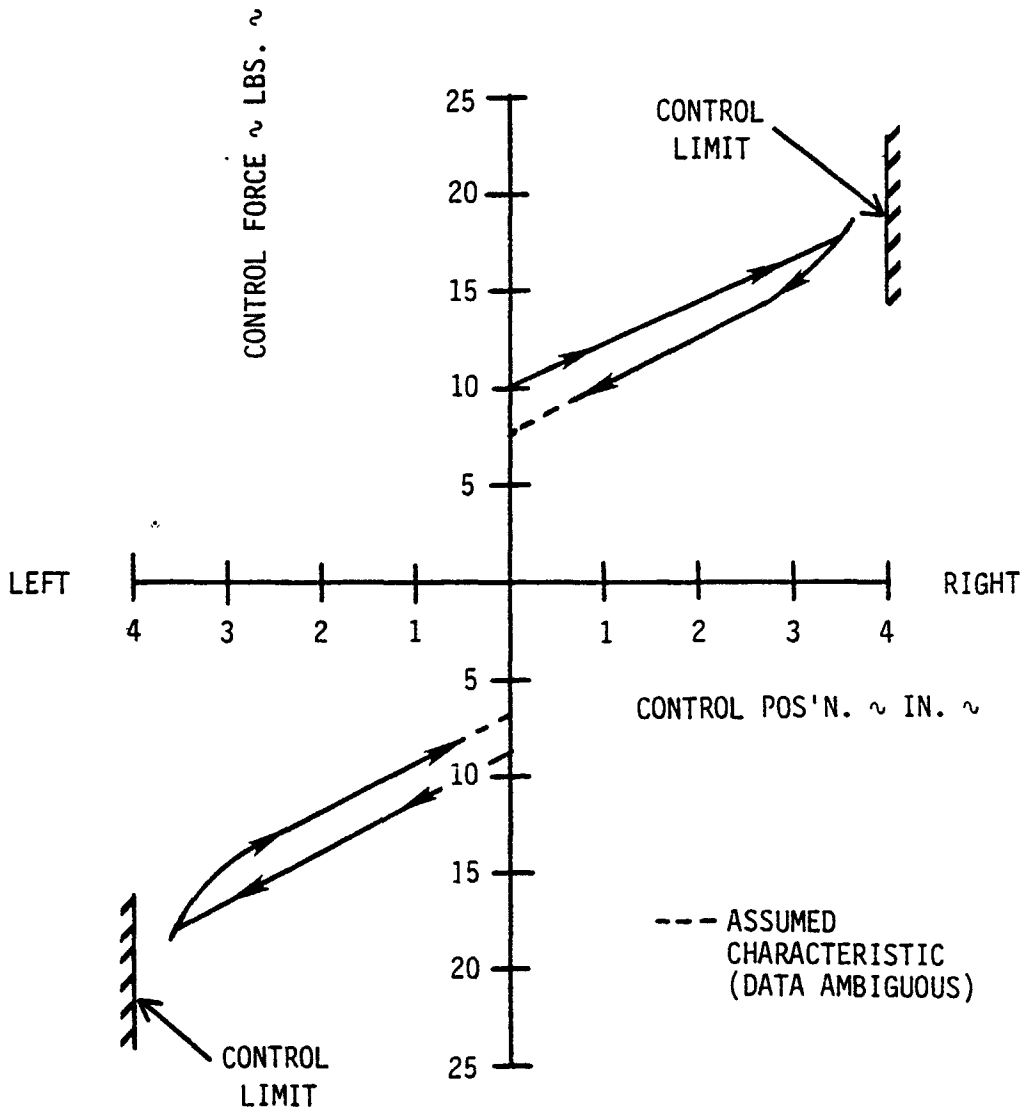


FIGURE 3-9

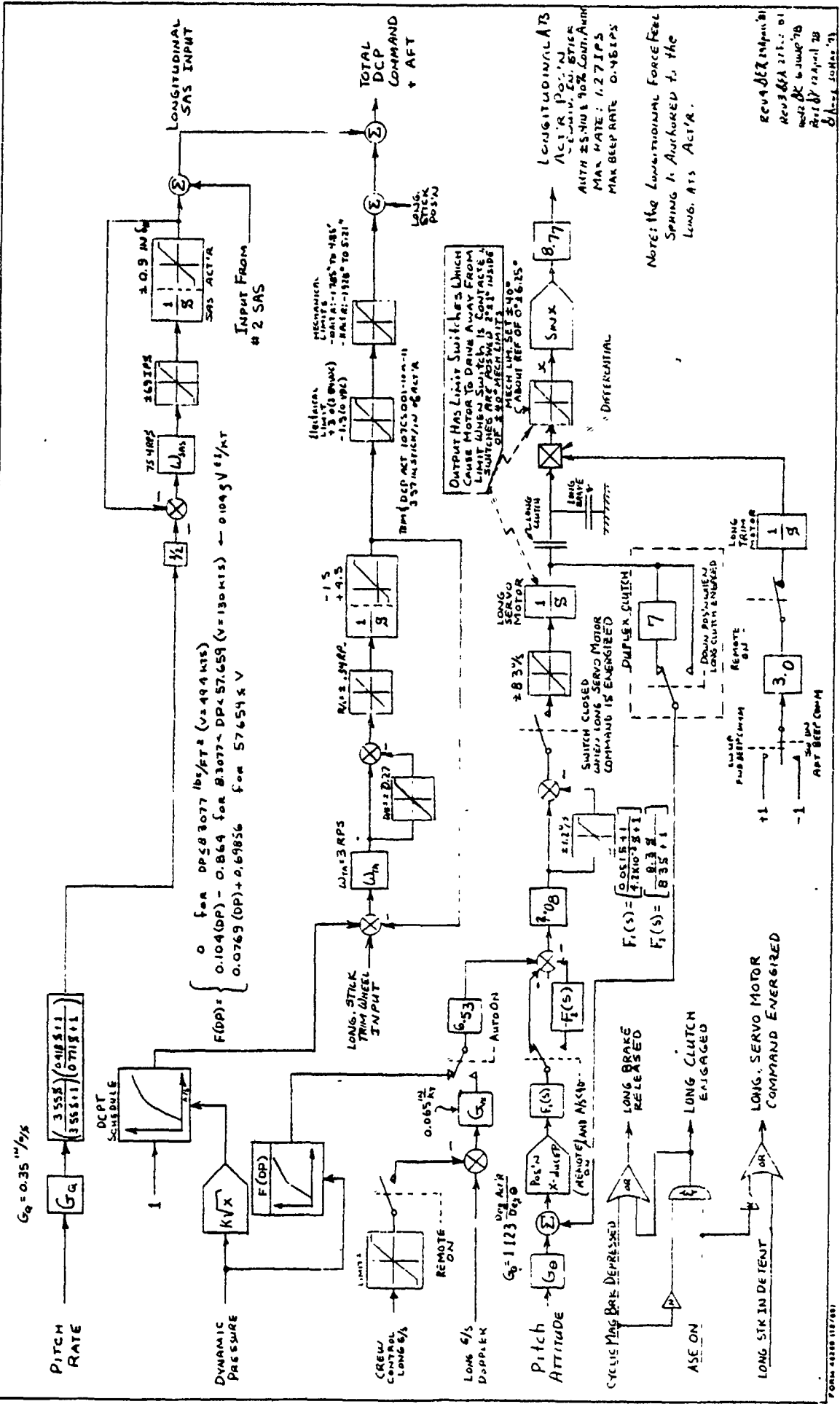
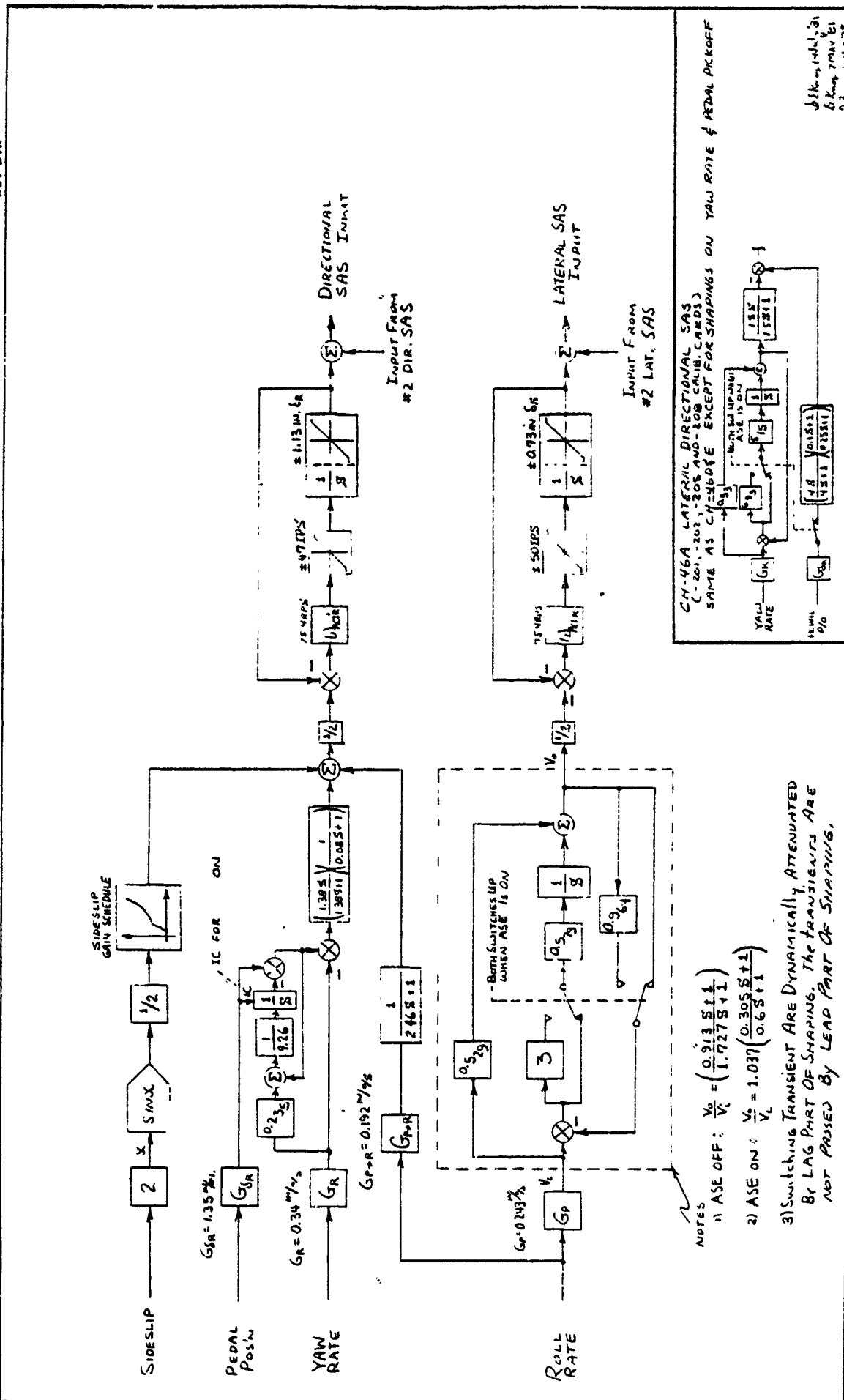


FIGURE 3-10 CH-46E LONGITUDINAL AFCS (SAS + ATS)

PREPARED BY:  
CHECKED BY:  
DATE:

MODEL NO.

NUMBER  
REV LTR



NOTES  
 1) ASE OFF:  $\frac{V_0}{V_c} = \left( \frac{0.913 S + 1}{1.727 S + 1} \right)$   
 2) ASE ON:  $\frac{V_0}{V_c} = 1.037 \left( \frac{0.305 S + 1}{0.6 S + 1} \right)$   
 3) Switching Transients are Dynamically Attenuated by Lag Part of Shaping. The Transients are Not Passed by Lead Part of Shaping.

CH-46A LATERAL DIRECTIONAL SAS (-201, -202, -203 AND -200 CALIB CARDS) SAME AS CH-46E EXCEPT FOR SHAPING ON YAW RATE & PEDAL PICKOFF

15V  
10V  
YAW RATE  
PEDAL PICKOFF

8/16/65 (REV. 2)  
 6/24/65 (REV. 1)  
 J.A.B. 10/15/65

FIGURE 3-11 CH-46E LATERAL-DIRECTIONAL SAS

SHEET





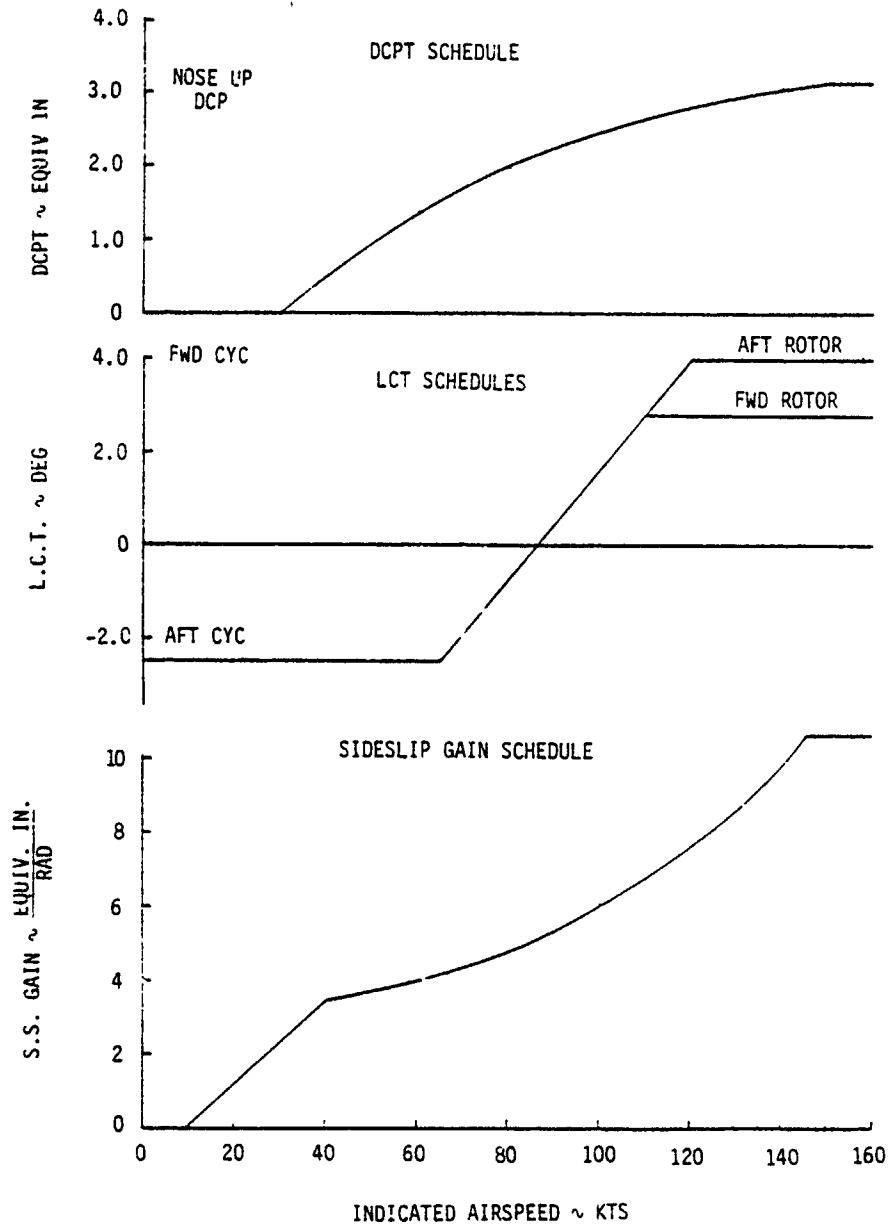


FIGURE 3-14 CH-46E TRIM SCHEDULE AND SIDESLIP GAIN

This Page Left Blank Intentionally

#### 4.0 TRIM CHARACTERISTICS

##### 4.1 TRIM ANALYSIS DATA

The trim data obtained from the Boeing Vertol Tandem Rotor Trim and Stability Analysis Program (A-97) for the CH-46E are presented in Volume 2. Data were obtained at alternate gross weight (24300 lb.) and at an intermediate gross weight (17500 lb.) for the following flight conditions.

- Level flight, from 40 knots rearward to envelope-limited maximum forward speed, at sea level and at service ceiling.
- Maximum power climb and autorotation from 60 knots to 120 knots at sea level, and from 70 knots to envelope-limited maximum speed at service ceiling.
- Constant altitude sideslips at sea level, to  $\pm 45$  deg at 50 knots,  $\pm 30$  deg at intermediate speed, and to power-limited sideslip angle at high speed.
- Sideward flight to 45 knots left and right at sea level.

For each flight condition considered, the four cockpit control positions, plus helicopter pitch and roll attitudes, are plotted vs. airspeed or sideslip angle. A sample of the plotted data for level flight at 17500 lb. gross weight is given in Figures 4-1 to 4-3.

Taking all the trim data as a whole, the following characteristics are noteworthy.

- The longitudinal stick gradient in level flight is strongly stable up to about 50 knots, and then approximately neutral to maximum speed.

- The trim variation between full power climb and autorotation, as indicated by change in stick and pedal position, is very small (less than 10%).
- In sideslips, lateral stick and pedal gradients are strongly stable.
- Large control margins exist for all controls at all flight conditions investigated.
- For flight above 6,000 ft. altitude, some of the trim characteristics show an abrupt change at 50 knots. This is due to the change from hover cyclic to full forward cyclic, as required by Reference 2 for flight above 6,000 feet.

A tabulation of minimum control margins for each control system axis is given in Table 4-1 for all the flight conditions considered.

#### 4.2 CORRELATION WITH FLIGHT TEST

Figures 4-4 to 4-15 display the correlation between predicted trim data obtained from program A-97, and actual flight test data extracted from the CH-46E SLEP II flight test. All flight test control position data has been reduced to the basic aircraft condition (DCPT and SAS off), obtained by adding flight test values of DCPT and SAS extension to the cockpit control positions. This was done to remove the effects of SAS offset at trim, poor DCPT schedule tracking, and any other potential AFCS actuator misbehavior. By adding actual SAS and DCPT contributions to the actual control positions, the "true" value at the rotors is obtained for comparison with unaugmented trim analysis values.

The following comments are offered on those figures in which correlation appears unsatisfactory.

Figure 4-4: Longitudinal stick correlation is good except for the speed sweep points above 88 knots. These flight test data were reduced by adding nominal DCPT values to the flight test stick position, since the actual DCPT values were not available (unserviceable actuator instrumentation for this flight). Since it is known that the basic aircraft has an unstable stick gradient above 60 knots, it is concluded that the DCPT actuator must have overextended in the speed range between 88 knots and 116 knots, at which point it began again to extend at the correct rate vs. airspeed, but displaced by about 8%. Disregarding these dubious flight test points, Figure 4-4 shows good correlation.

Figure 4-5: Pedal position correlation at low speed is not good, perhaps due to the poor prediction of lateral flapping at low speed, which is inherent in the uniform inflow assumption of A-97. Above 80 knots, correlation is good, except for the isolated autorotation point at 126 knots.

Figure 4-7: Longitudinal stick shows the correct trend with airspeed, but displaced 4%. Correlation is good for climb and descent points. At hover, actual stick positions are forward of the predicted value, due probably to the fact that, if any wind exists, hover is performed while headed into the wind, requiring forward stick to hold position.

Figure 4-8: Lateral stick correlation is good at cruise, but more than 5% in error in climb and autorotation.

Figure 4-10: Longitudinal stick correlation in sideslip is in error by up to 8%, but the trend is correct.

Figure 4-11: Lateral stick gradient at 106 knots is not as stable as predicted. Pedal gradients are accurately predicted, but displacement is in error by about 5%.

Figure 4-13: Longitudinal stick gradient appears to be more unstable than predicted, but other well-established data show that the basic aircraft is not that unstable.

Figure 4-14: Poor pedal position correlation at high speed is unexplained, but trend of flight test data versus airspeed conflicts with similar data in Figures 4-5 and 4-8. The flight test data is therefore suspect.

### CH-46E TRIM CHARACTERISTICS LEVEL FLIGHT

DCPT ON	○	GW 17500 LB	CG 20 IN AFT	HD 0 FT
SAS ON	□	17500 LB	40 IN FWD	0 FT
TRIM 0 IN.	△	17500 LB	20 IN AFT	14000 FT

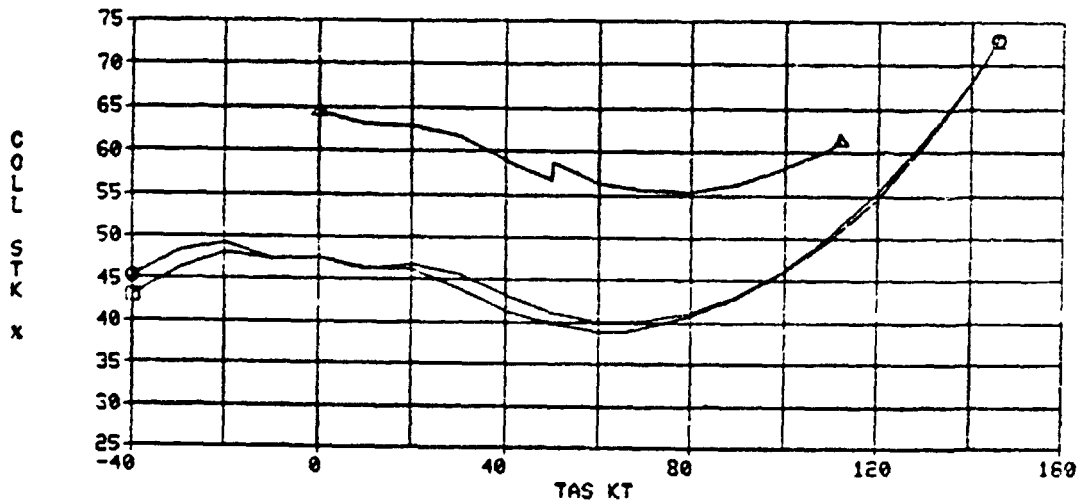
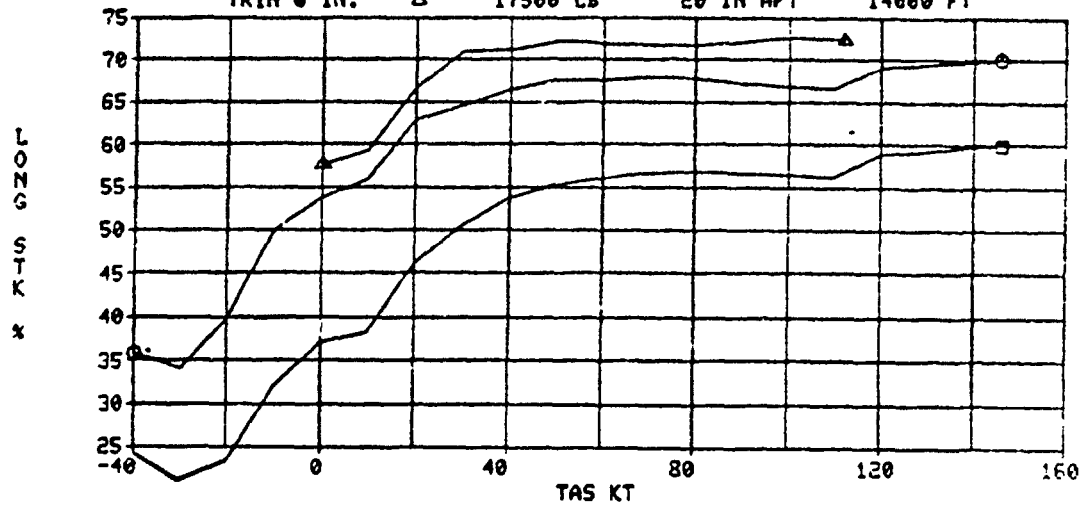


FIGURE 4-1

### CH-46E TRIM CHARACTERISTICS LEVEL FLIGHT

DCPT ON	○	GW 17500 LB	CG 20 IN AFT	HD 0 FT
SAS ON	□	17500 LB	20 IN FWD	0 FT
TRIM 0 IN.	△	17500 LB	20 IN AFT	14000 FT

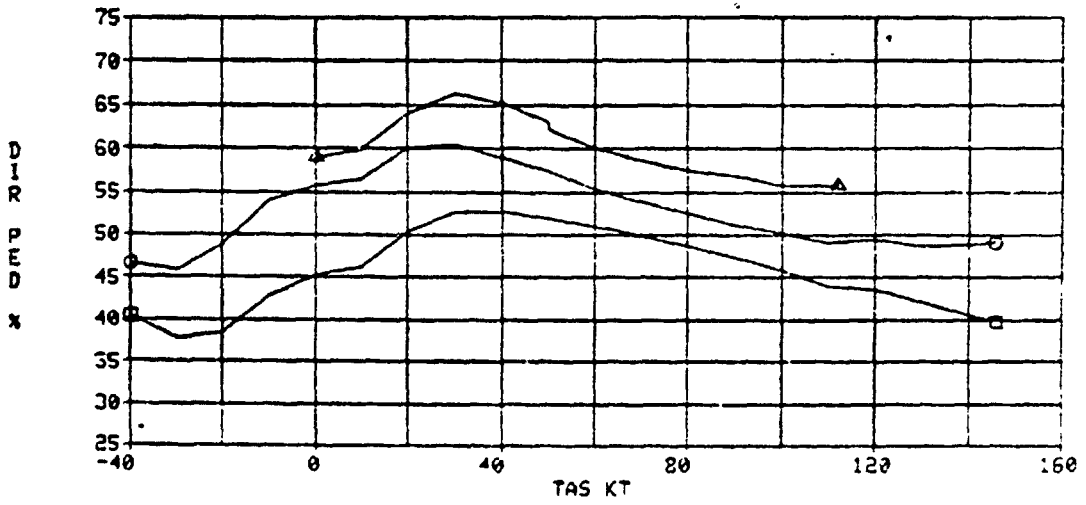
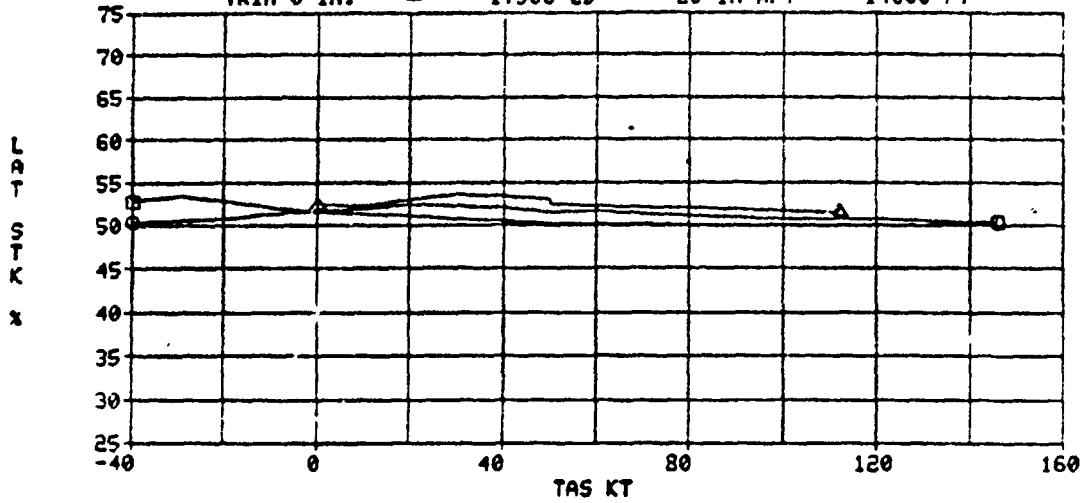


FIGURE 4-2

### CH-46E TRIM CHARACTERISTICS LEVEL FLIGHT

DCPT ON	○	GW 17500 LB	CG 20 IN AFT	HD 0 FT
SAS ON	□	17500 LB	40 IN FWD	0 FT
TRIM 0 IN.	△	17500 LB	20 IN AFT	14000 FT

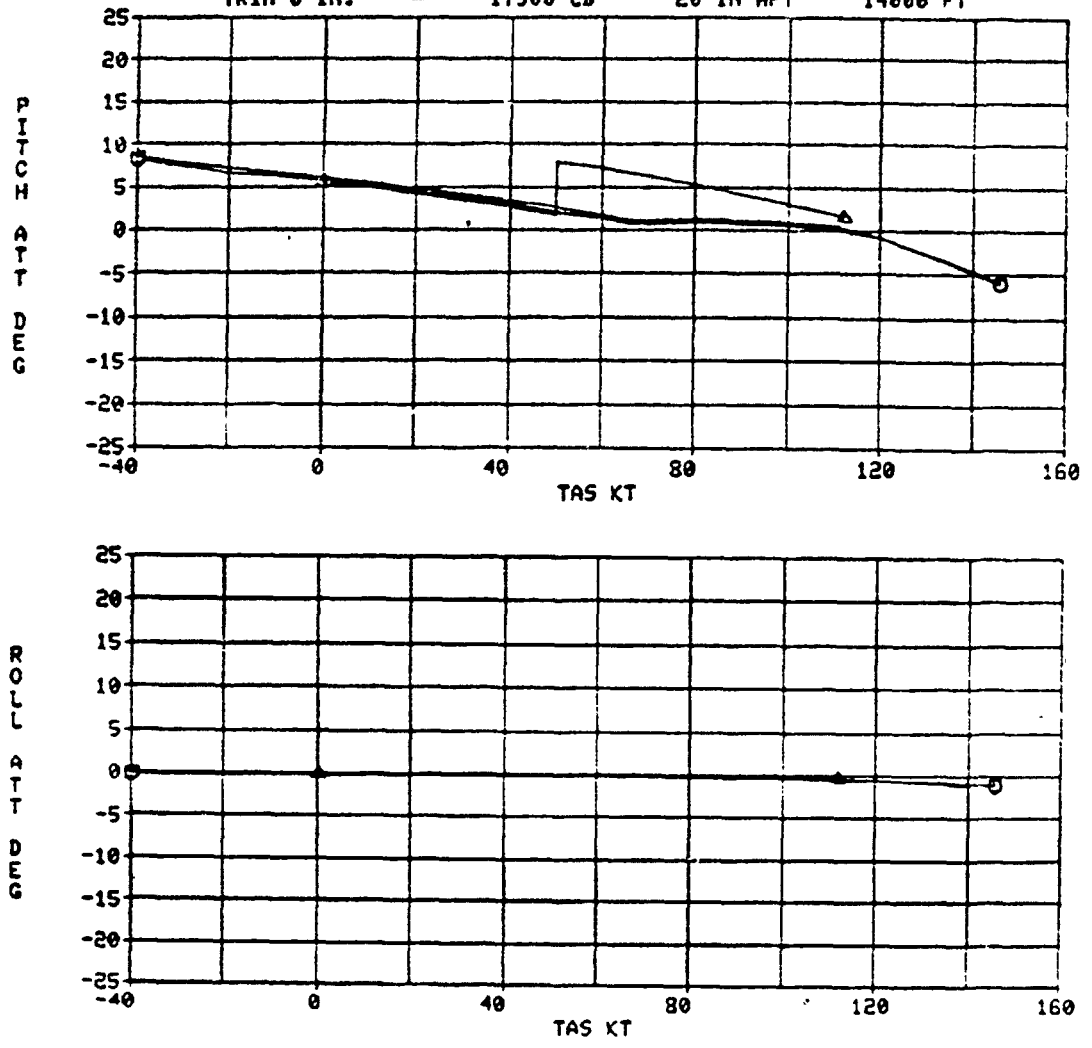


FIGURE 4-3

TABLE 4-1

CRITICAL CONTROL MARGIN SUMMARY

FLIGHT REGIME	CRITICAL FLIGHT CONDITION							CONTROL MARGINS		
	G.W. (lb.)	C.G. (in.)	h <sub>D</sub> (ft.)	T.A.S. (kt.)	R/C (f'/min)	B (deg.)	CRITICAL STOP	(INS.)	(%)	
LEVEL FLIGHT	17500	40 F	0	-30	0	0	LONGITUDINAL AFT	2.9	21	
	17500	20 A	14000	112		0	FWD	3.8	27	
	17500	40 F	0	66	0	0	COLLECTIVE DN	4.7	38	
	17500	20 A	0	146	0	0	UP	3.3	27	
MIL. POWER CLIMB AND AUTOROTATION	17500	20 A	14000	101	1414	0	LONGITUDINAL AFT	4.2	30	
	17500	20 A	0	126	-3987	0	FWD	0	0	
	17500	20 A	14000	101	1414	0	COLLECTIVE DN	0	0	
							UP	3.0	24	
SIDESLIP	17500	20 A	0	140	0	0	LONGITUDINAL AFT	4.2	30	
	24300	6 F	0	90	0	-30	FWD	2.5	24	
	24300	6 F	0	90	0	30	LF	2.4	23	
	24300	6 F	0	90	0	30	RT	1.4	19	
	24300	6 F	0	50	0	-45	LF	1.5	21	
							RT			
SIDEWARD FLIGHT	24300	6 F	0	45 L	0	-90	LATERAL LF	3.8	37	
	24300	6 F	0	45 R	0	90	RT	3.6	35	
	24300	6 F	0	45 R	0	90	DIRECTIONAL LF	3.5	48	
	24300	6 F	0	45 L	0	-90	RT	3.2	44	

### CH-46E TRIM CHARACTERISTICS FLIGHT TEST CORRELATION LEVEL FLIGHT & AUTOROTATION

DCPT OFF  
SAS OFF  
TRIM 0 IN.

GW 24200 LB  
CG 6 IN FWD

HD 3500 FT  
RPM 100 %

LEVEL FLIGHT ○  
AUTOROTATION ▽

F/T A-97

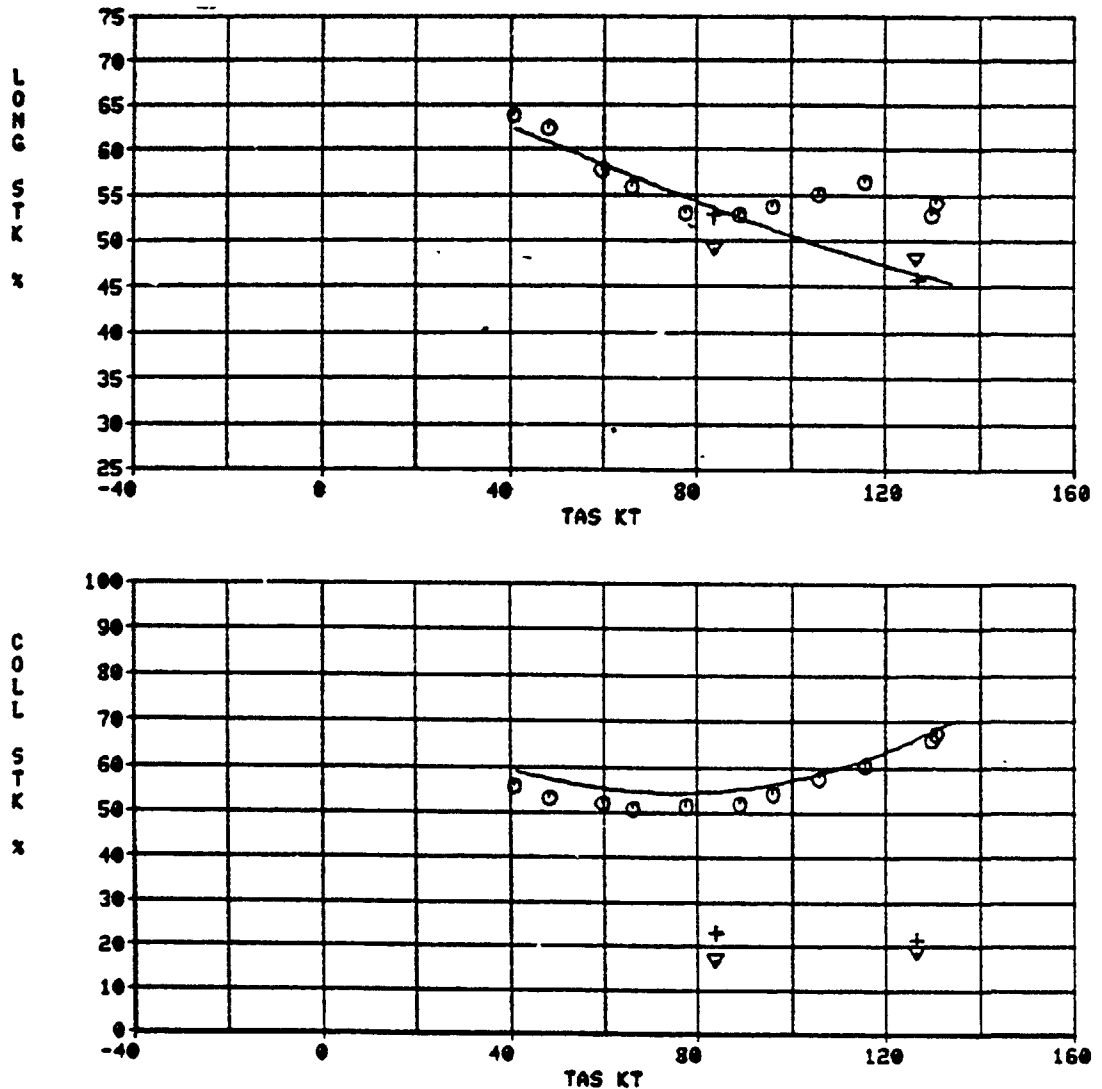


FIGURE 4-4

### CH-46E TRIM CHARACTERISTICS FLIGHT TEST CORRELATION LEVEL FLIGHT & AUTOROTATION

DCPT OFF	GW 24200 LB	HD 3500 FT	F/T A-97
SAS OFF	CG 6 IN FWD	RPM 100 %	LEVEL FLIGHT ○ -
TRIM 0 IN.			AUTOROTATION ▽ +

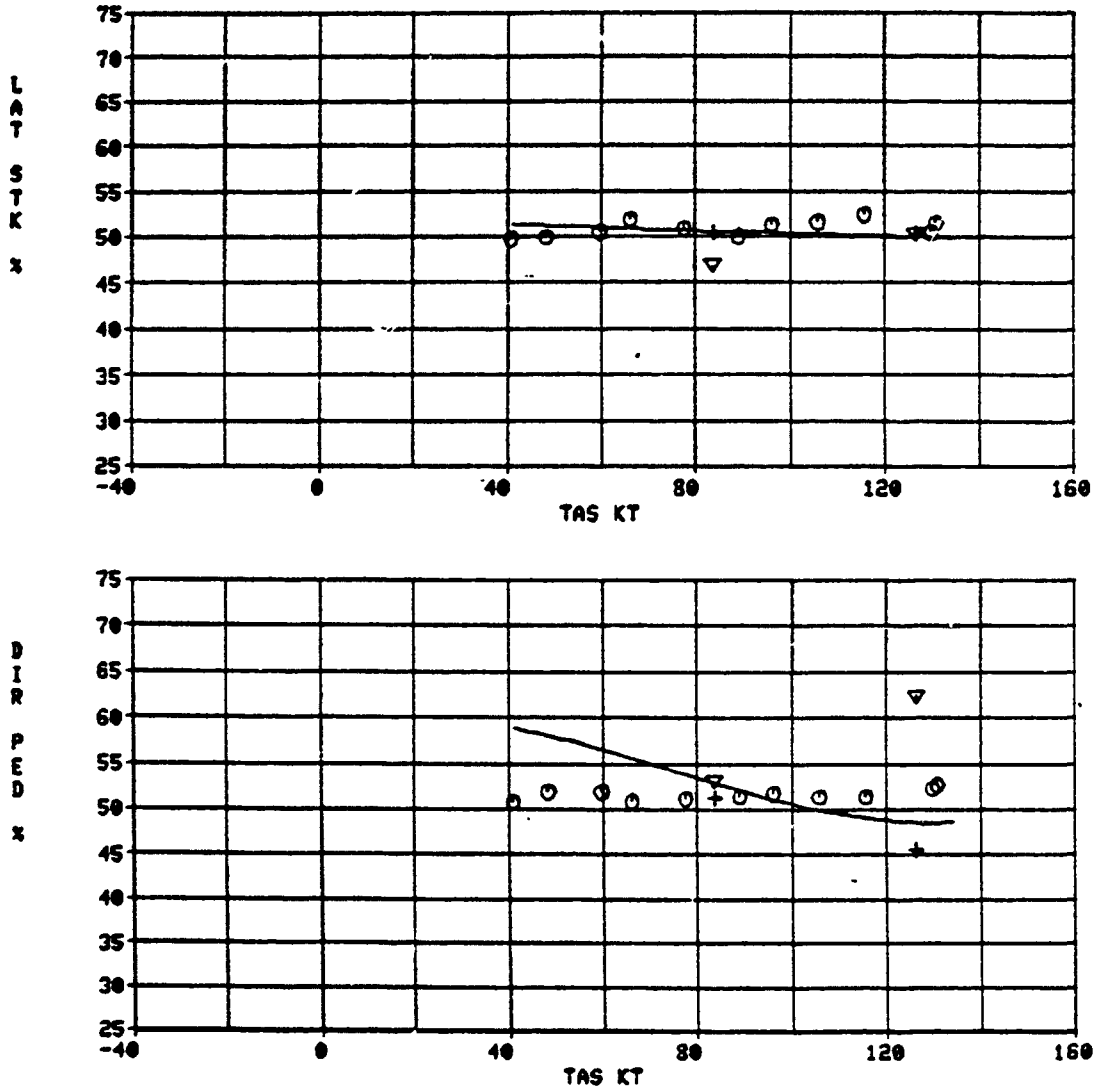


FIGURE 4-5

### CH-46E TRIM CHARACTERISTICS FLIGHT TEST CORRELATION LEVEL FLIGHT & AUTOROTATION

DCPT OFF	GW 24200 LB	HD 3500 FT	F/T A-97
SAS OFF	CG 6 IN FWD	RPM 100 %	LEVEL FLIGHT ○ -
TRIM 0 IN.			AUTOROTATION ▽ +

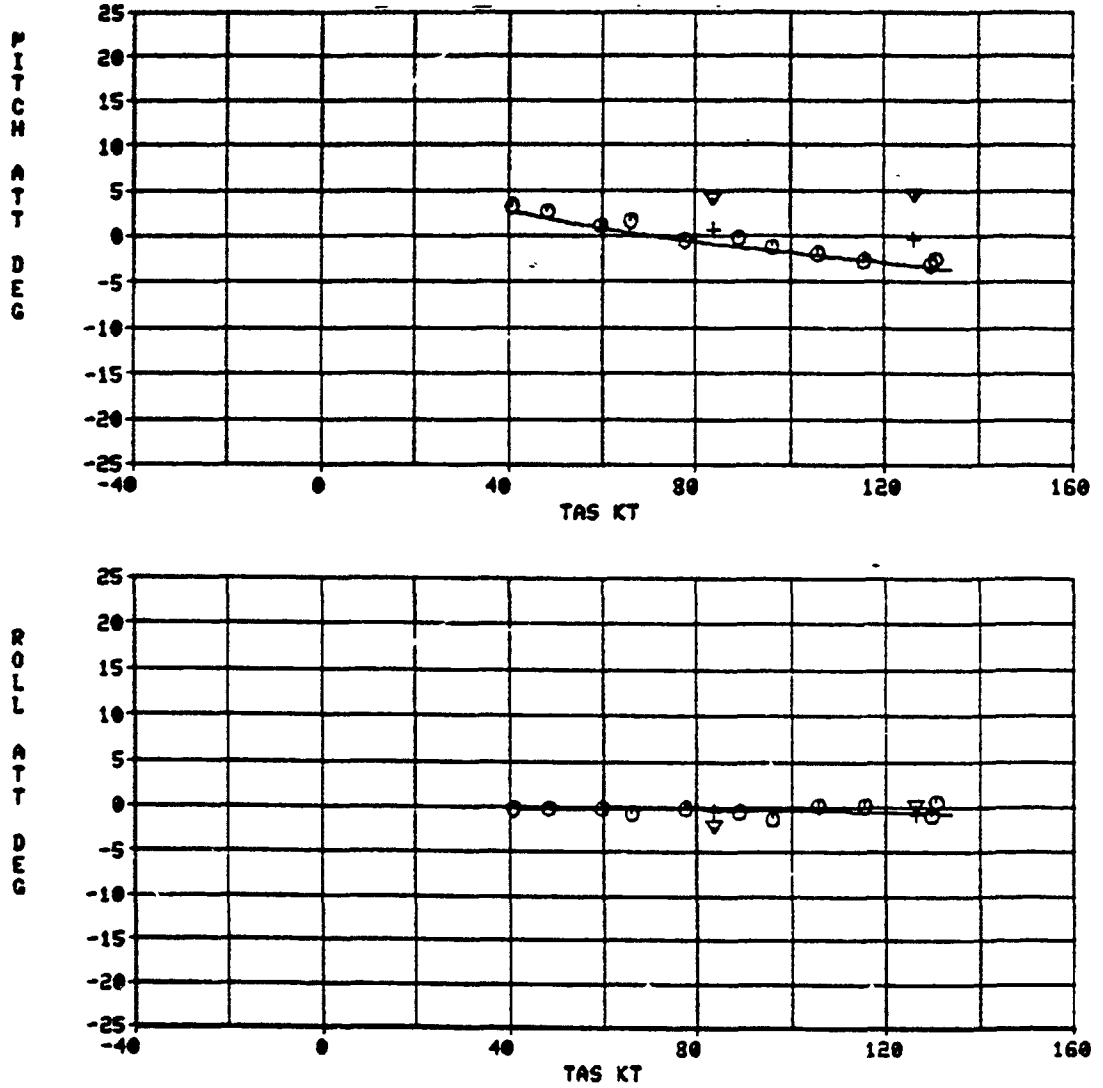


FIGURE 4-6

### CH-46E TRIM CHARACTERISTICS FLIGHT TEST CORRELATION HOVER, LEVEL FLIGHT, CLIMB & DESCENT

DCPT OFF    GU 24350 LB    XHD 4000 FT    LEVEL FLIGHT ○    -  
SAS OFF    CG 6 IN FWD    RPM 100 %    HOVER □    +  
TRIM 0 IN.    \* EXCEPT HOVER IGE    CLIMB △    +  
DESCENT ▽    +

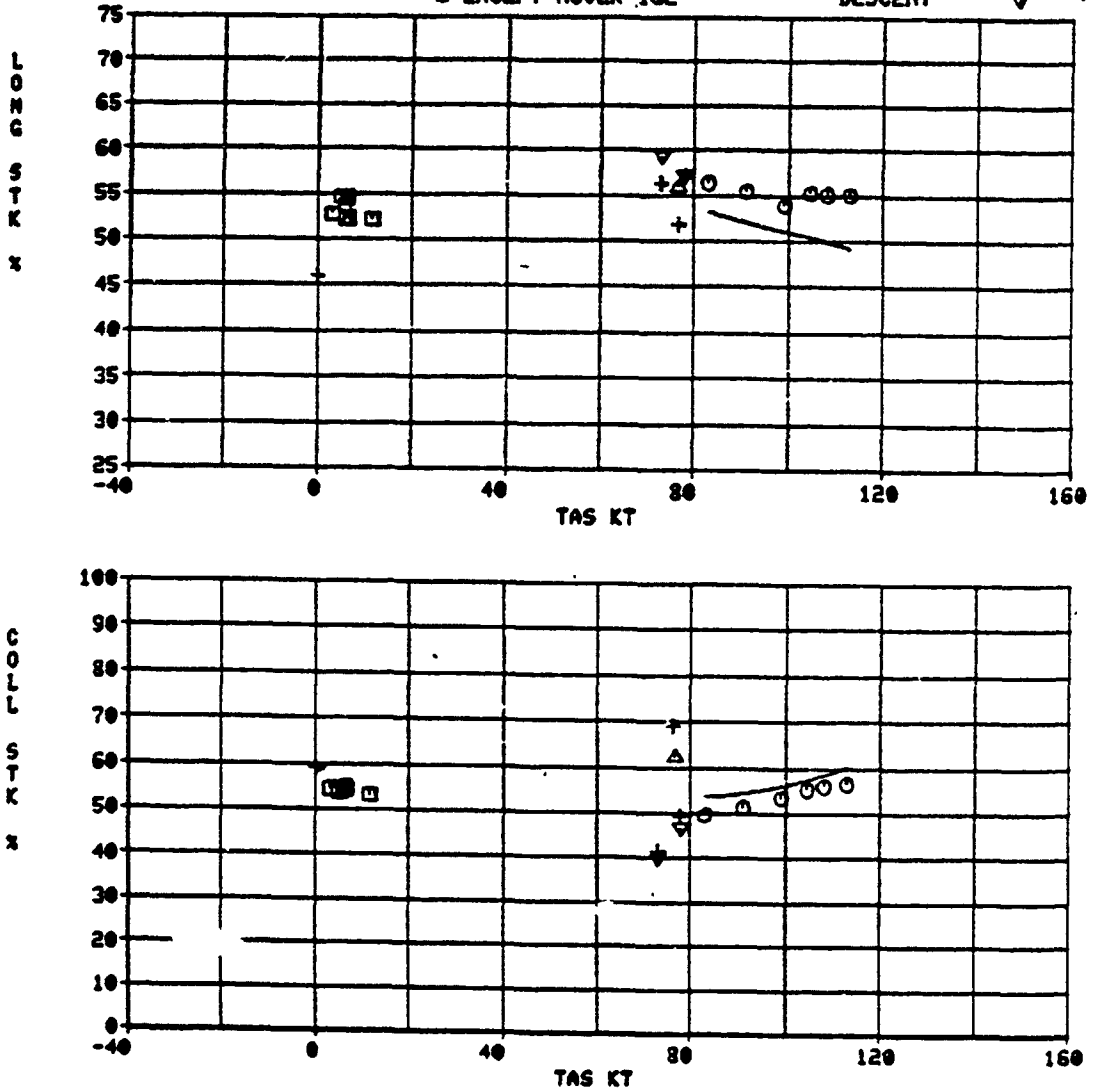


FIGURE 4-7

### CH-46E TRIM CHARACTERISTICS FLIGHT TEST CORRELATION HOVER, LEVEL FLIGHT, CLIMB & DESCENT

DCPT OFF	GW 24350 LB	XHD 4000 FT	F/T	A-97
SAS OFF	CG 6 IN FWD	RPN 100 %	LEVEL FLIGHT	○ -
TRIM 0 IN.			HOVER	□ +
			CLIMB	△ +
			DESCENT	▽ +

\* EXCEPT HOVER IGE

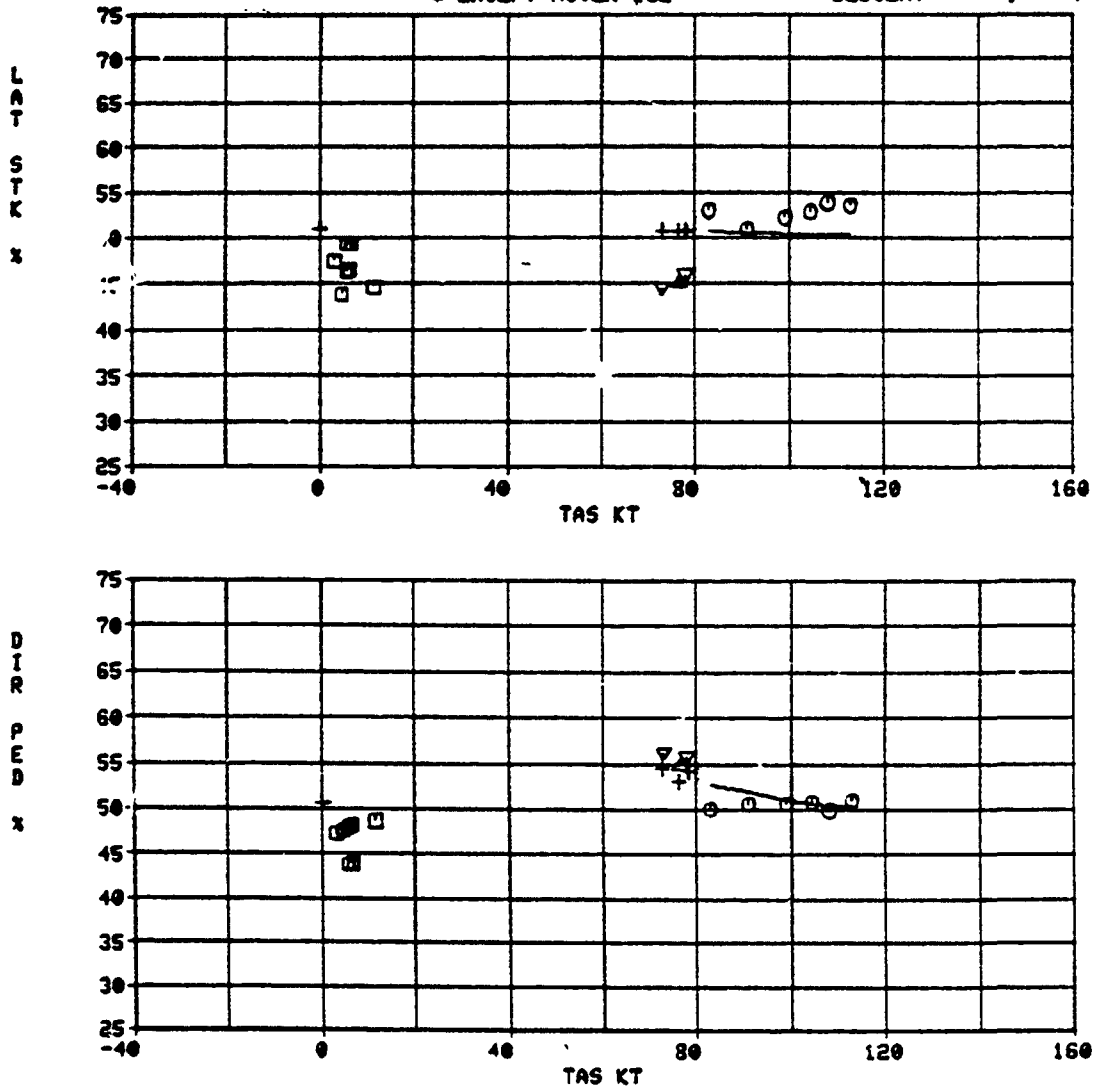


FIGURE 4-8

### CH-46E TRIM CHARACTERISTICS FLIGHT TEST CORRELATION HOVER, LEVEL FLIGHT, CLIMB & DESCENT

DCPT OFF	GW 24350 LB	XHD 4000 FT	F/T A-97
SAS OFF	CG 6 IN FWD	RPM 100 %	LEVEL FLIGHT ○ -
TRIM 0 IN.			HOVER □ +
			CLIMB △ +
			DESCENT ▽ +

3 EXCEPT HOVER ICE

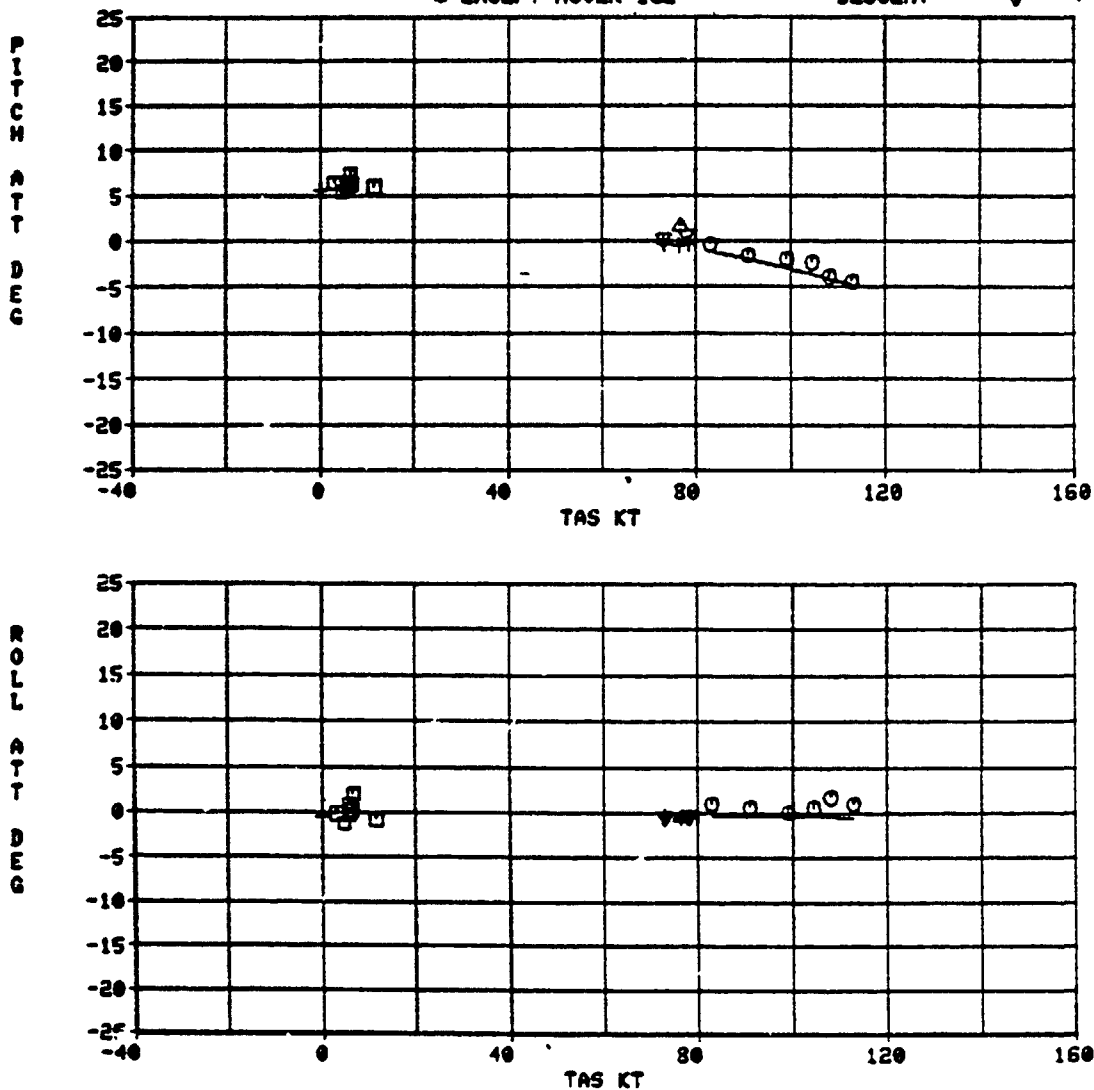


FIGURE 4-9

### CH-46E TRIM CHARACTERISTICS FLIGHT TEST CORRELATION SIDESLIP

DCPT OFF	GU 23900 LB	HD 4800 FT	TAS 64 KT ○	F/T A-97
SAS OFF	CG 6 IN FWD	RPM 100 %	106 KT □	-
TRIM 0 IN.				

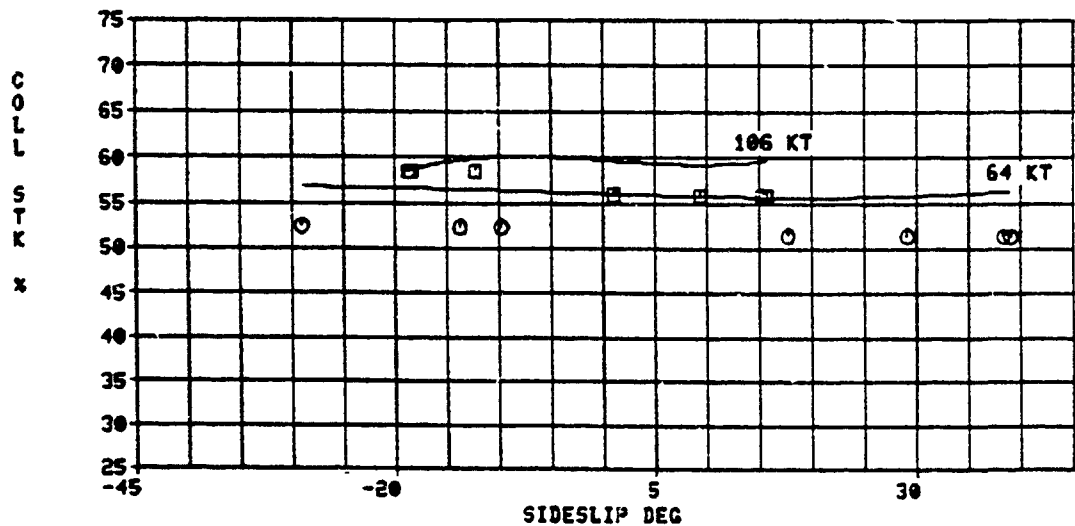
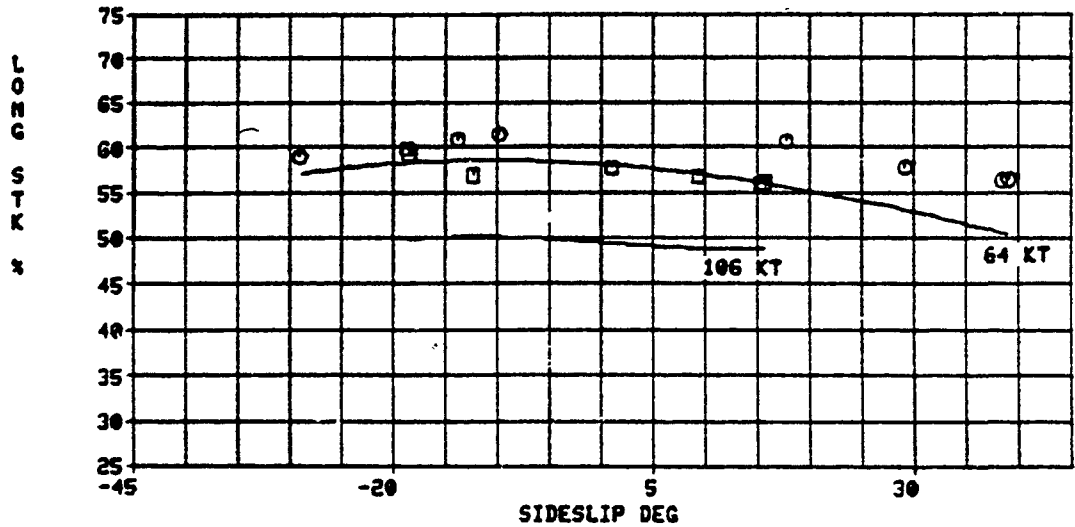


FIGURE 4-10

### CH-46E TRIM CHARACTERISTICS FLIGHT TEST CORRELATION SIDESLIP

DCPT OFF      GU 23900 LB      HD 4800 FT      TAS 64 KT ○      F/T A-97  
 SAS OFF      CG 6 IN FWD      RPM 100 X      106 KT □      -  
 TRIM 0 IN.

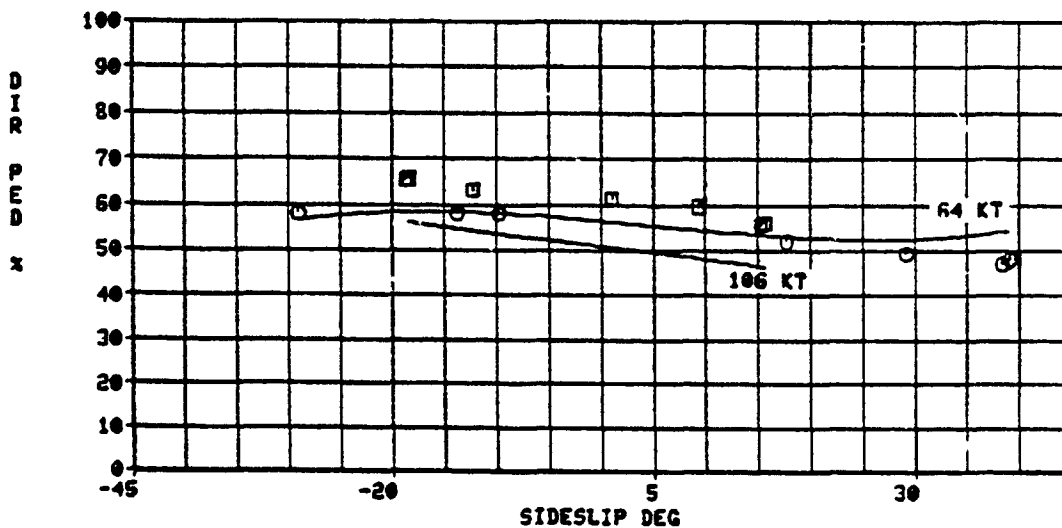
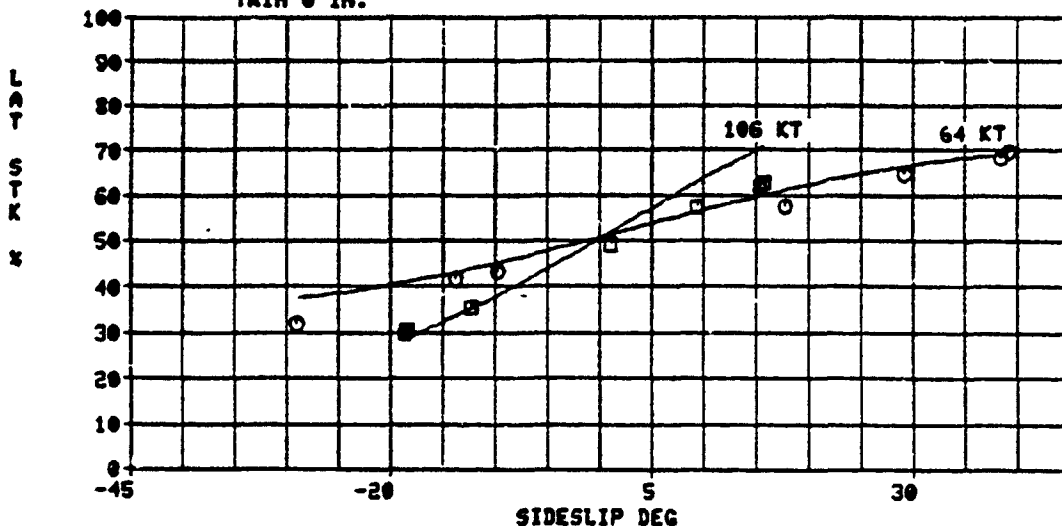


FIGURE 4-11

### CH-46E TRIM CHARACTERISTICS FLIGHT TEST CORRELATION SIDESLIP

DCPT OFF  
SAS OFF  
TRIM @ IN.

GU 23900 LB  
CG 6 IN FWD

HD 4800 FT  
RPM 100 %

TAS 64 KT  $\square$  F/T A-97  
106 KT  $\circ$  -

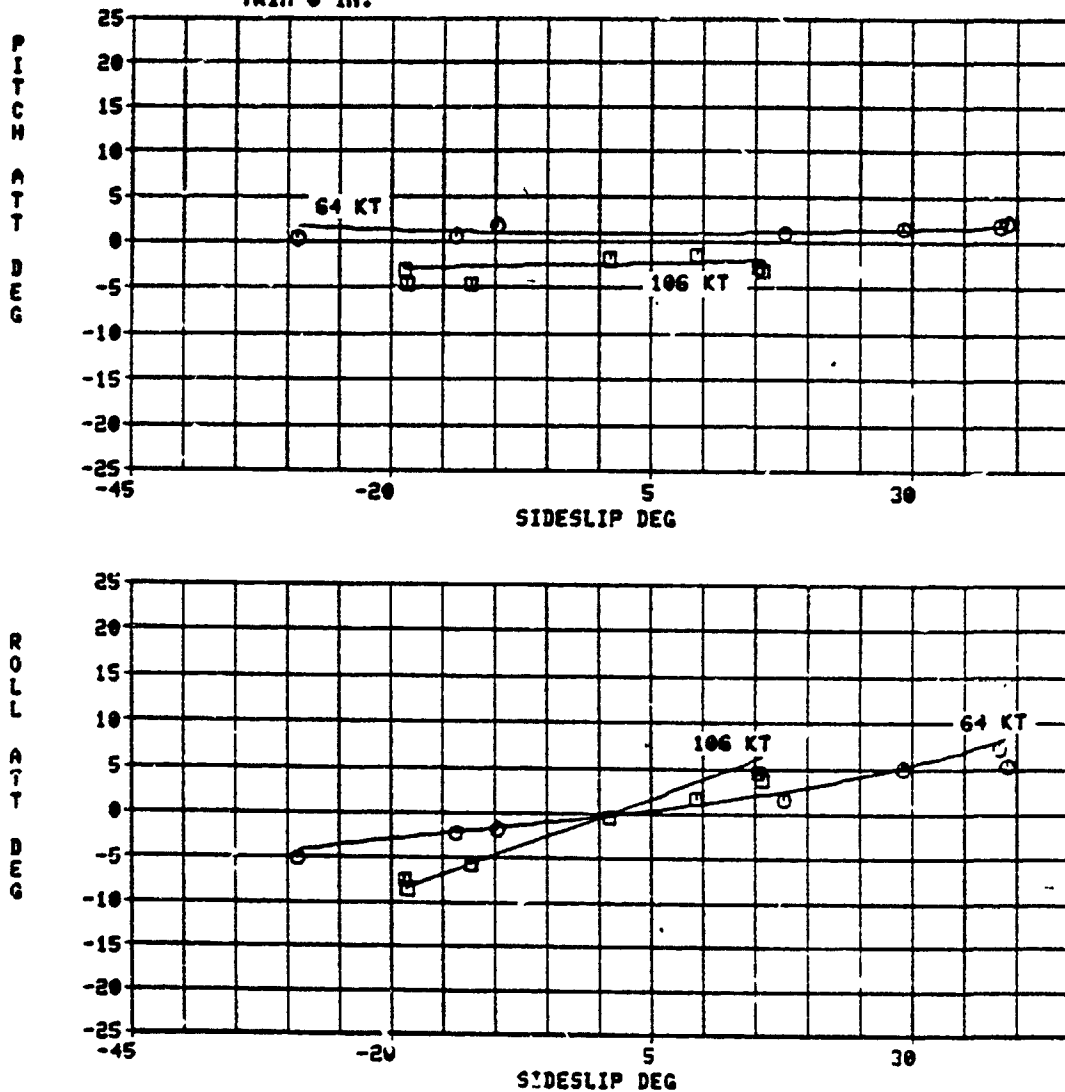


FIGURE 4-12

### CH-46E TRIM CHARACTERISTICS FLIGHT TEST CORRELATION LEVEL FLIGHT

DCPT OFF  
SAS OFF  
TRIM 0 IN.

GW 21050 LB  
CG 8 IN AFT  
HD 2100 FT  
RPM 100 %

F/T A-97  
MANUAL CYCLIC A ○ -  
MANUAL CYCLIC B □ -

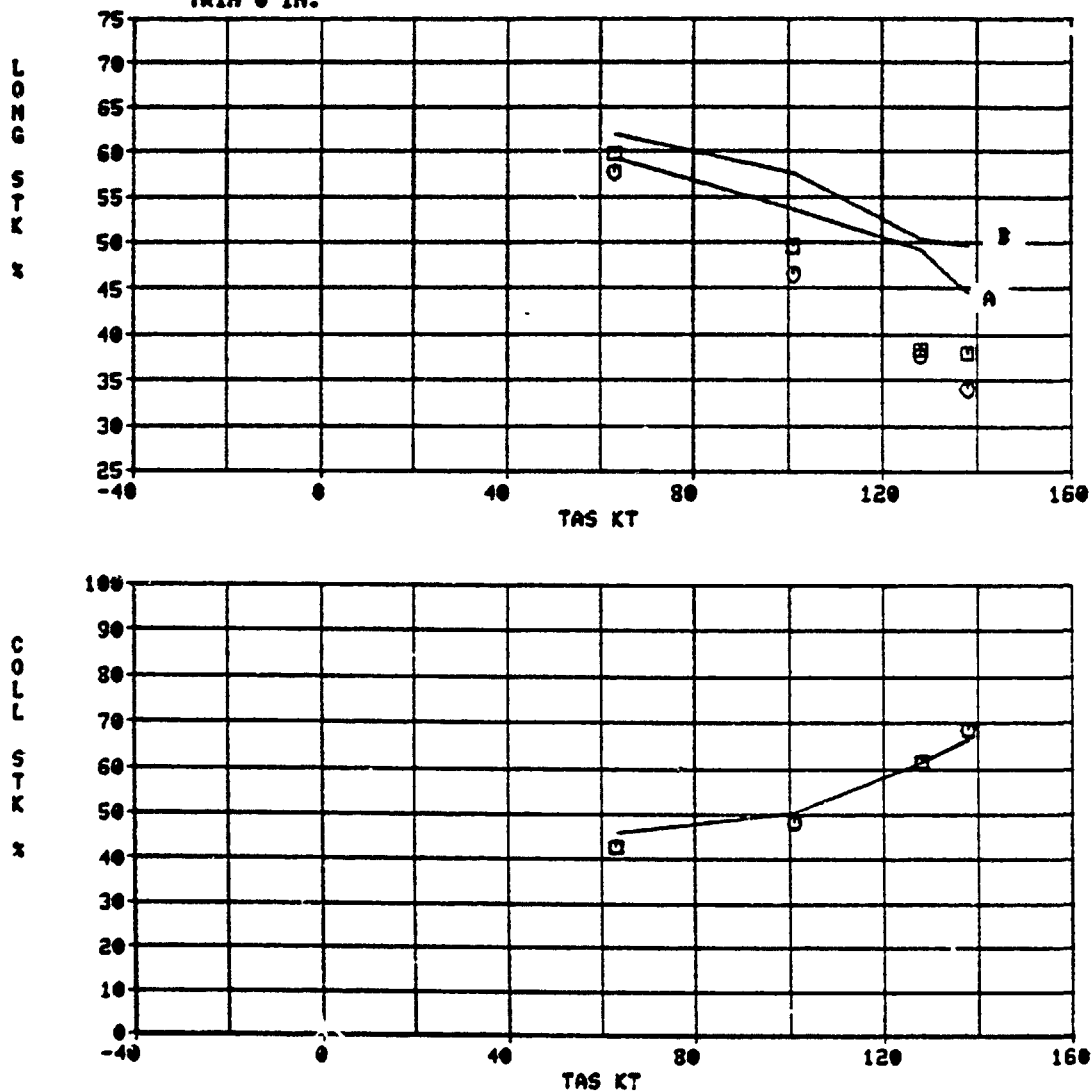


FIGURE 4-13

### CH-46E TRIM CHARACTERISTICS FLIGHT TEST CORRELATION LEVEL FLIGHT

\* DCPT OFF      GU 21050 LB      HD 2100 FT      MANUAL CYCLIC A ○      F/T A-97  
 SAS OFF      CG 8 IN AFT      RPM 100 %      MANUAL CYCLIC B □      -  
 TRIM 0 IN.

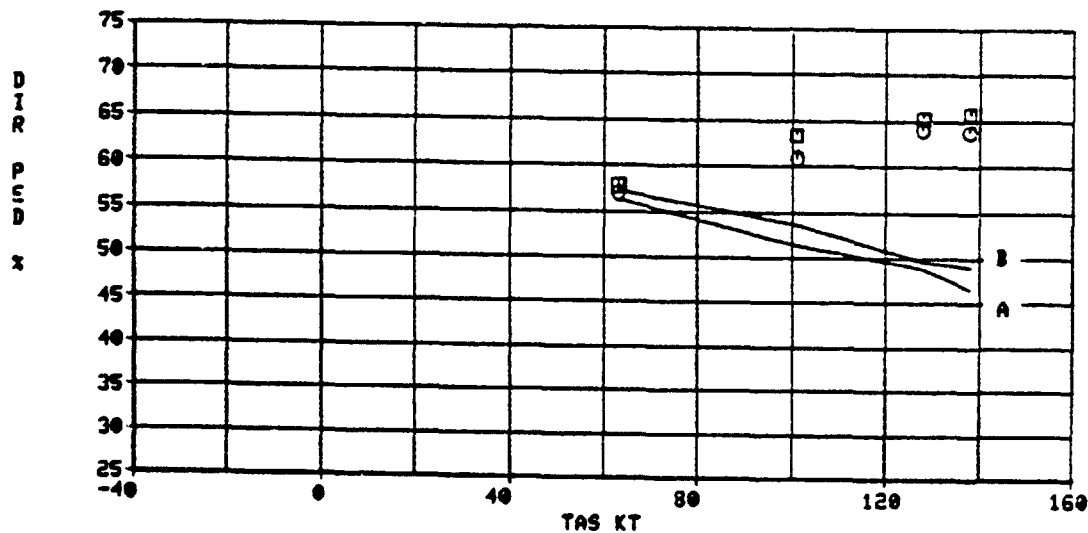
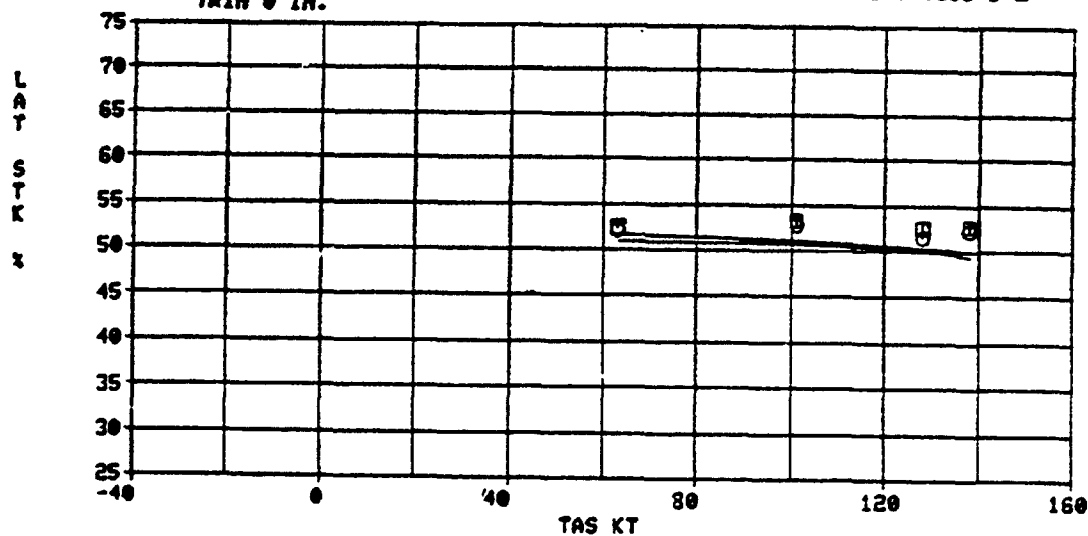


FIGURE 4-14

### CH-46E TRIM CHARACTERISTICS FLIGHT TEST CORRELATION LEVEL FLIGHT

DCPT OFF	CU 21050 LB	HD 2100 FT	F/T A-97
SAS OFF	CG 8 IN AFT	RPM 100 %	MANUAL CYCLIC A ○ -
TRIM 0 IN.			MANUAL CYCLIC B □ -

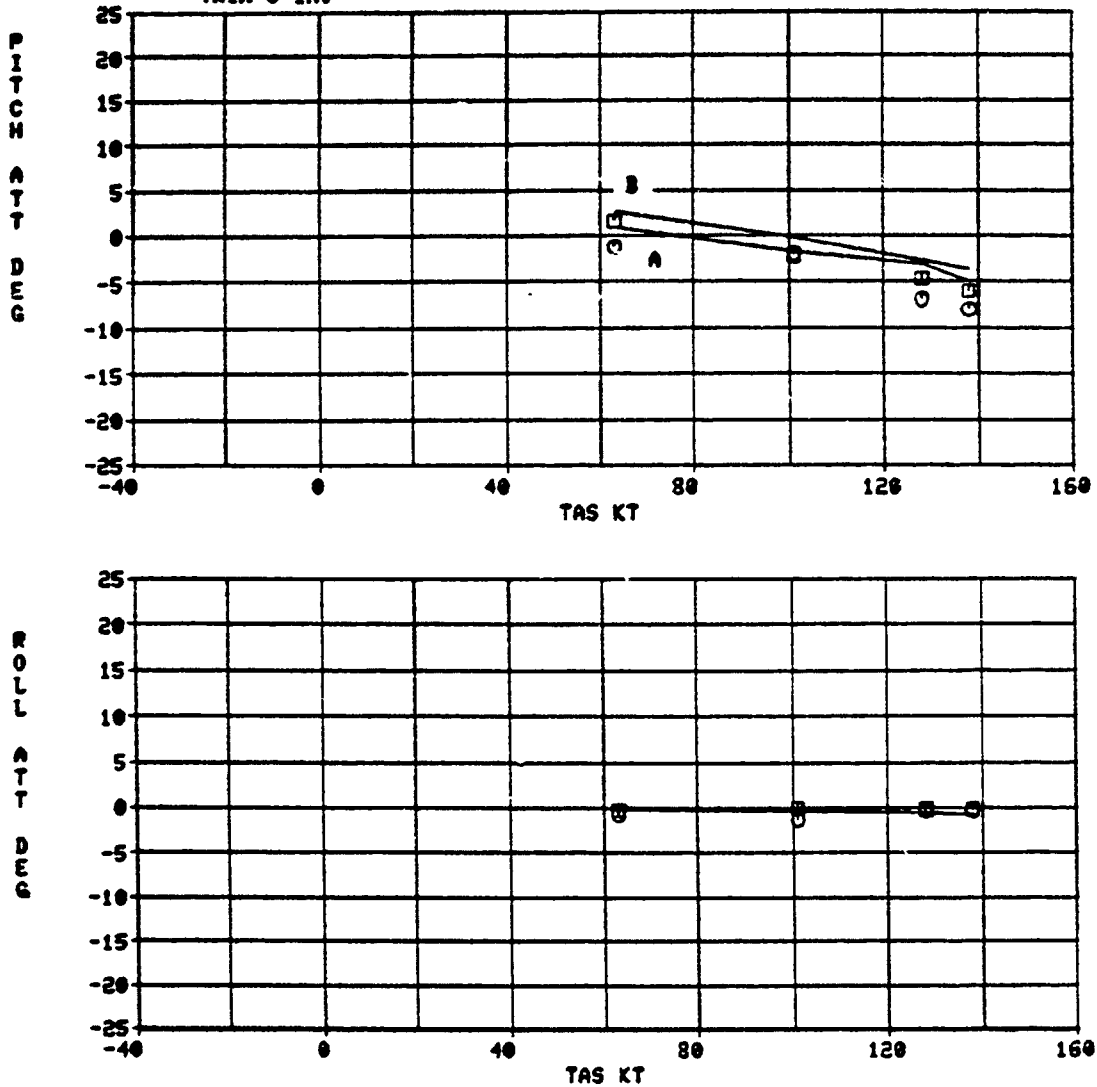


FIGURE 4-15

## 5.0 STATIC STABILITY CHARACTERISTICS

### 5.1 LONGITUDINAL STATIC STABILITY

The longitudinal static stability characteristics of the CH-46E, as predicted by the A-97 Trim Analysis Program, are shown in Figure 5-1 for level flight at sea level and 8,000 feet, and in Figure 5-2 for autorotation and transmission-limited full power climb. Longitudinal stick position gradient and force gradient with airspeed are shown, in which positive gradients represent stability.

Because the available flight test data was limited in scope, and because predicted longitudinal stick position gradients agree well with trim flight test data in Section 4.2, it was decided that predicted static stability characteristics would be meaningful, and would allow a wider range of flight conditions to be addressed.

The predicted data were obtained by the same method as in flight testing, namely at constant collective with DCPT and ATS on. As airspeed is varied above and below the level flight trim points, the resulting rates of climb and descent are accepted as collective is kept constant. In climb and autorotation, the collective is likewise kept constant, and the rate of climb or descent increases or decreases about the steady trim value as airspeed varies.

The stick force data were obtained by entering the ATS-ON longitudinal stick force plots (Figures 3-5 to 3-7) with the stick positions of Figures 5-1 and 5-2, and reading the corresponding forces. The discontinuity in the force data at the trim points is due to the breakout force required to move the stick from the established trim position.

In general, the CH-46E is shown to be slightly unstable at 50 knots in level flight, neutrally stable at 80 to 90 knots in level flight and autorotation, and stable in an 80 knot climb and at 130 knot level flight. These characteristics agree well with existing flight test data, except that the existing data show slight positive stability at 80 knots.

## 5.2 LATERAL - DIRECTIONAL STATIC STABILITY

The predicted lateral-directional static stability characteristics of the CH-46E are shown in Figures 5-3 and 5-4 for level flight at three airspeeds at sea level, and in Figures 5-5 and 5-6 for level flight at 8,000 feet and for autorotation at sea level. Lateral stick and pedal position, and longitudinal stick and roll attitude, are shown versus sideslip angle. Positive lateral stick and negative pedal gradients represent stability.

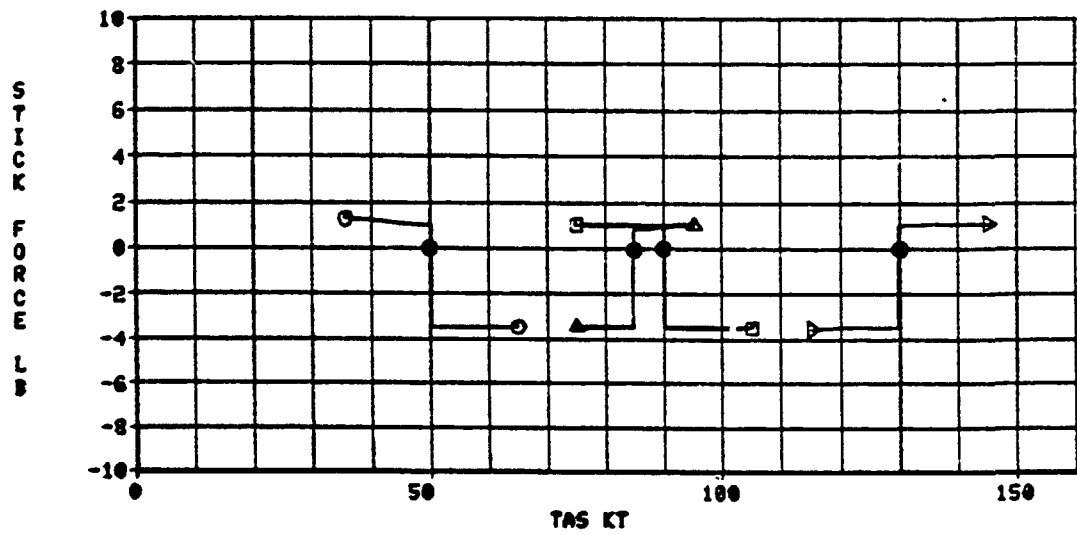
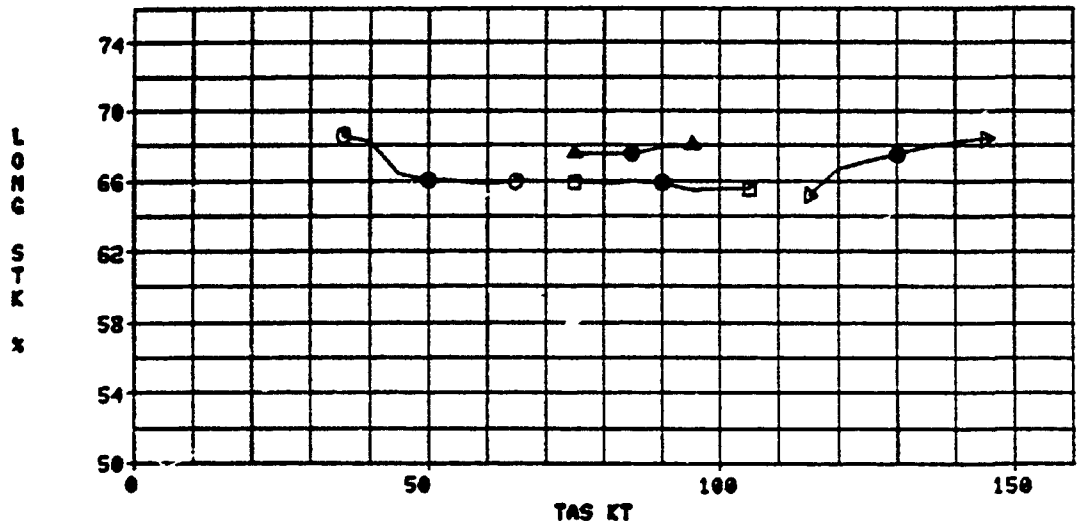
Predicted data are used for the same reasons as set forth in Section 5.1, namely limited flight test data, good agreement of predicted gradient with available flight test data, and the possibility of addressing a wider range of flight conditions.

In a manner analogous to Section 5.1, the predicted lateral-directional data were obtained at constant collective with SAS and ATS on, accepting the variations in rate of climb and descent as sideslip angle is varied.

In general, the CH-46E is shown to have lateral-directional stability characteristics which are good at low speed and excellent at high speed. At the larger sideslip angles, the pedal gradient loses linearity, but remains stable to 30 deg. This reduction of directional stability is attributable mainly to the loss of effectiveness of the artificial stability channel of the yaw SAS at large sideslip angles.

### CH-46E LONGITUDINAL STATIC STABILITY LEVEL FLIGHT

DCPT ON	○	GW	24300 LB	CG	6 IN FWD	HD	0 FT	TAS	50 KT
SAS ON	□		24300 LB		6 IN FWD		0 FT		90 KT
TRIM 0 IN.	▷		24300 LB		6 IN FWD		0 FT		130 KT
	△		24300 LB		6 IN FWD		8000 FT		85 KT

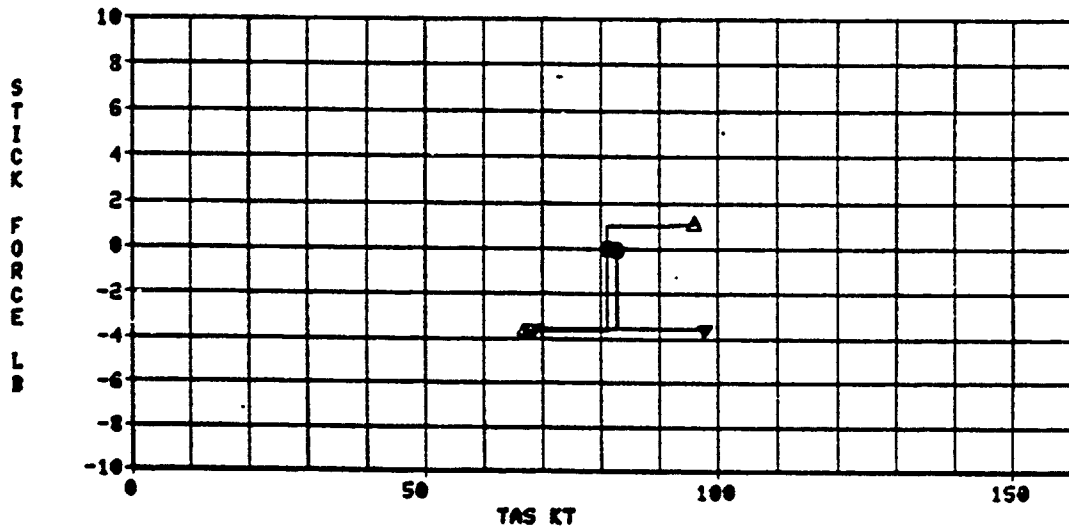
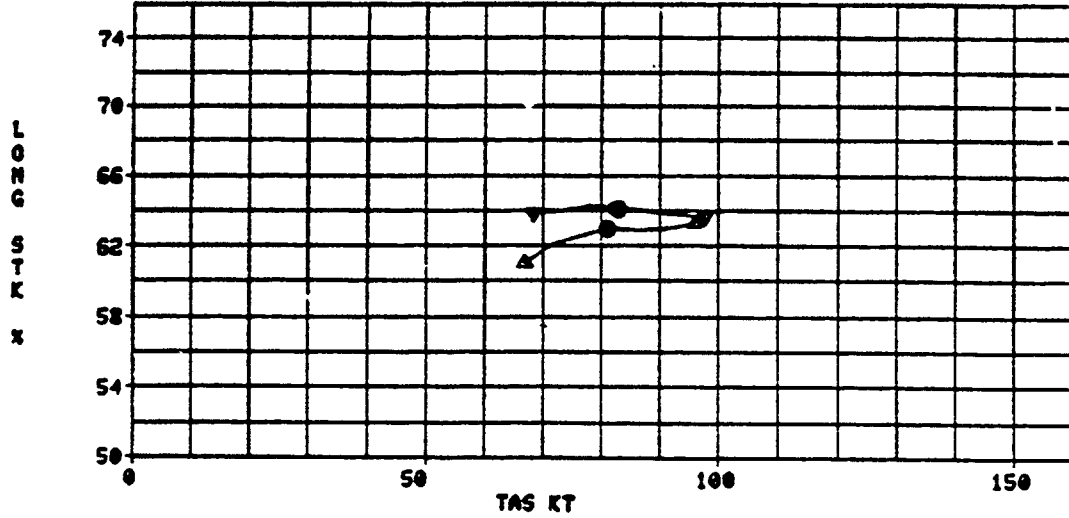


● TRIM POINT

FIGURE 5-1

### CH-46E LONGITUDINAL STATIC STABILITY MAX POWER CLIMB & AUTOROTATION

DCPT ON ▽ GW 24300 LB CG 6 IN FWD HD 0 FT TAS 80 KT AUTO  
 SAS ON Δ 24300 LB 6 IN FWD 0 FT 80 KT CLIMB  
 TRIM 0 IN.

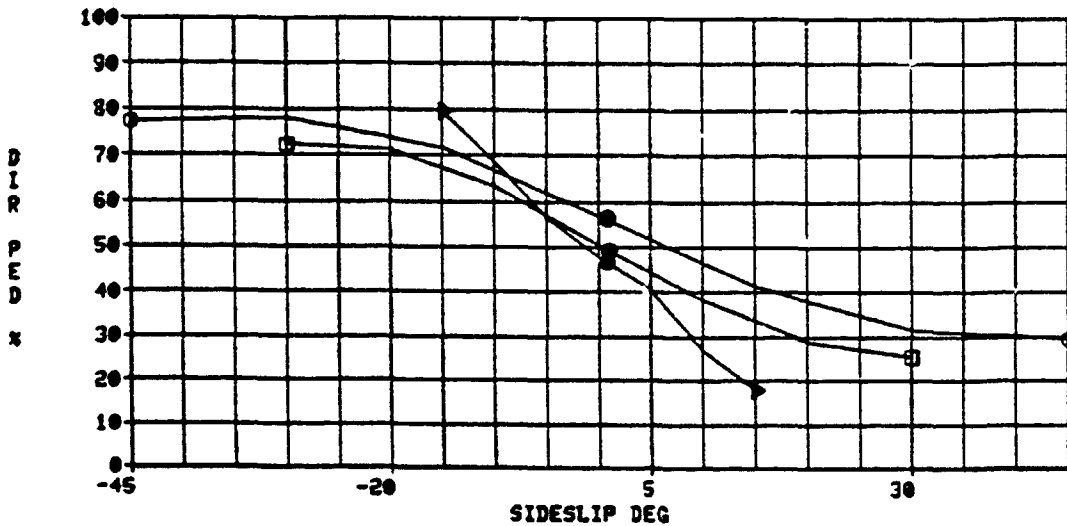
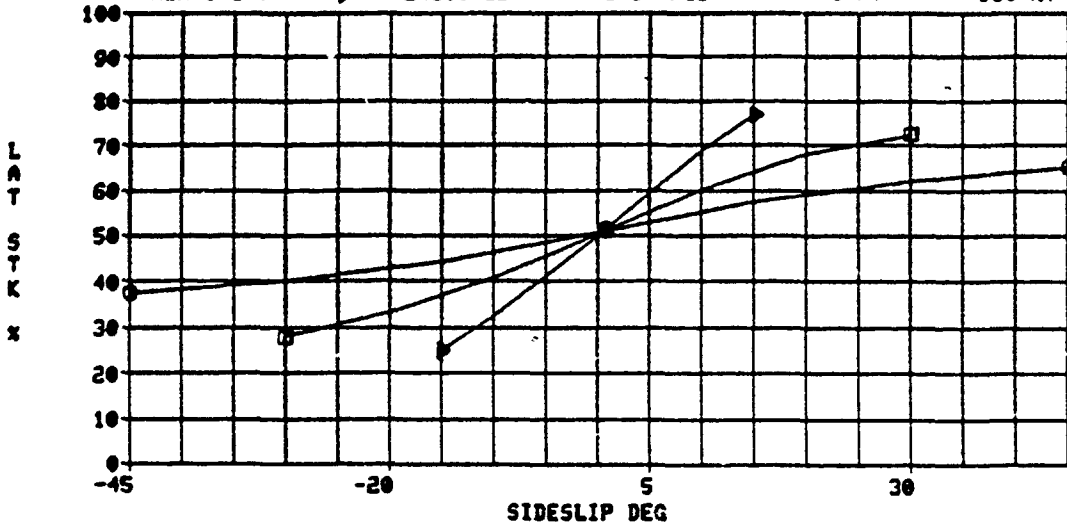


● TRIM POINT

FIGURE 5-2

### CH-46E LATERAL-DIRECTIONAL STATIC STABILITY LEVEL FLIGHT

DCPT ON	○ GW 24300 LB	CG 6 IN FWD	HD 0 FT	TAS 50 KT
SAS ON	□ 24300 LB	6 IN FWD	0 FT	90 KT
TRIM 0 IN.	▷ 24300 LB	6 IN FWD	0 FT	130 KT

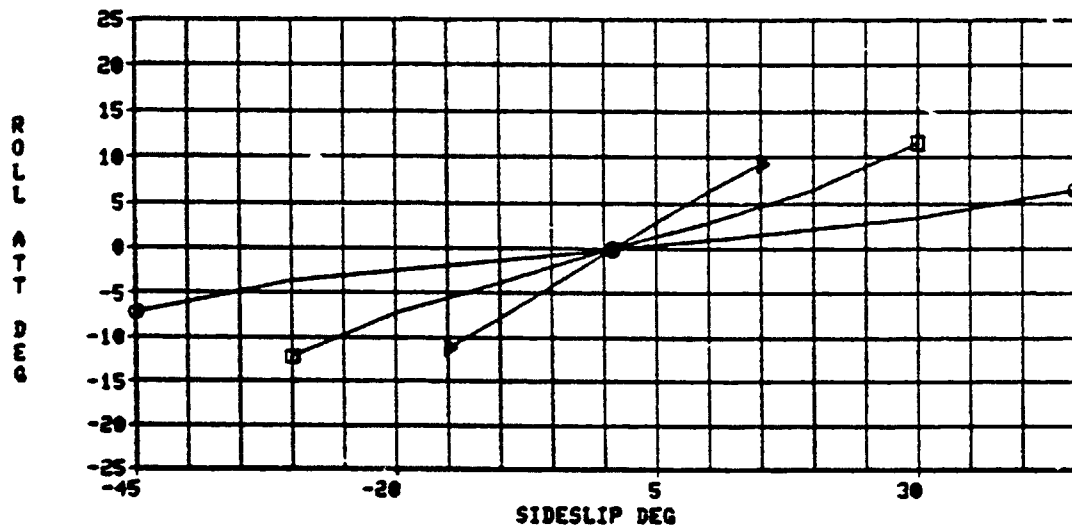
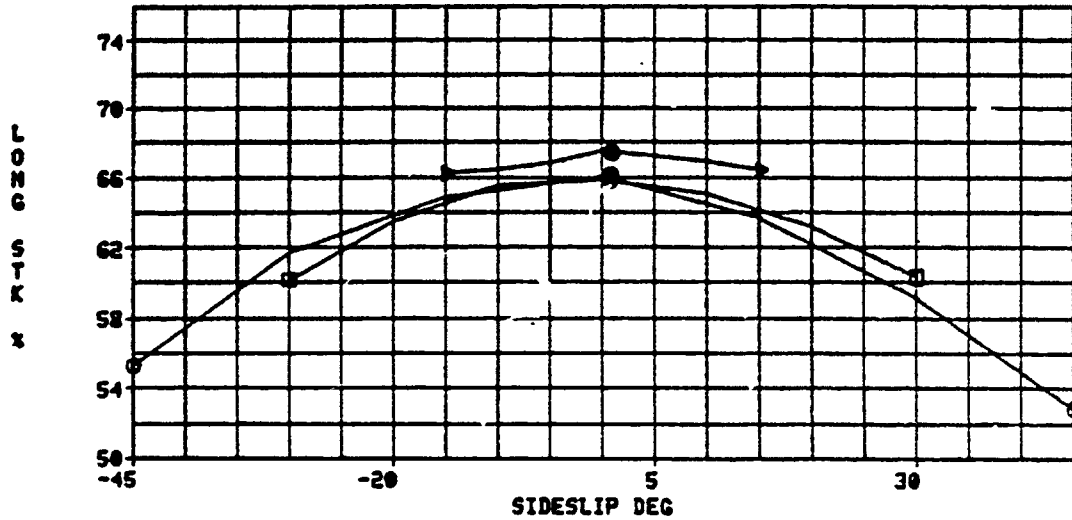


● TRIM POINT

FIGURE 5-3

### CH-46E LATERAL-DIRECTIONAL STATIC STABILITY LEVEL FLIGHT

DCPT ON	○ GW 24300 LB	CG 6 IN FWD	HD 0 FT	TAS 50 KT
SAS ON	□ 24300 LB	6 IN FWD	0 FT	90 KT
TRIM 0 IN.	▷ 24300 LB	6 IN FWD	0 FT	130 KT

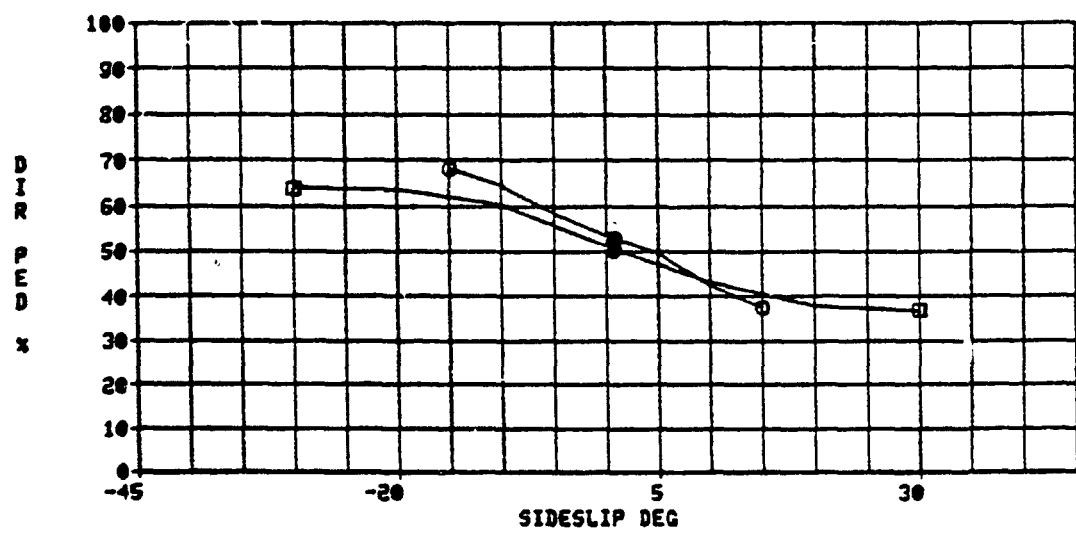
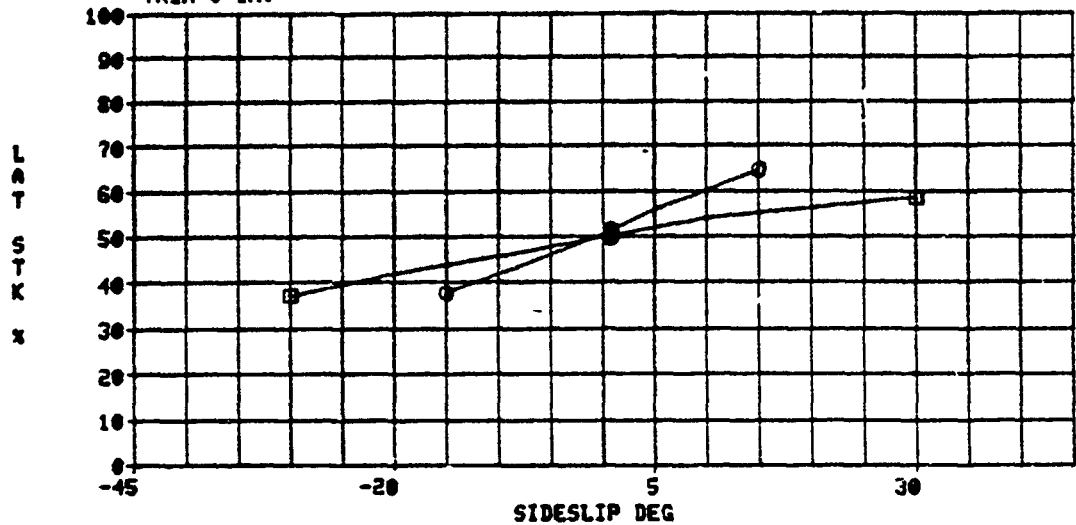


● TRIM POINT

FIGURE 5-4

### CH-46E LATERAL-DIRECTIONAL STATIC STABILITY LEVEL FLIGHT & AUTOROTATION

DCPT ON      ○ GW 24300 LB    CG 6 IN FWD    HD 8000 FT    TAS 90 KT LEVEL  
SAS ON       □ 24300 LB       6 IN FWD       0 FT         80 KT AUTO  
TRIM 0 IN.

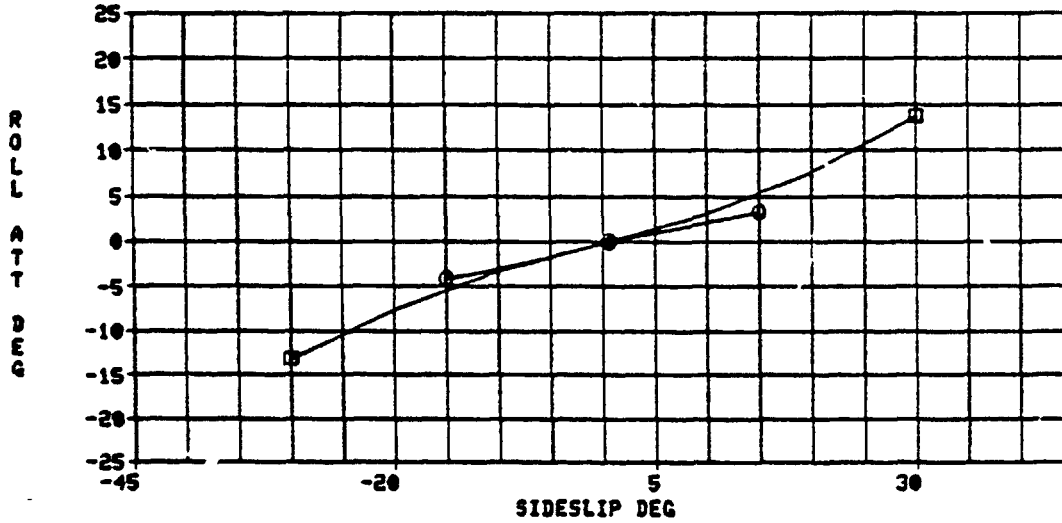
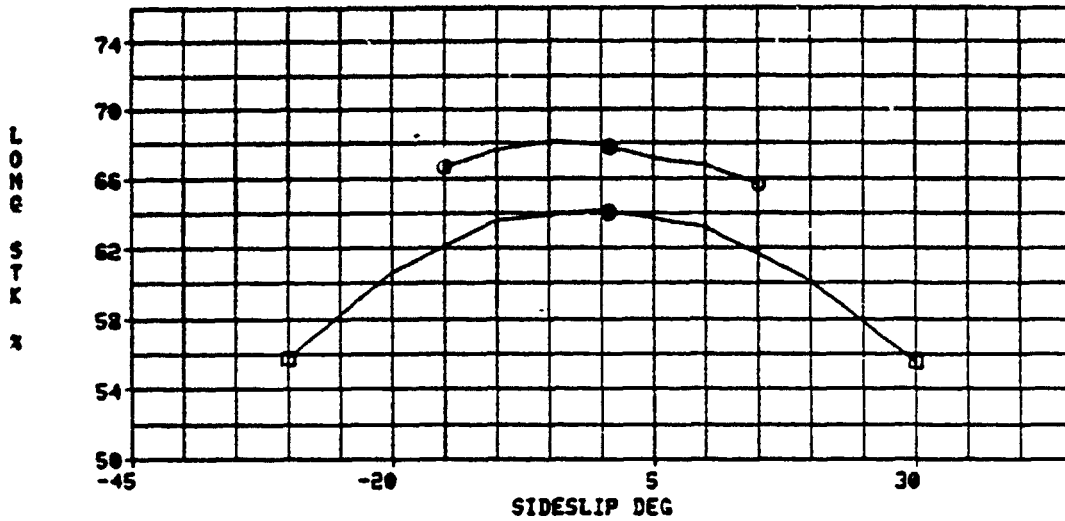


● TRIM POINT

FIGURE 5-5

### CH-46E LATERAL-DIRECTIONAL STATIC STABILITY LEVEL FLIGHT & AUTOROTATION

DCPT ON      ○ GW 24300 LB    CG 6 IN FWD    HD 8000 FT    TAS 90 KT LEVEL  
 SAS ON      □ 24300 LB       6 IN FWD       0 FT         80 KT AUTO  
 TRIM 0 IN.



● TRIM POINT

FIGURE 5-6

## 6.0 CONTROL SENSITIVITY

The control response and sensitivity characteristics of the CH-46E at 24300 lb. and 6 in. fwd CG are summarized for the longitudinal, lateral and directional control axes in Figures 6-1 to 6-3. Data are shown for hover IGE, and for cruise at approximately 112 knot TAS at 4750 feet.

These characteristics were extracted from the control response data obtained during the SLEP II flight test program. At each flight condition, a series of increasingly large control step inputs was made in the positive and negative directions for each control axis. The maximum response rate during the first second, and the attitude deviation at the end of one second, were read directly from the helicopter response data. The initial acceleration was obtained by reading the maximum slope of the rate response trace, which always occurs at the beginning of the response.

The control sensitivity requirements of Reference 4 are also shown in each figure. The CH-46E meets these requirements by comfortable margins at the conditions tested.

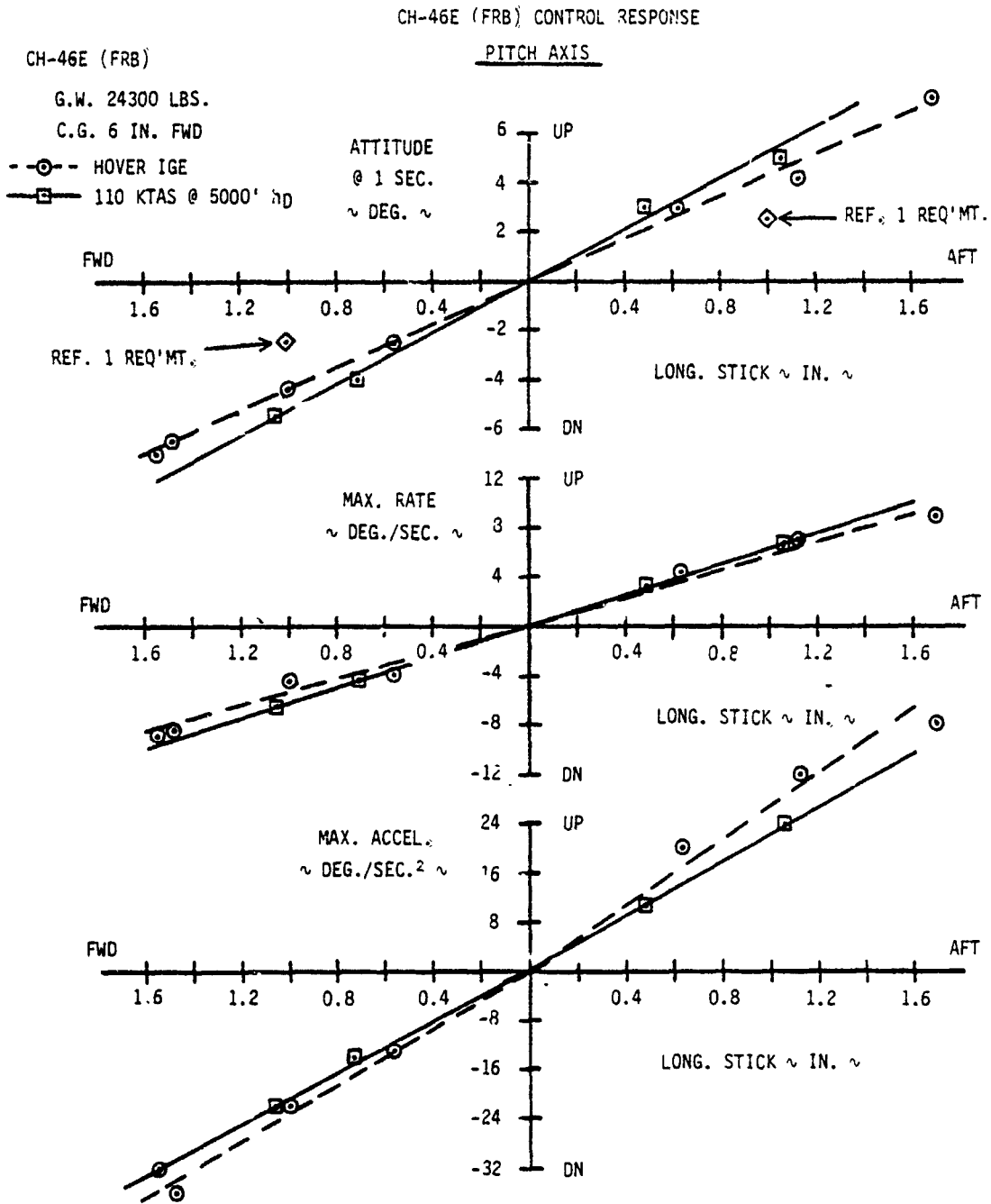


FIGURE 6-1

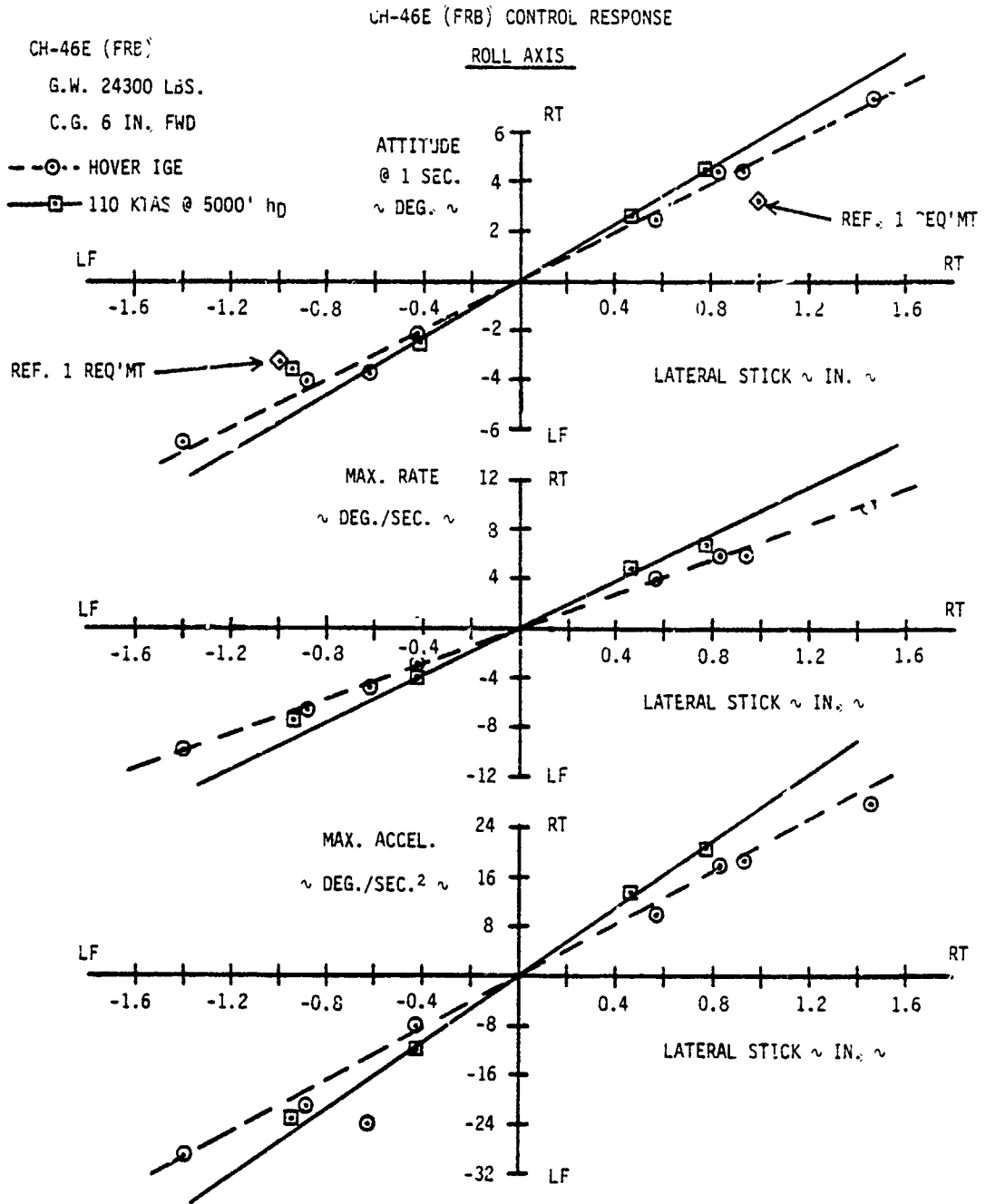


FIGURE 6-2

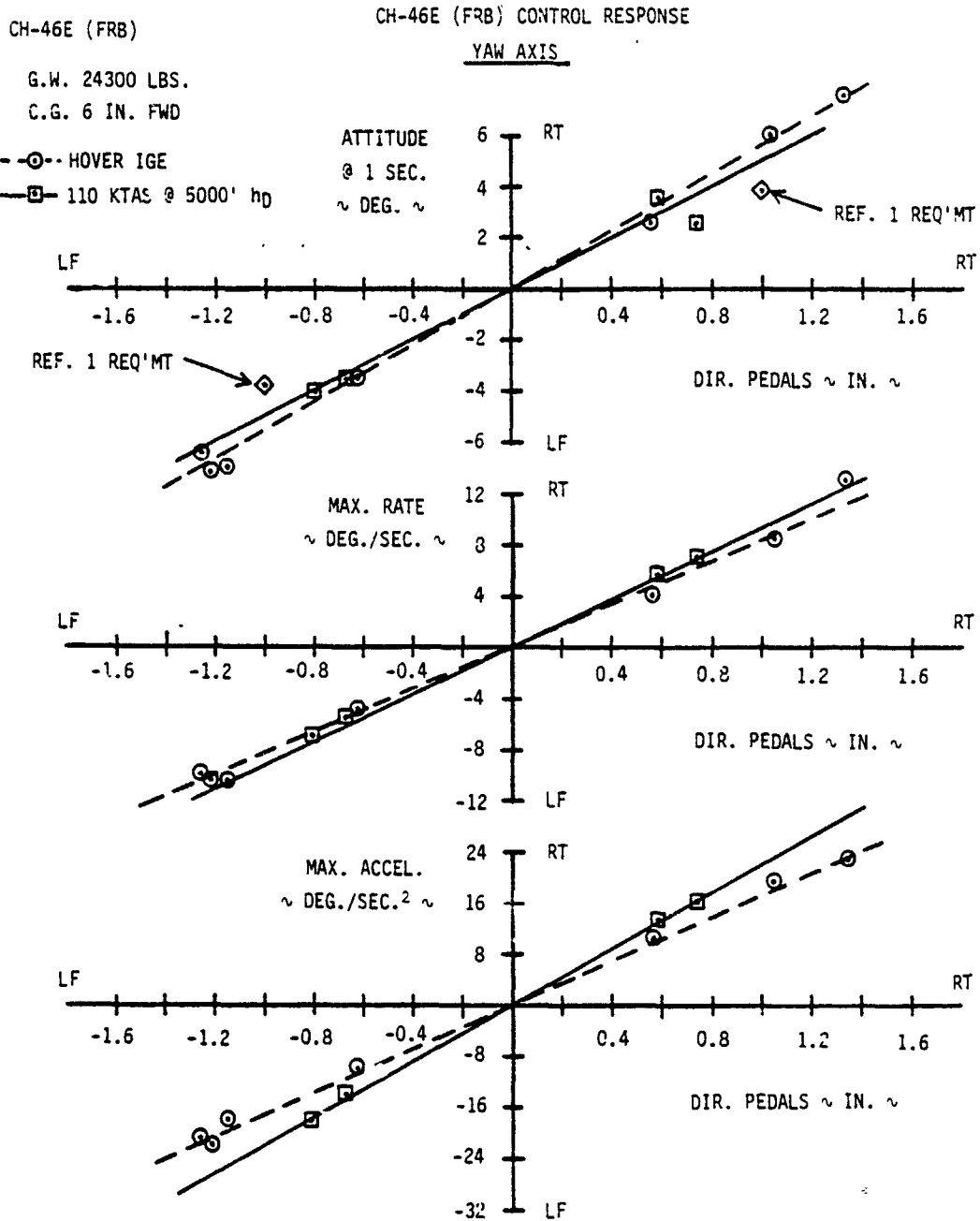


FIGURE 6-3

## 7.0 TIME-HISTORY DATA

### 7.1 GENERAL

The transient time-history data extracted from the CH-46E SLEP II flight test program are contained in Volume 3. These data were obtained at one gross weight and CG only, namely 24300 lb. and 6 in. fwd, at low to moderate altitude. Four general types of data are presented.

- Dynamic stability (longitudinal pulse response) at hover and cruise conditions.
- Control responses (longitudinal, lateral and directional step response) at hover and cruise conditions.
- SAS failures (longitudinal, lateral and directional hard-over SAS response) at cruise conditions. Failures during dual SAS operation (dual-to-single) and failures during single SAS operation (single-to-none) are both considered.
- Engine failure (single engine step reduction to ground idle) at cruise conditions.

In each record, the response of the helicopter in the axis of disturbance (control input, SAS failure, etc.) is thoroughly described by time-histories of six to eight relevant parameters in that axis, while interaxis coupling is assessed by a sampling of four parameters from each of the remaining axes.

### 7.2 DYNAMIC STABILITY

A representative set of dynamic stability time-histories for a longitudinal pulse input is presented in Figures 7-1 to 7-8. The flight conditions are noted on the figures. The first four figures describe the helicopter response in the axis of

disturbance (longitudinal), while the remaining four describe any interaxis coupling into the other axes.

The pitch response of the CH-46E is well damped. Pitch rate returns rapidly to zero as soon as the input is removed, and normal force is reduced. There seems to be some oscillatory motion in roll, but it is not clear that this is necessarily a response to the longitudinal pulse. A slight response in yaw rate is also noted.

### 7.3 CONTROL RESPONSE

A typical set of control response time-histories for a lateral step input is presented in Figures 7-9 to 7-15. The flight conditions are noted. The first three figures describe the resulting helicopter response in roll, while the next four describe any coupling into the yaw and pitch axes.

The roll response to lateral stick is a steady roll rate with an initial overshoot of about 50%. A slight yaw rate develops in one second, and a negligible pitch rate after two seconds.

### 7.4 SAS FAILURES

A representative SAS failure time-history for a dual-to-single yaw SAS failure is presented in Figures 7-16 to 7-22. The first three figures describe the helicopter yaw axis response, and the last four describe interaxis coupling.

The directional pedal trace shows a delay time of 1.8 sec before recovery input. Additional time might have been demonstrated, since the resultant yaw rate and attitude excursions are not large. However, droop stop pounding is sometimes a problem during recoveries from yaw SAS failures at cruise, and the pilot's anticipation of this may have led him to recover early. The strong interaxis coupling of yaw into

roll (dihedral effect) also influences the manner of recovery. The strategy followed here was to convert the combined right yaw and roll excursions into a coordinated right turn, from which recovery is readily achieved. The coupling of the yaw and roll excursions into the pitch axis is small, considering the magnitude of the peak yaw and roll rates.

#### 7.5 ENGINE FAILURES

A typical engine failure time-history for a dual-to-single failure is shown in Figures 7-23 to 7-32. The first three figures describe the engine, rotor, and helicopter vertical response. Subsequent figures deal with the helicopter pitch, roll and yaw responses.

In spite of the high torque condition at which the engine failure is initiated, there are no appreciable helicopter excursions in any axis, except for rotor RPM decay to 91%. The delay time for collective reduction exceeds 5.0 seconds.

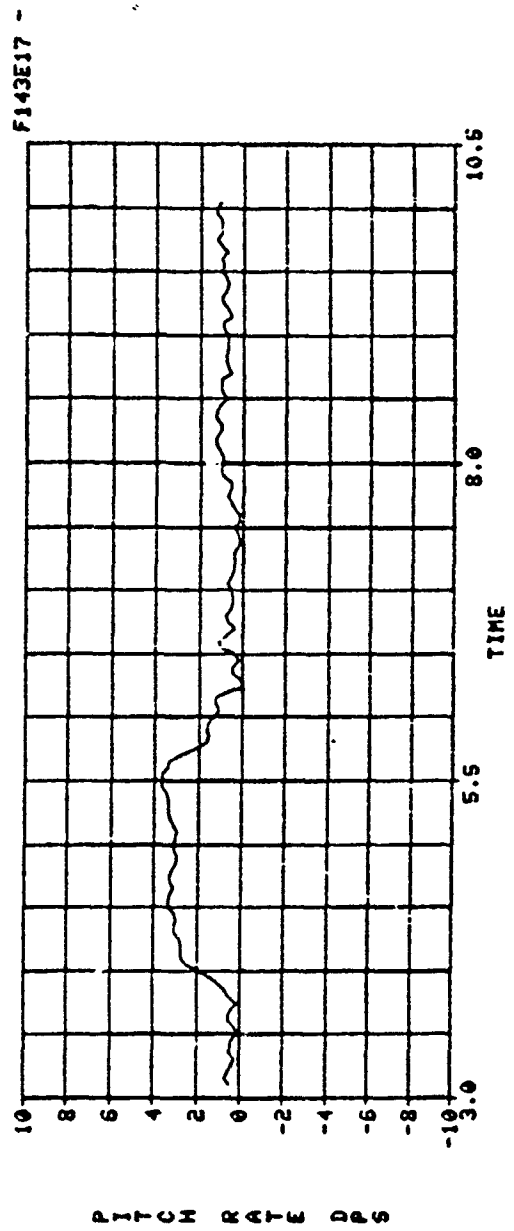
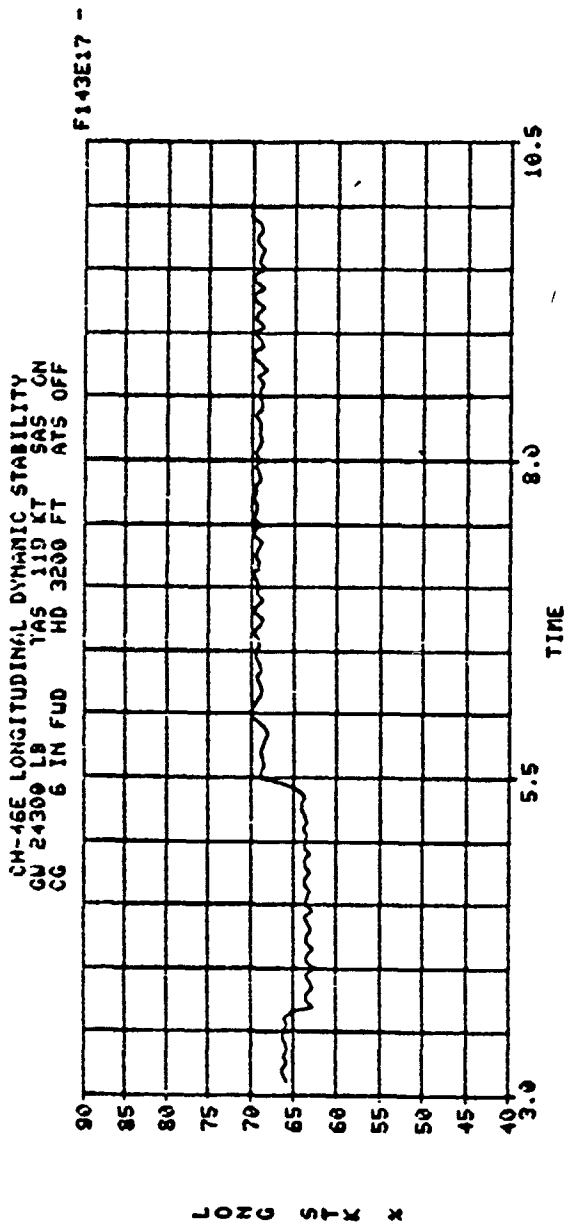


FIGURE 7-1

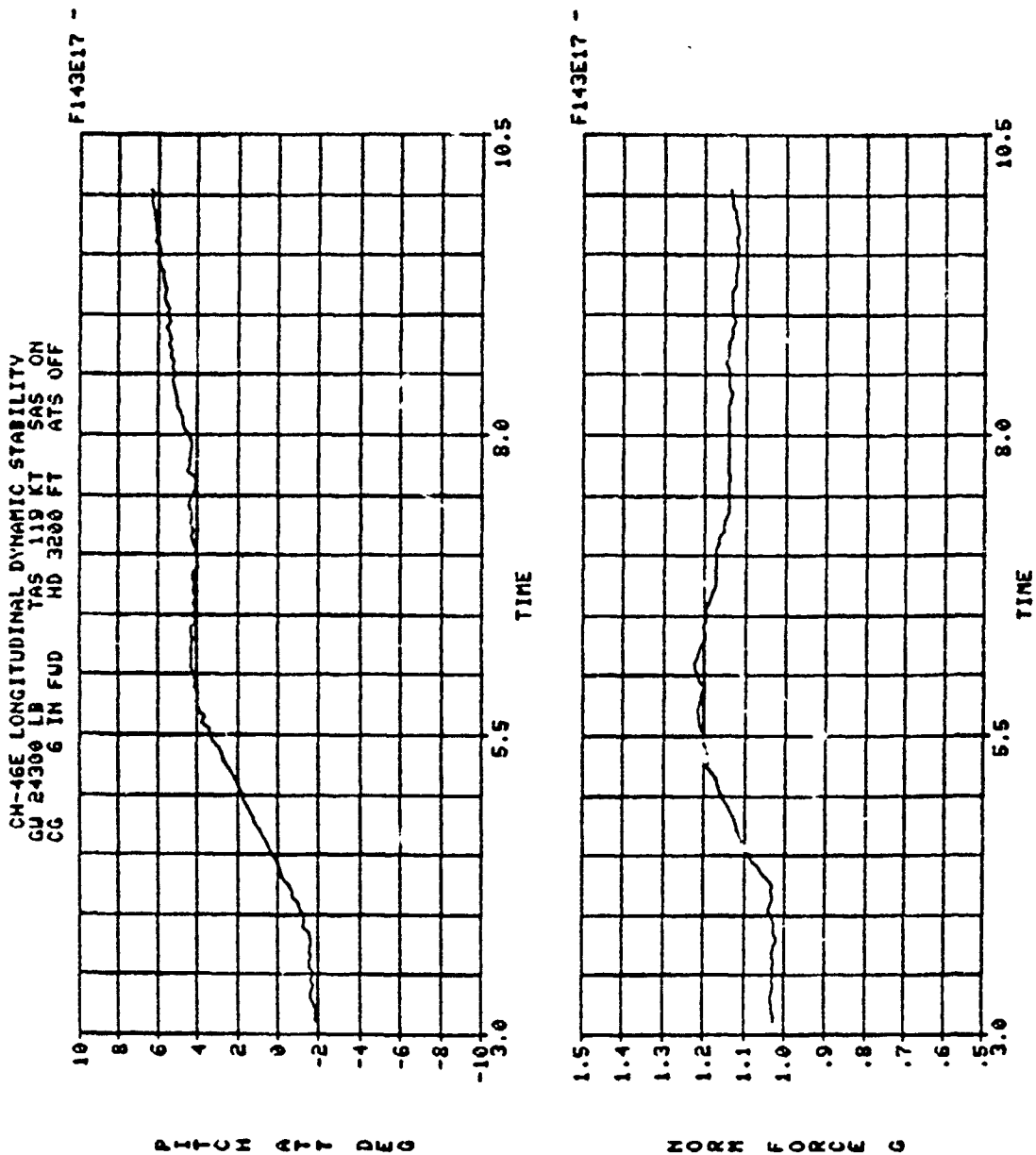


FIGURE 7-2

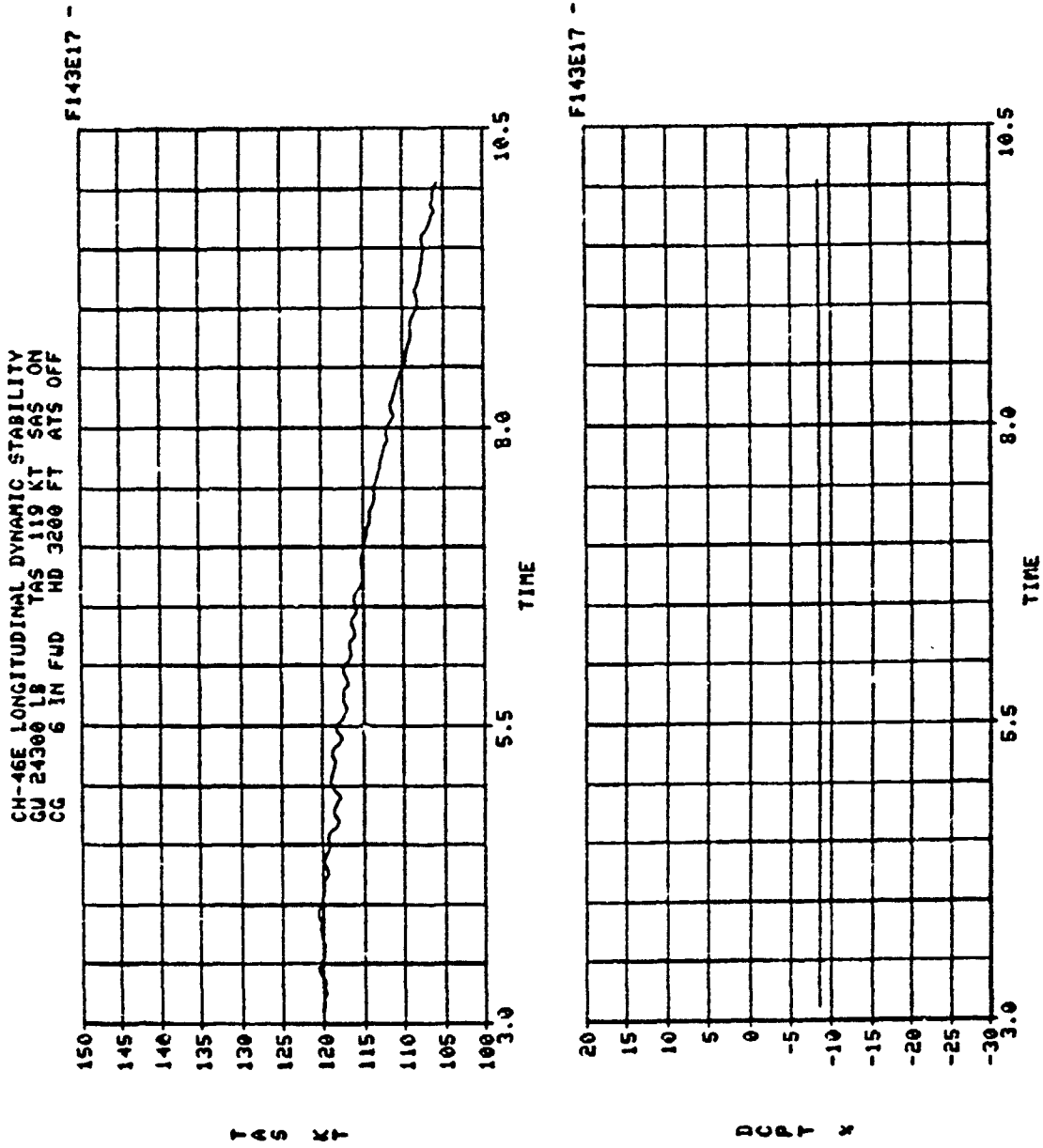


FIGURE 7-3

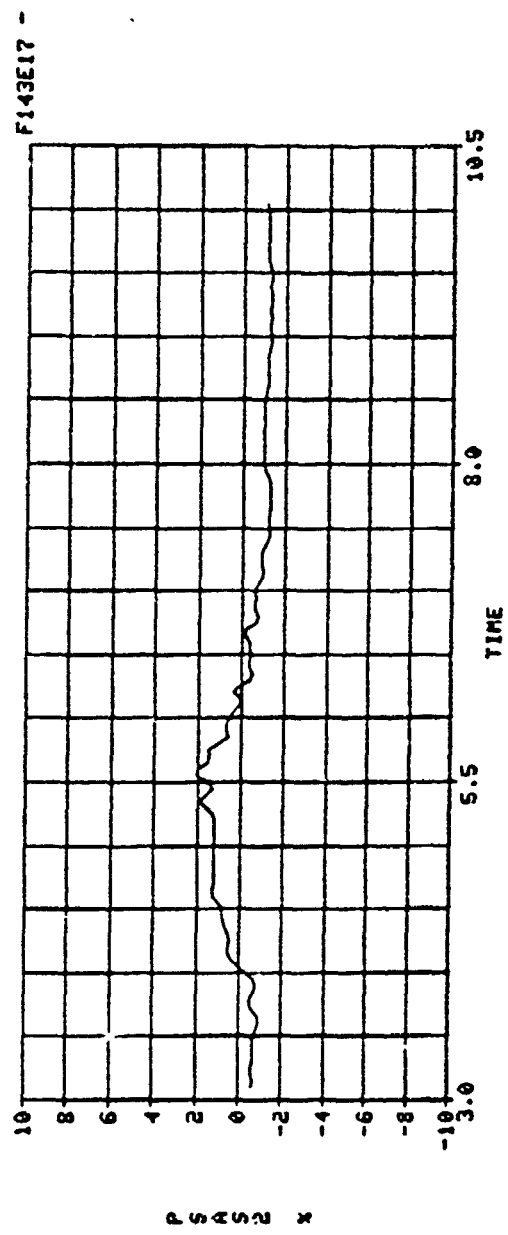
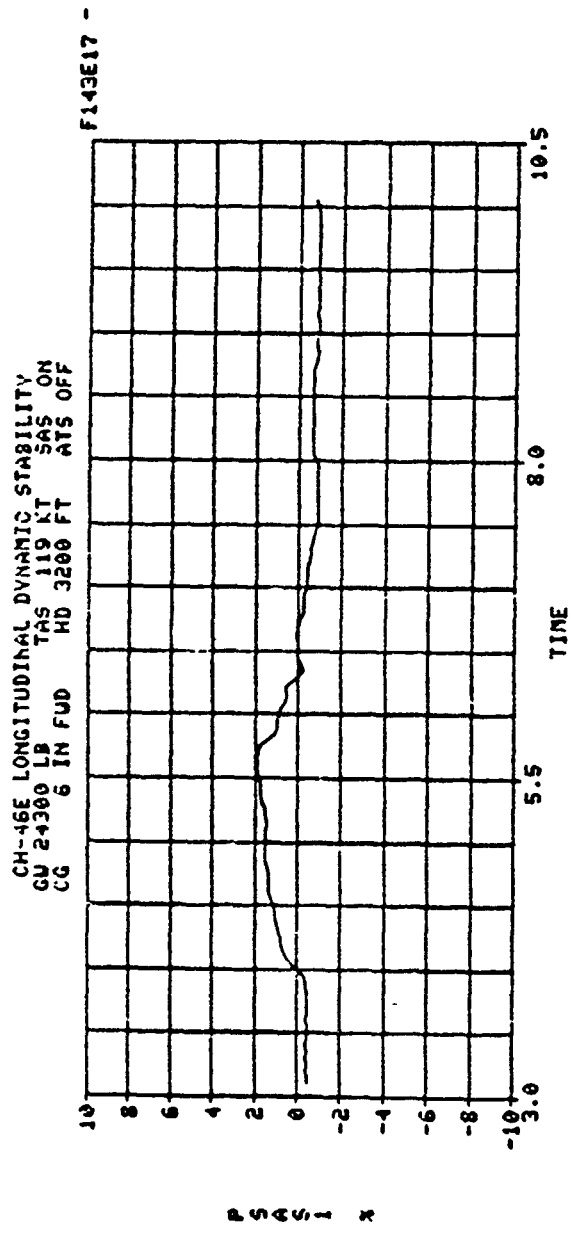


FIGURE 7-4

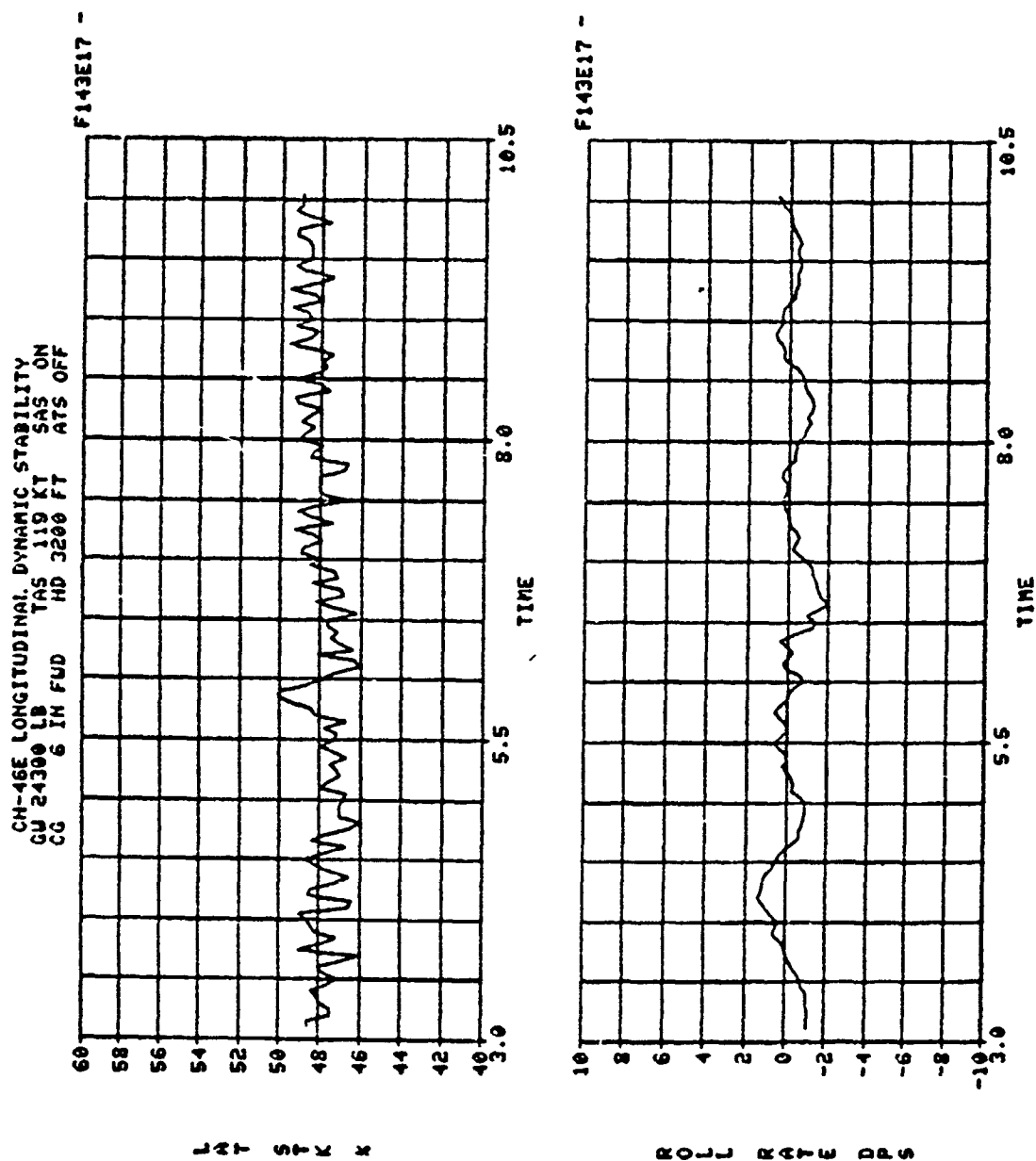


FIGURE 7-5

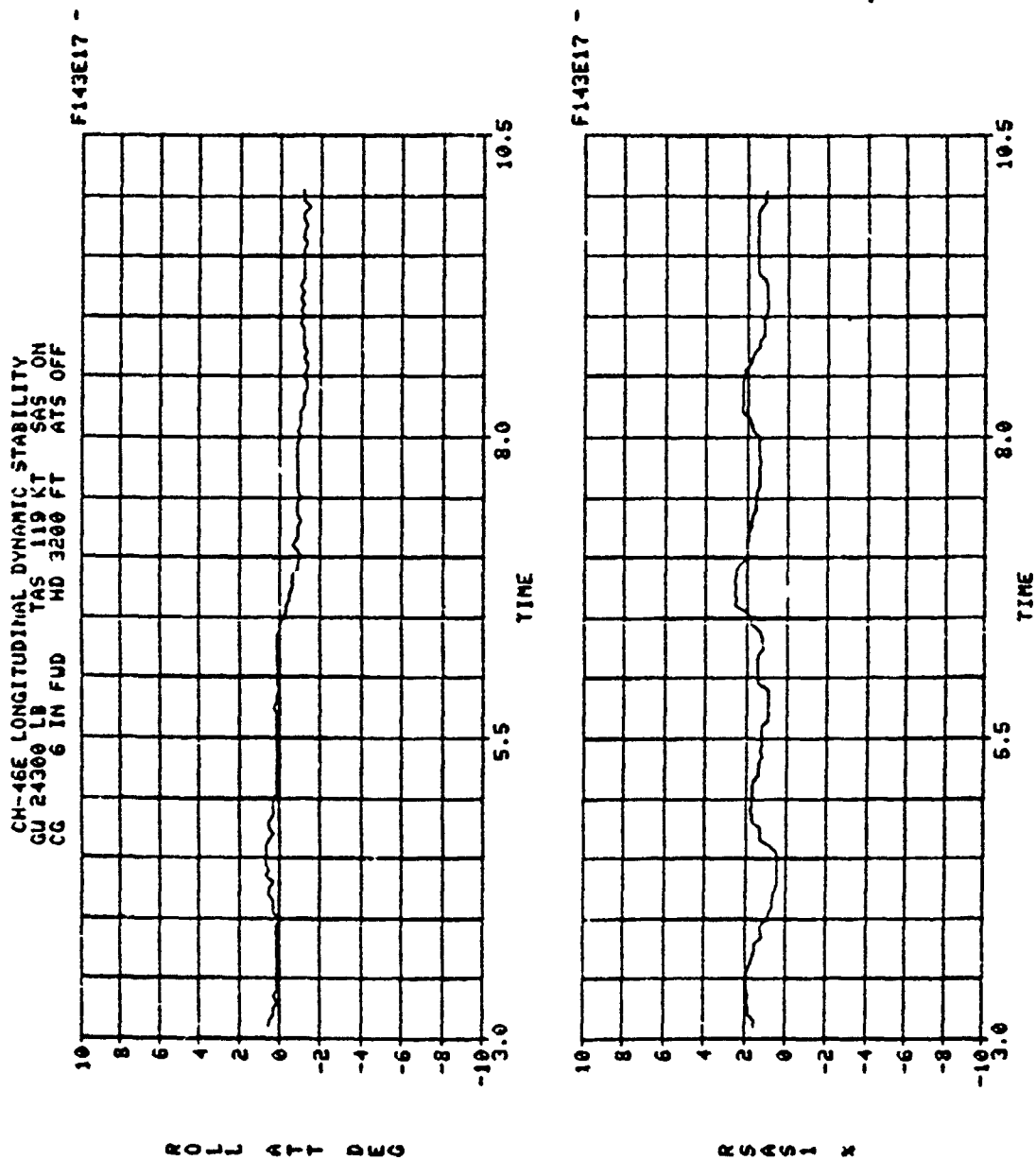


FIGURE 7-6

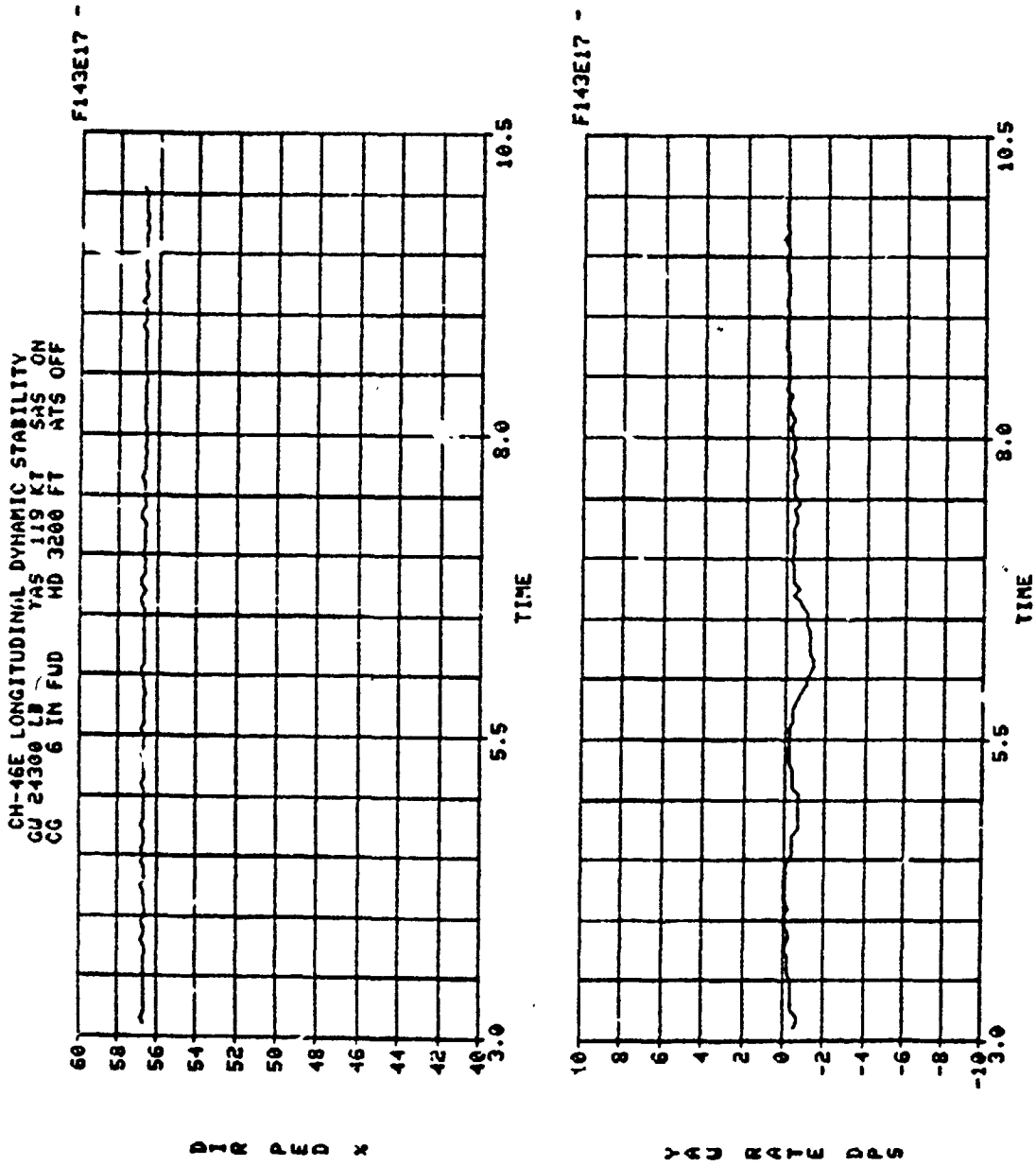


FIGURE 7-7

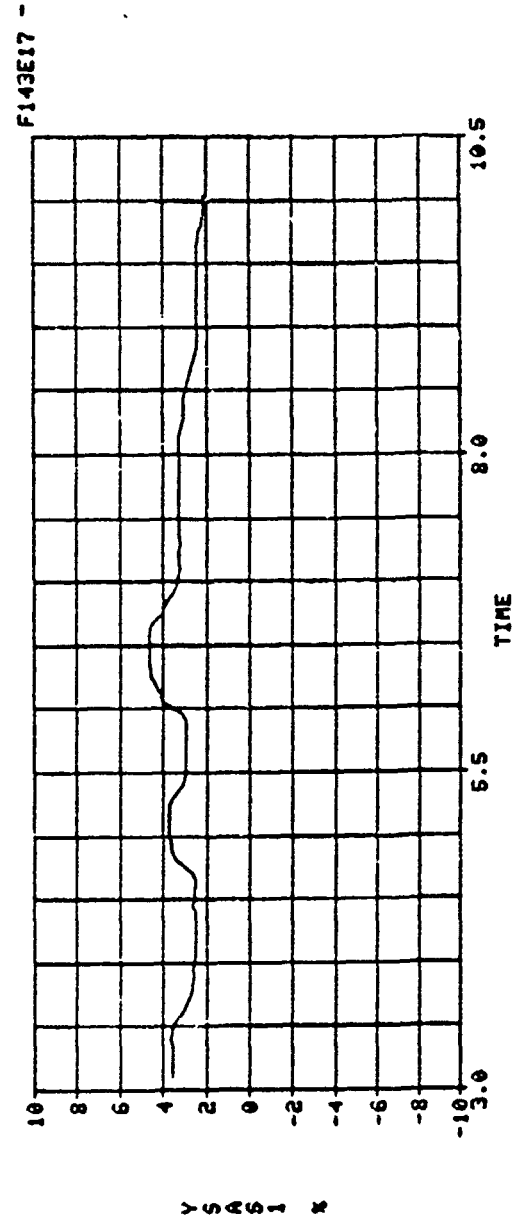
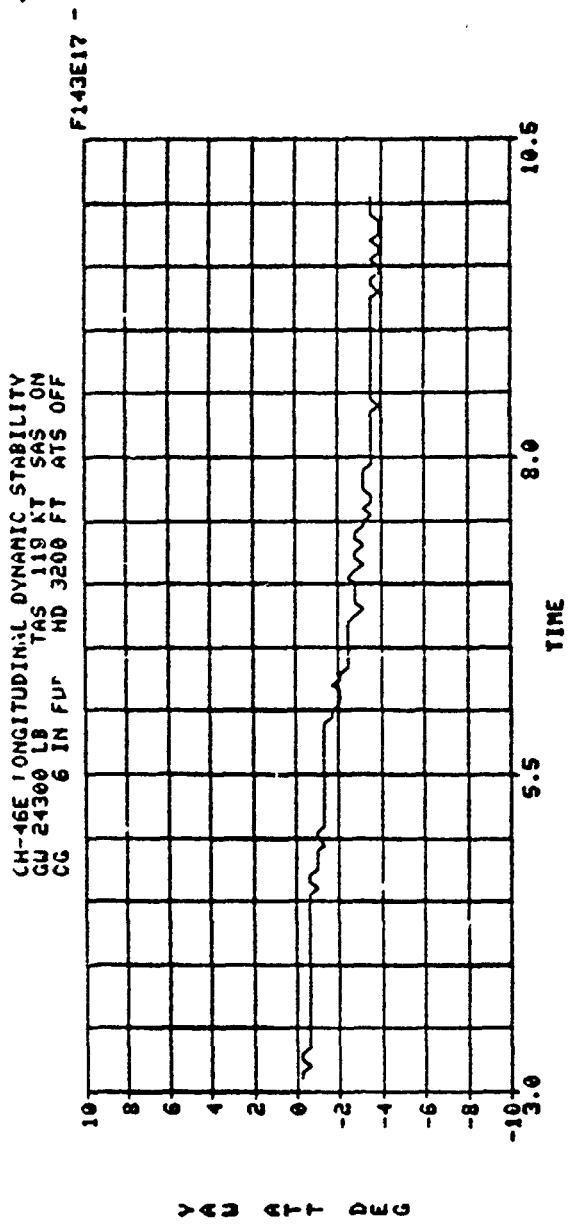


FIGURE 7-8

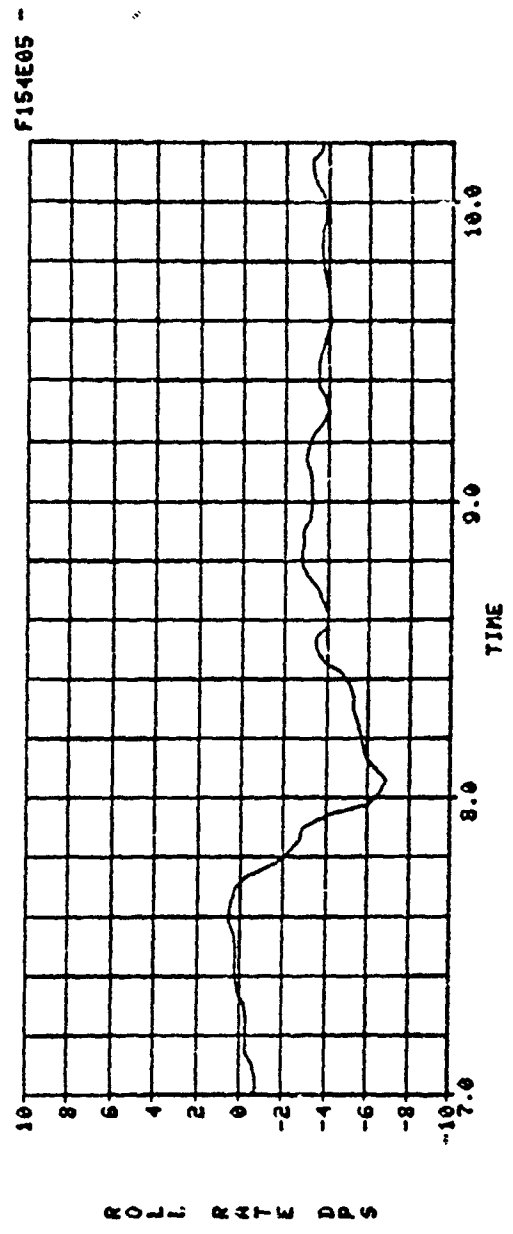
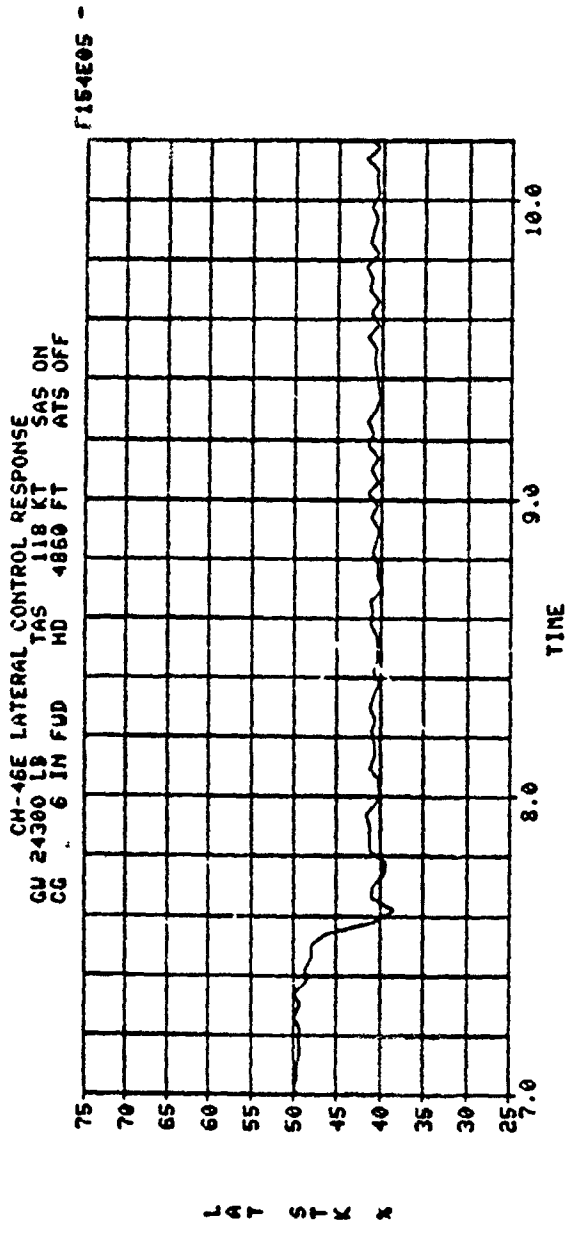


FIGURE 7-9

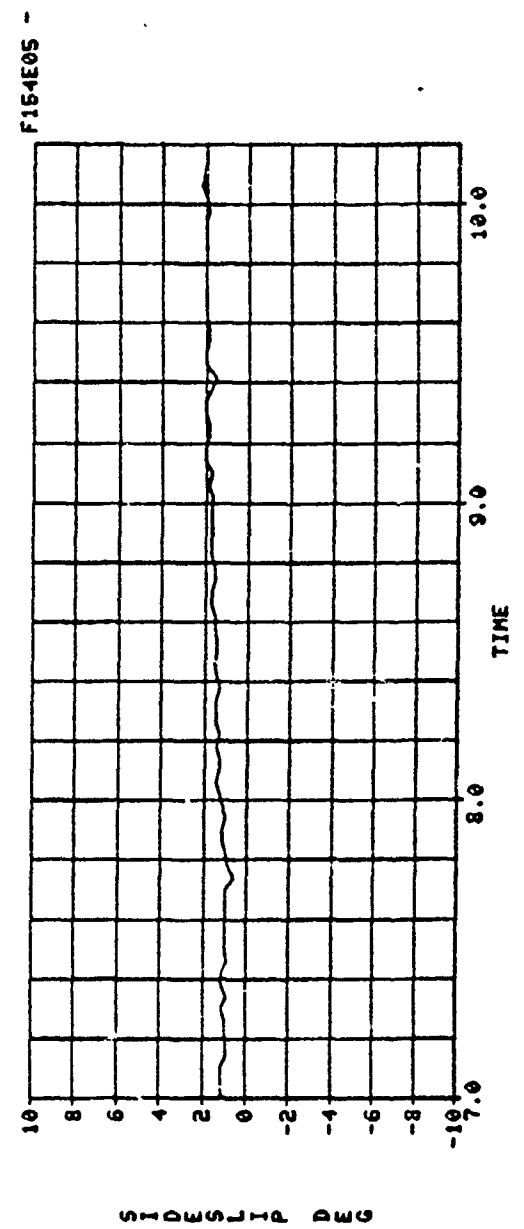
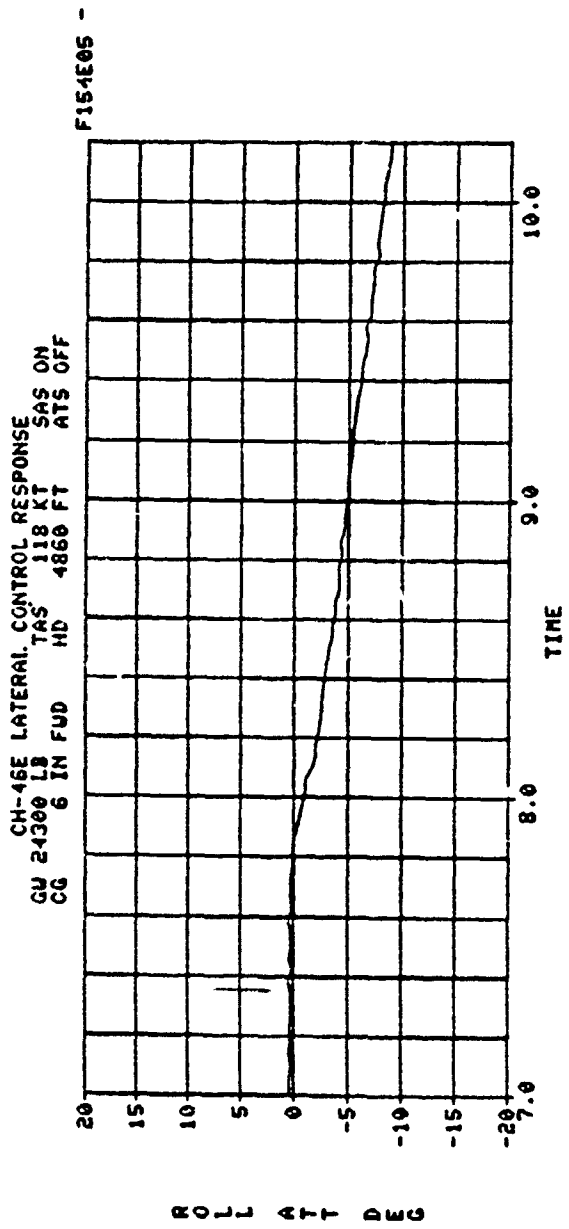


FIGURE 7-10

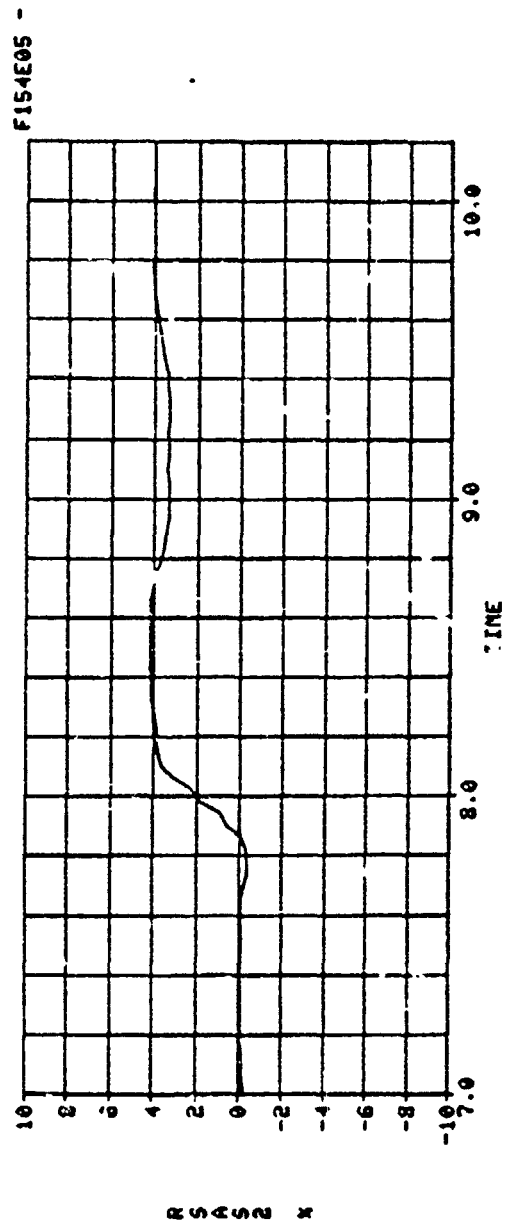
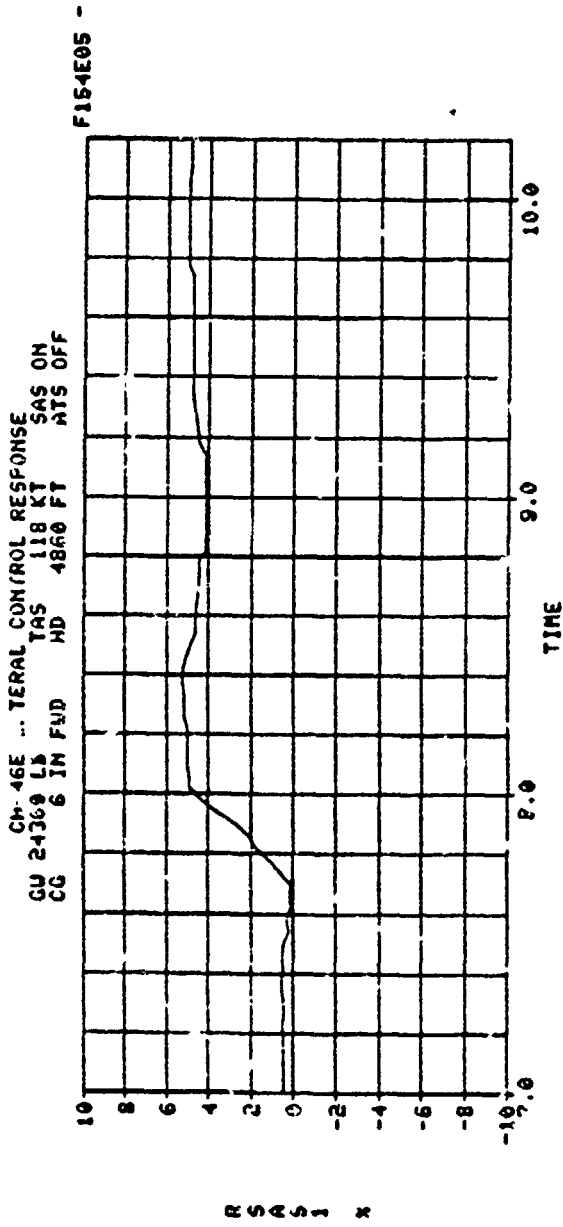


FIGURE 7-11

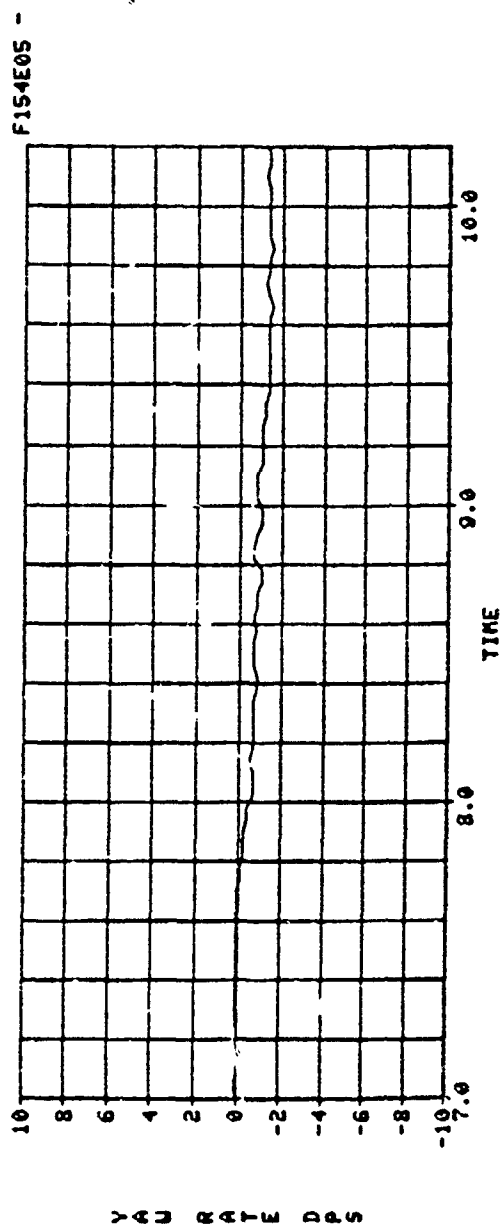
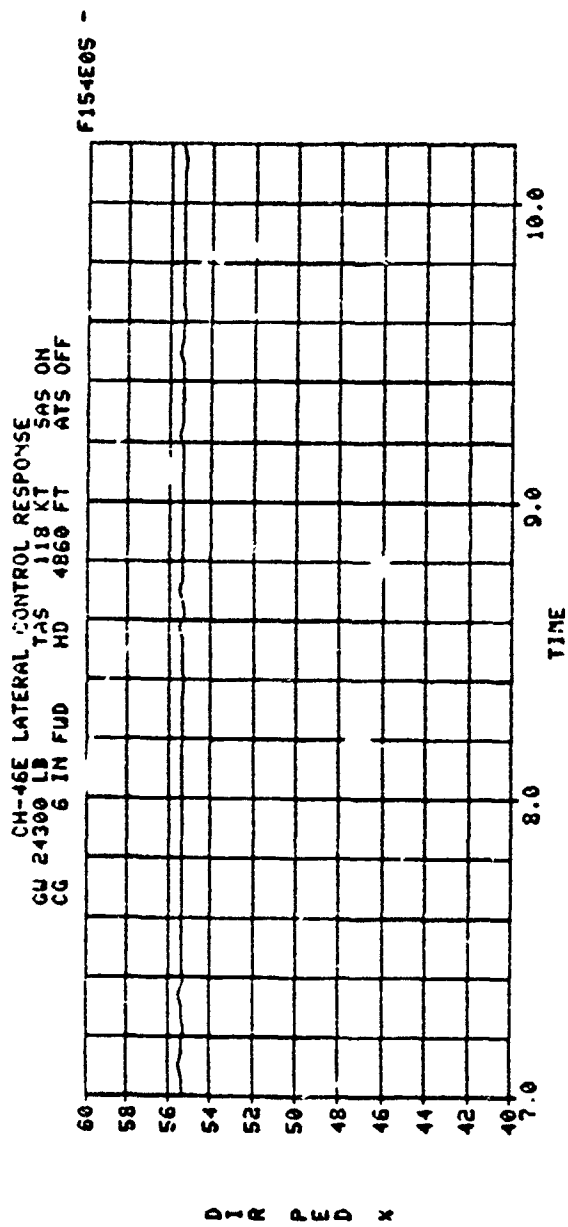


FIGURE 7-12

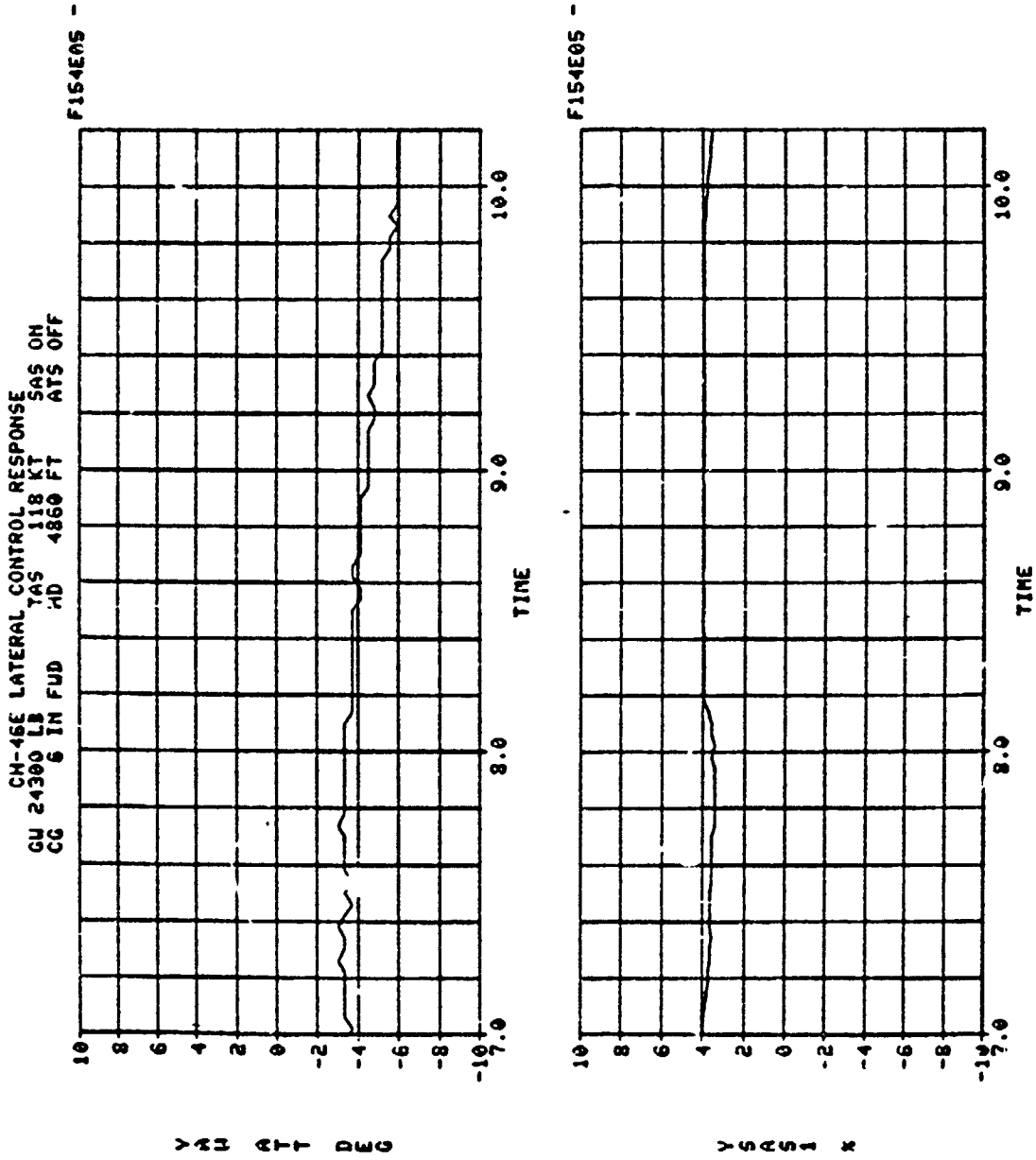


FIGURE 7-13

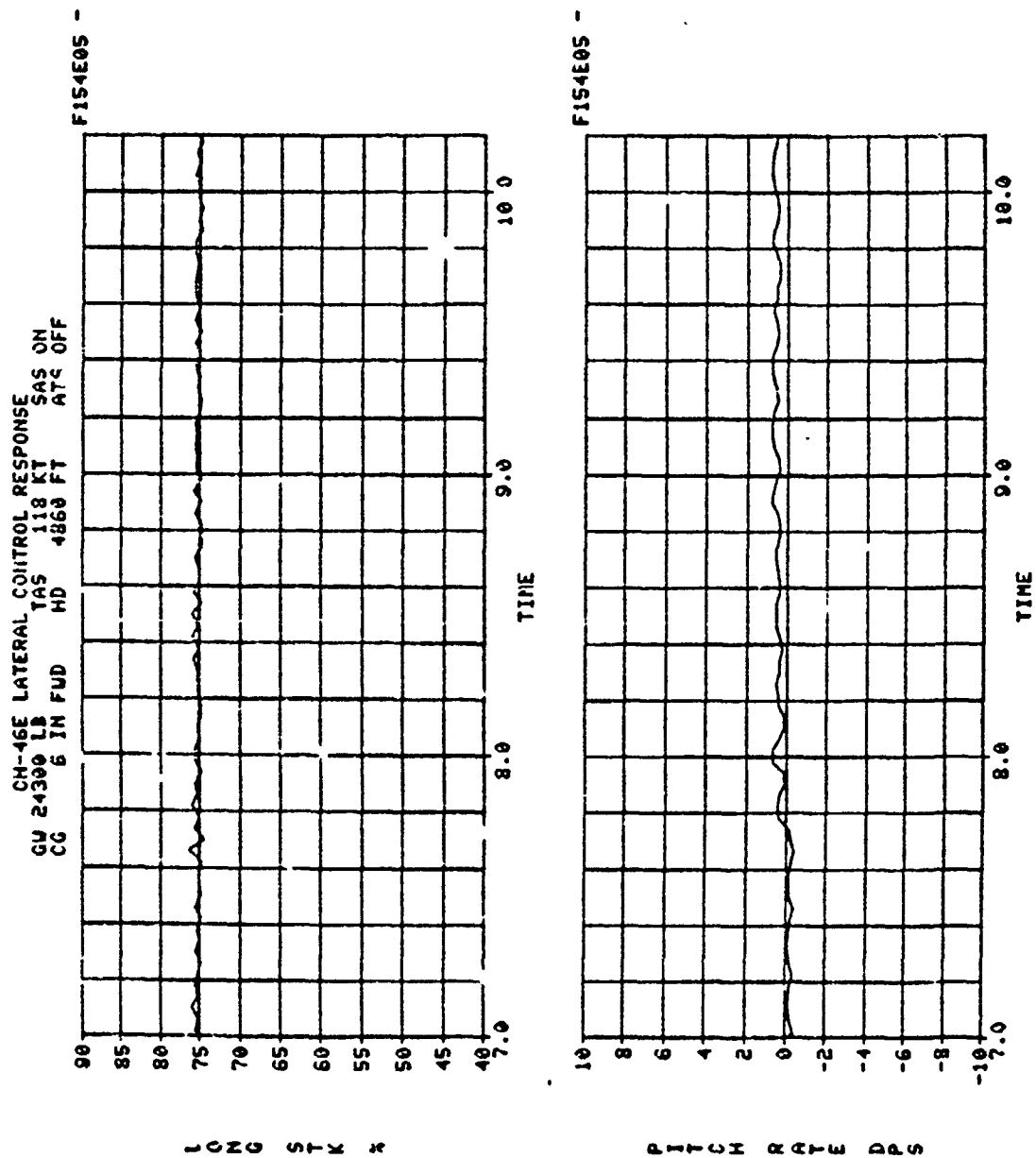


FIGURE 7-14

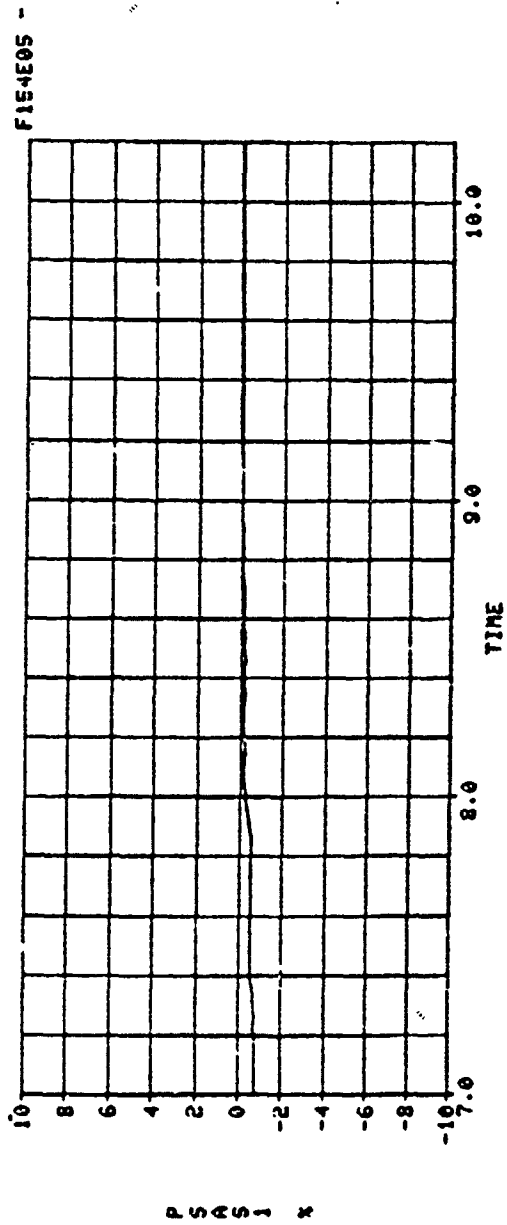
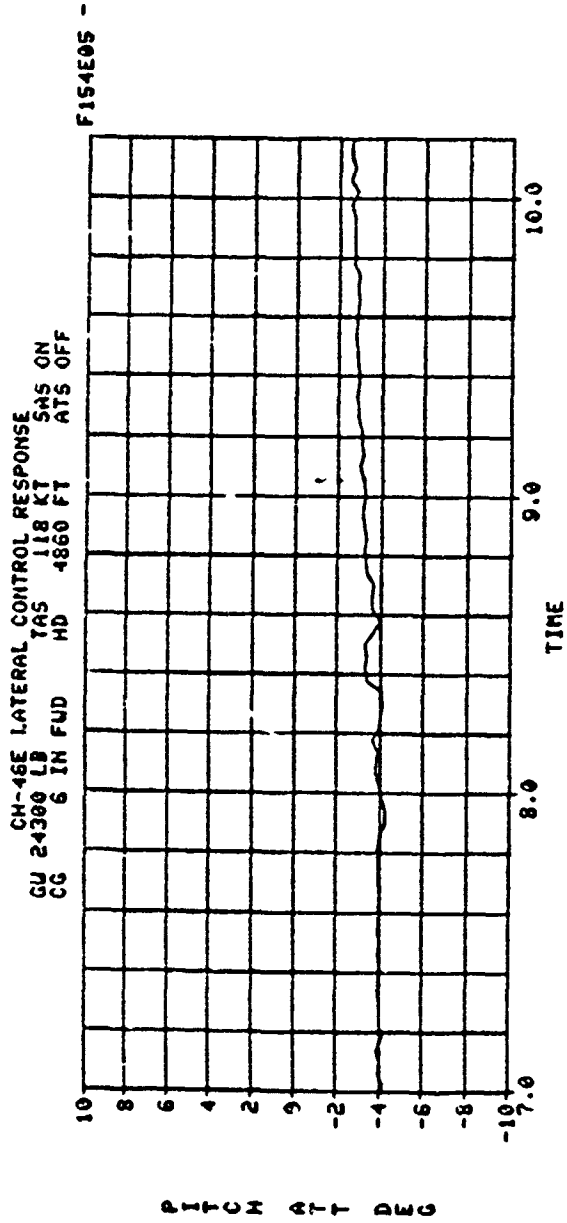


FIGURE 7-15

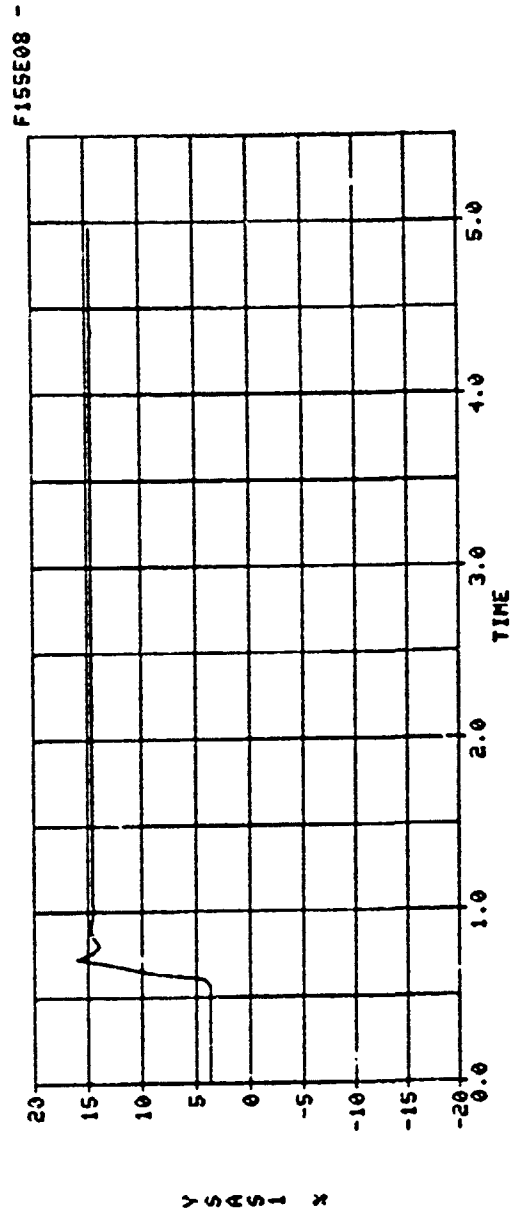
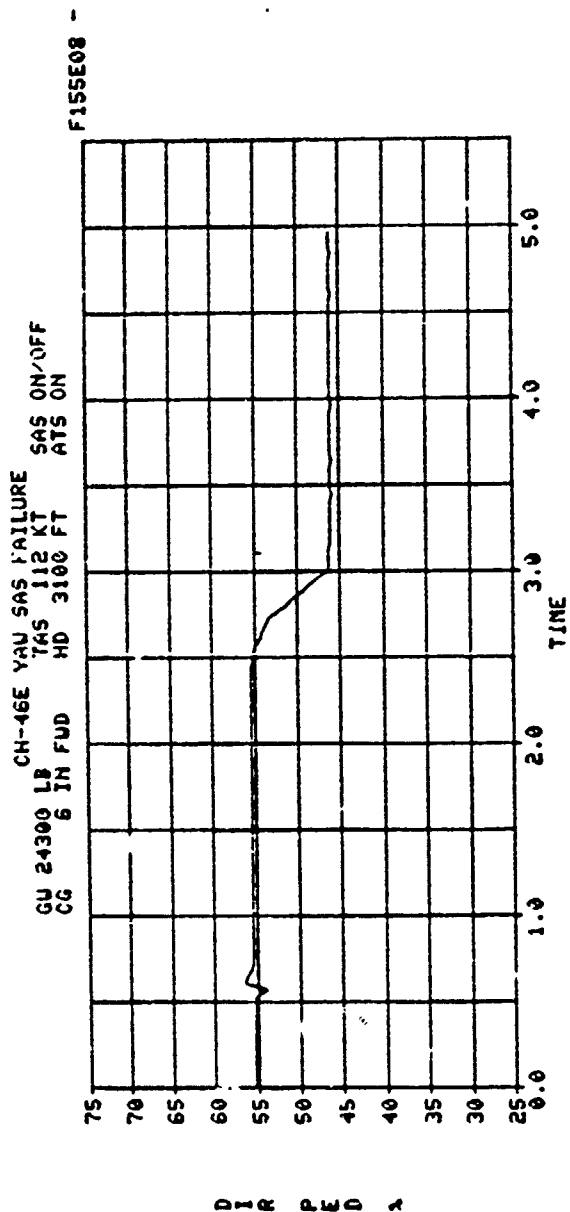


FIGURE 7-16

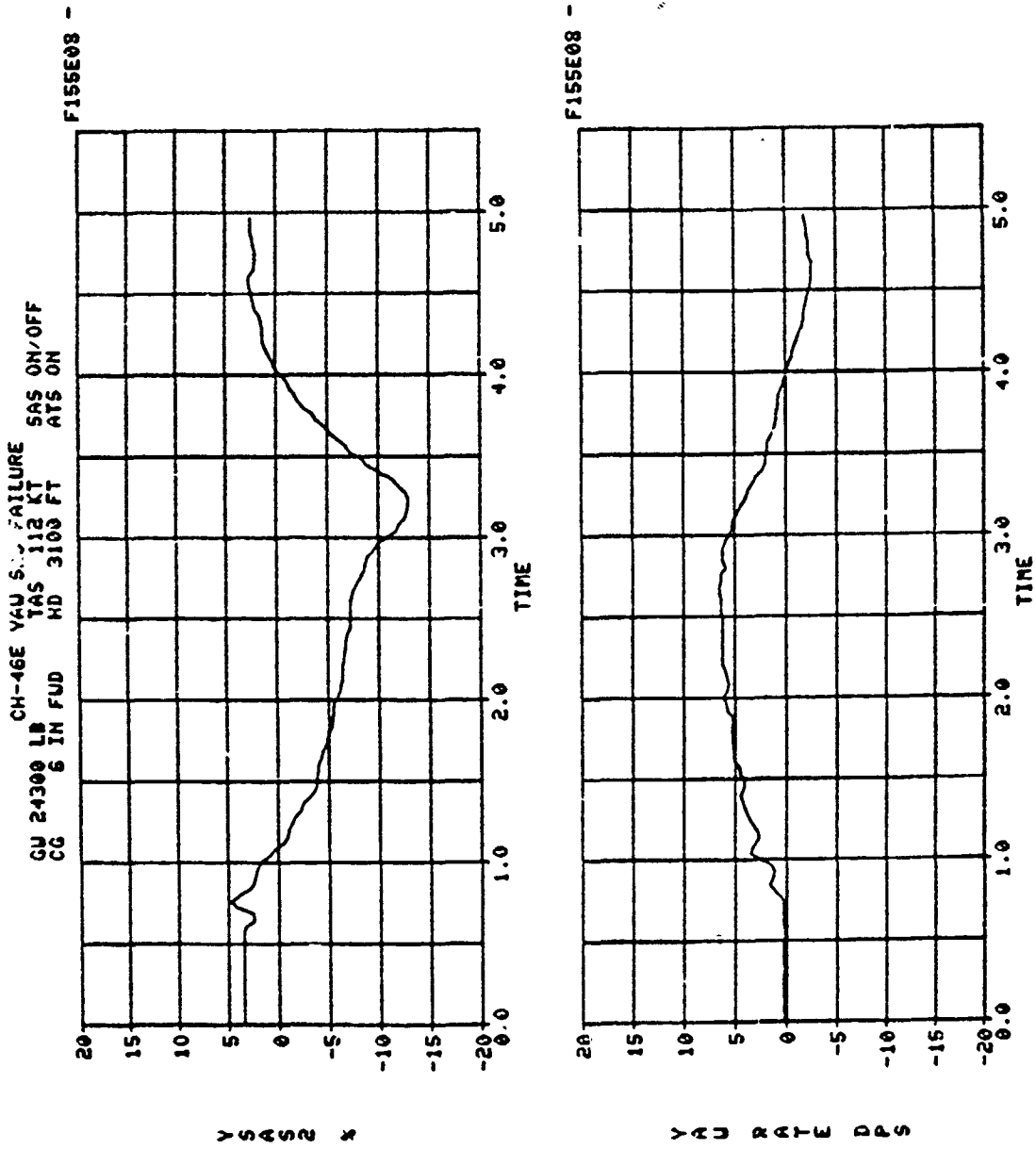


FIGURE 7-17

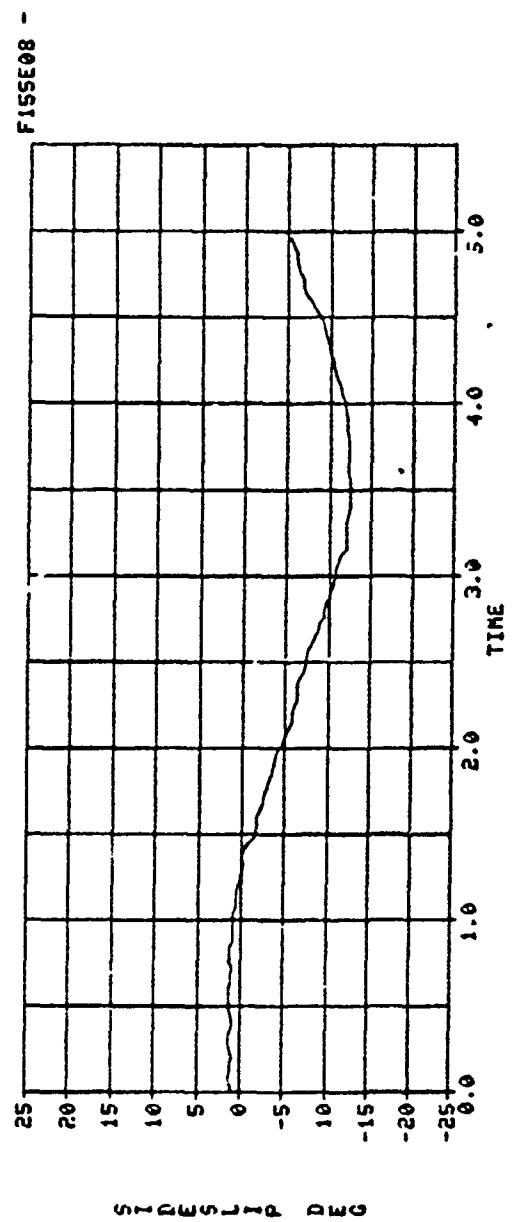
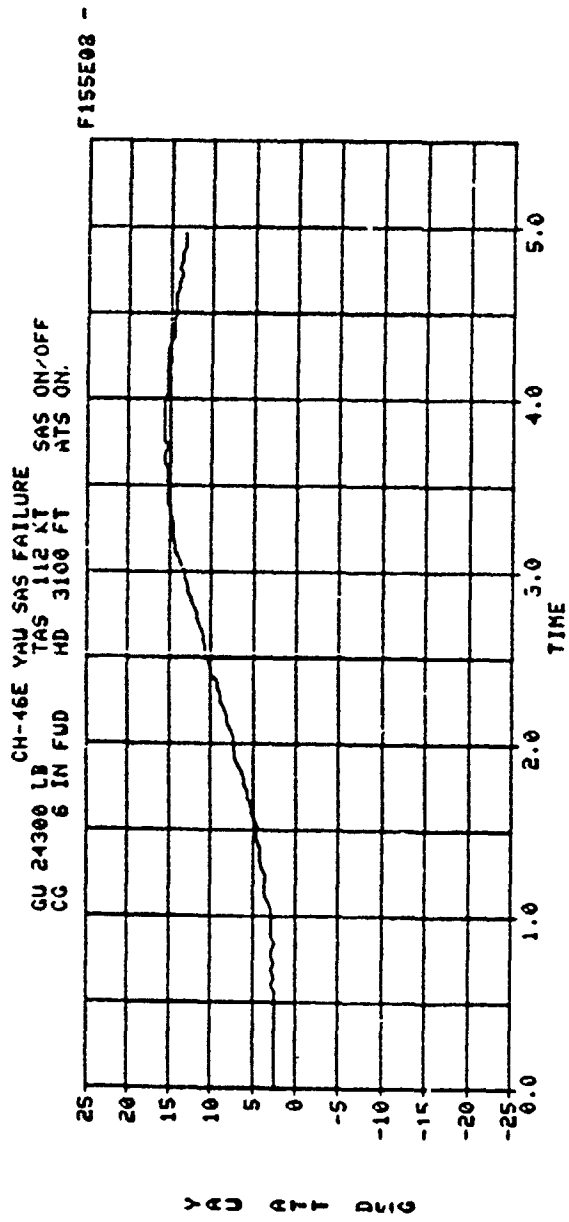


FIGURE 7-18

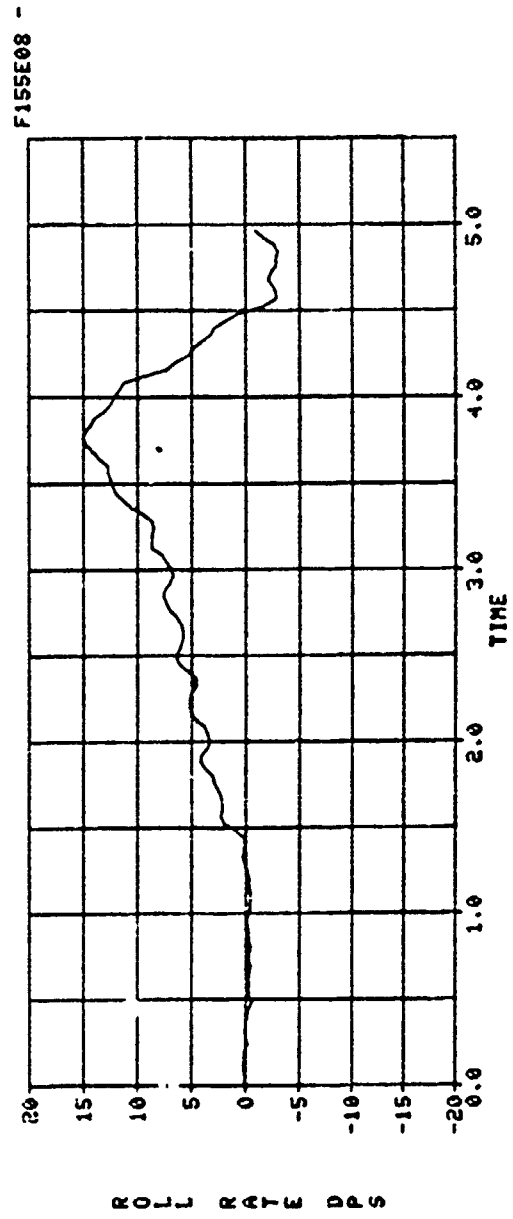
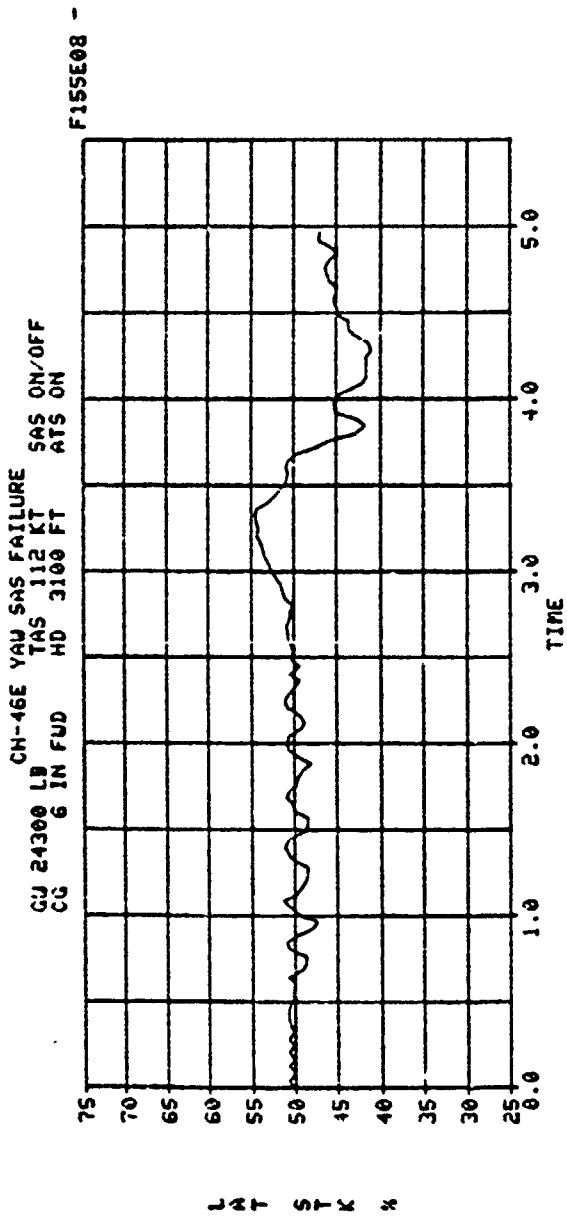


FIGURE 7-19

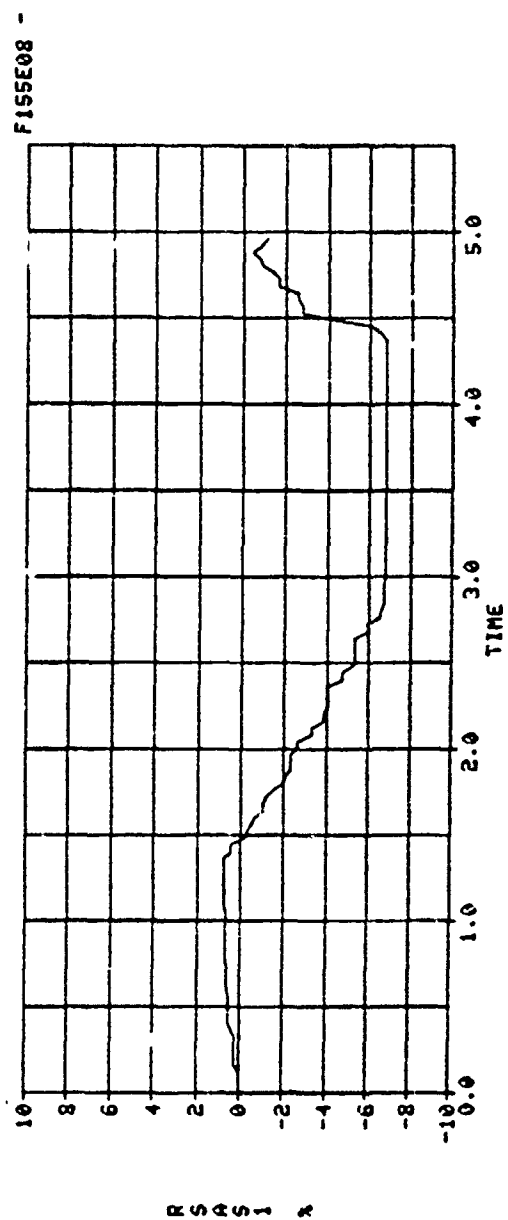
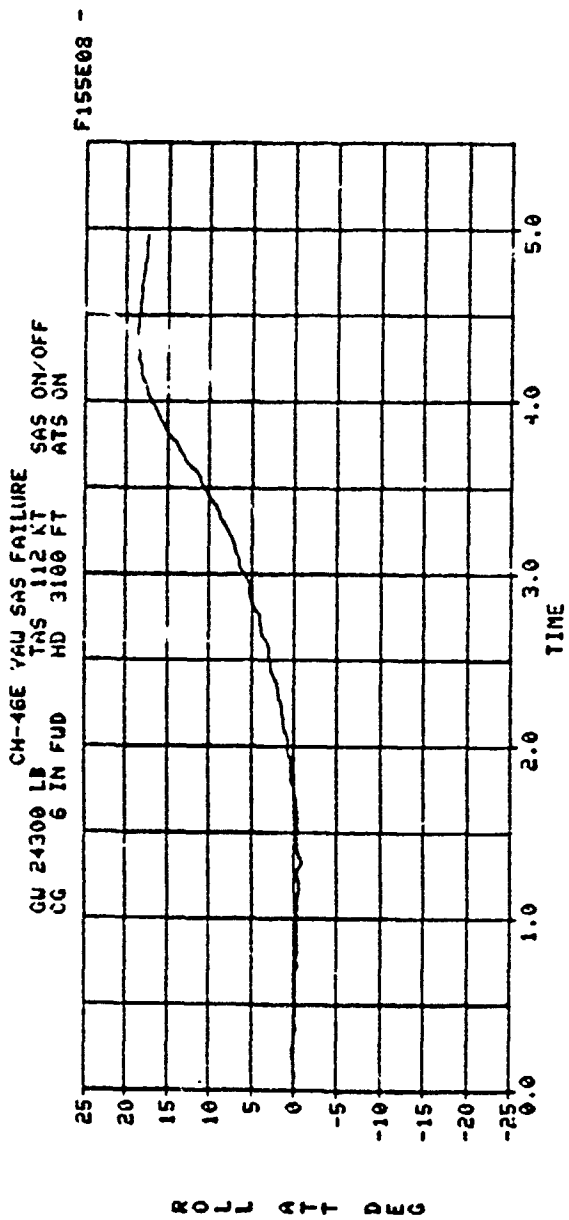


FIGURE 7-20

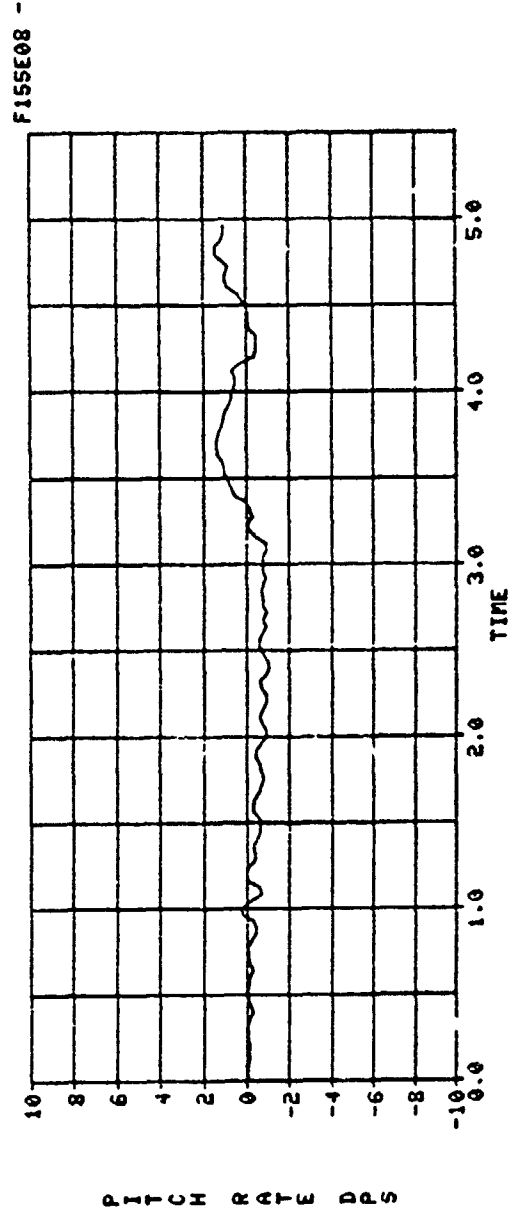
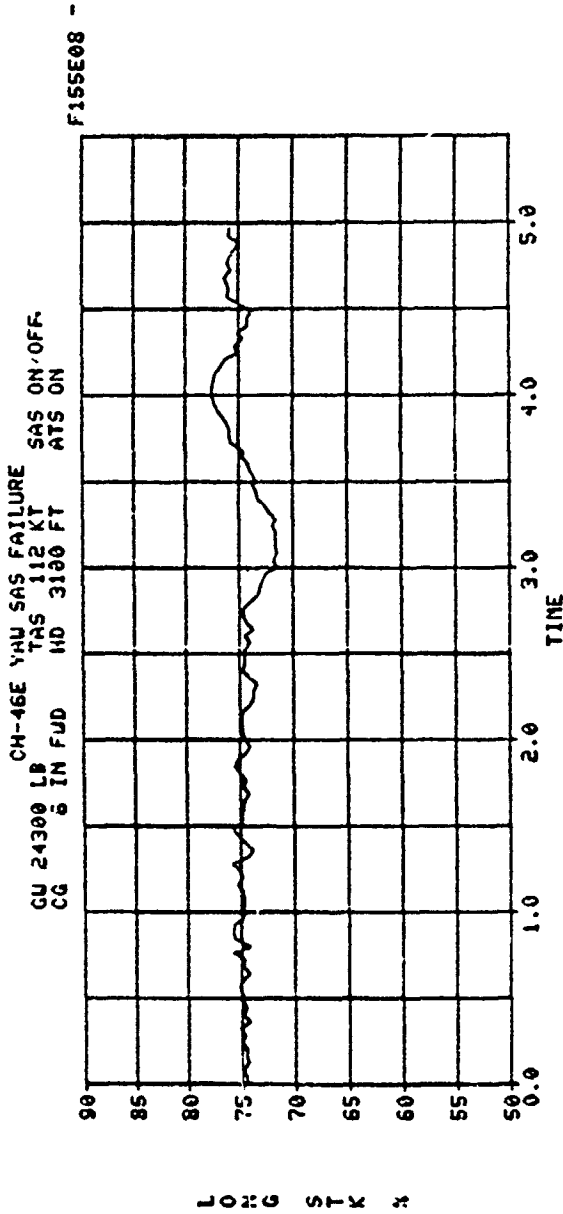


FIGURE 7-21

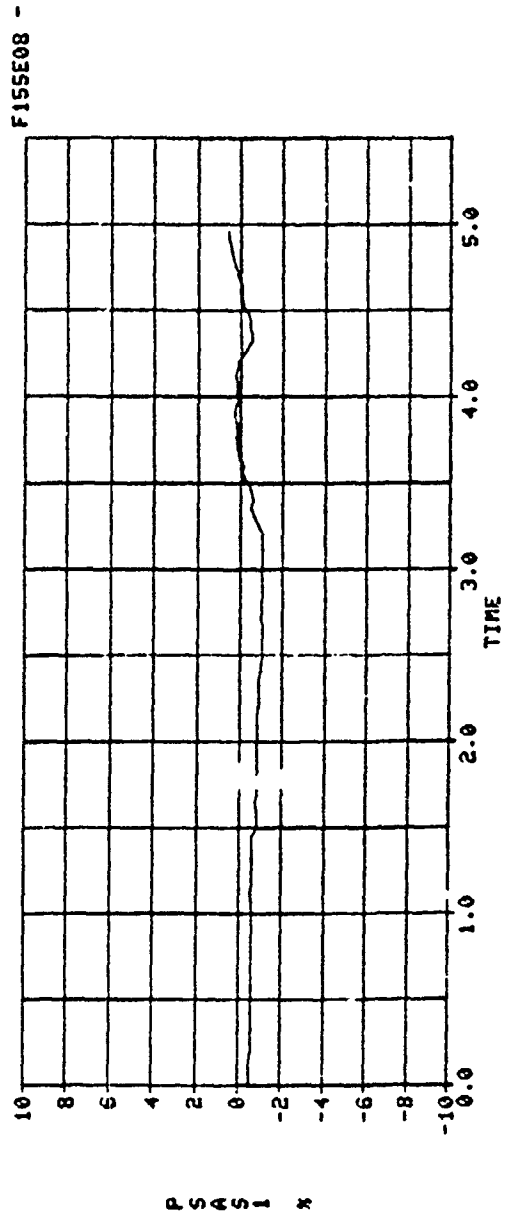
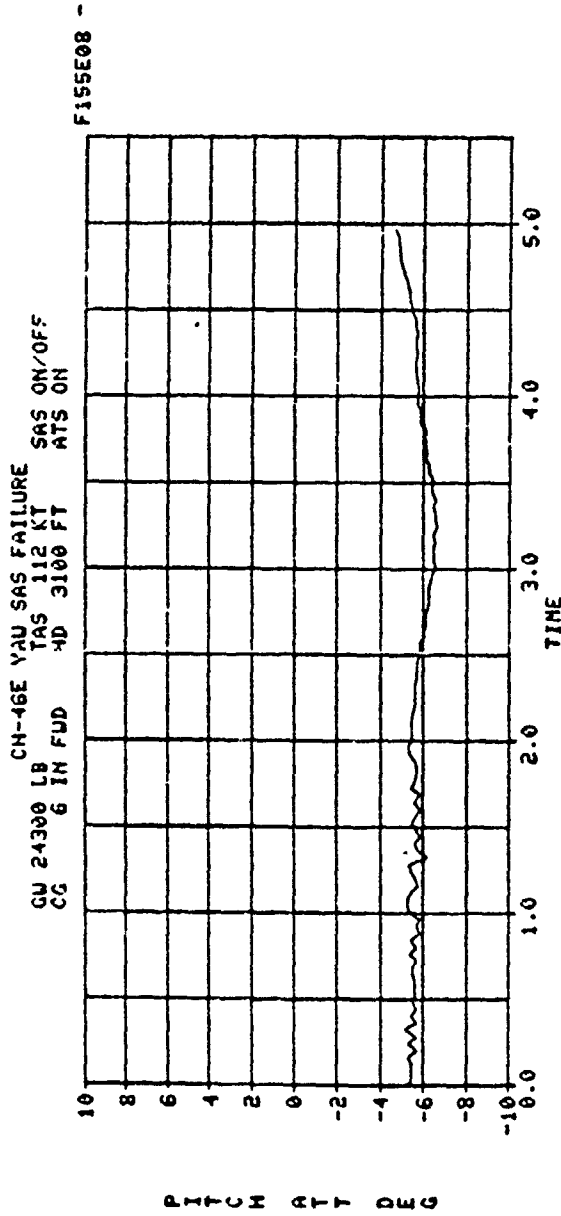


FIGURE 7-22

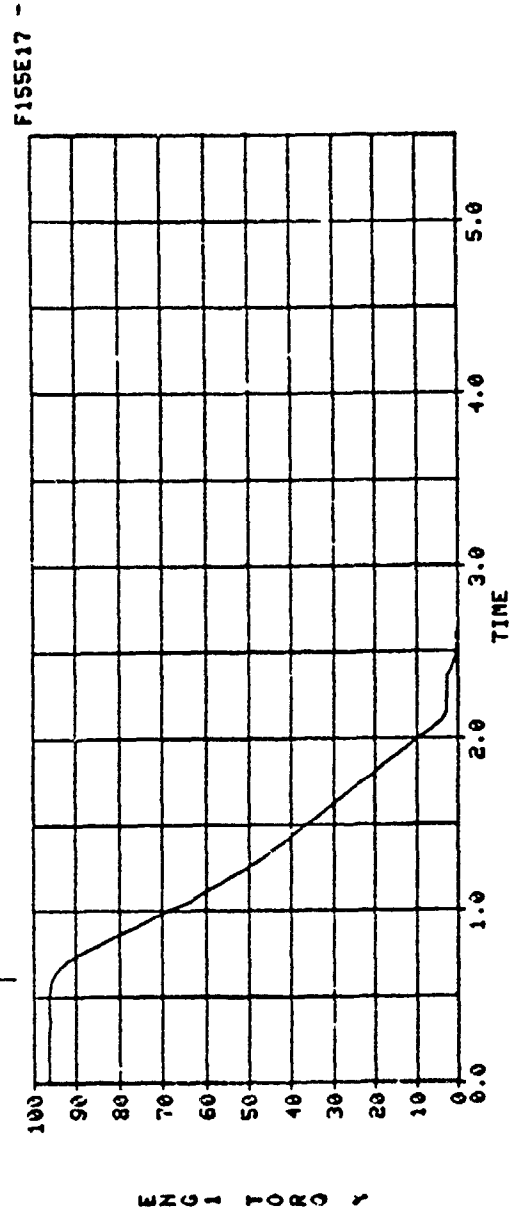
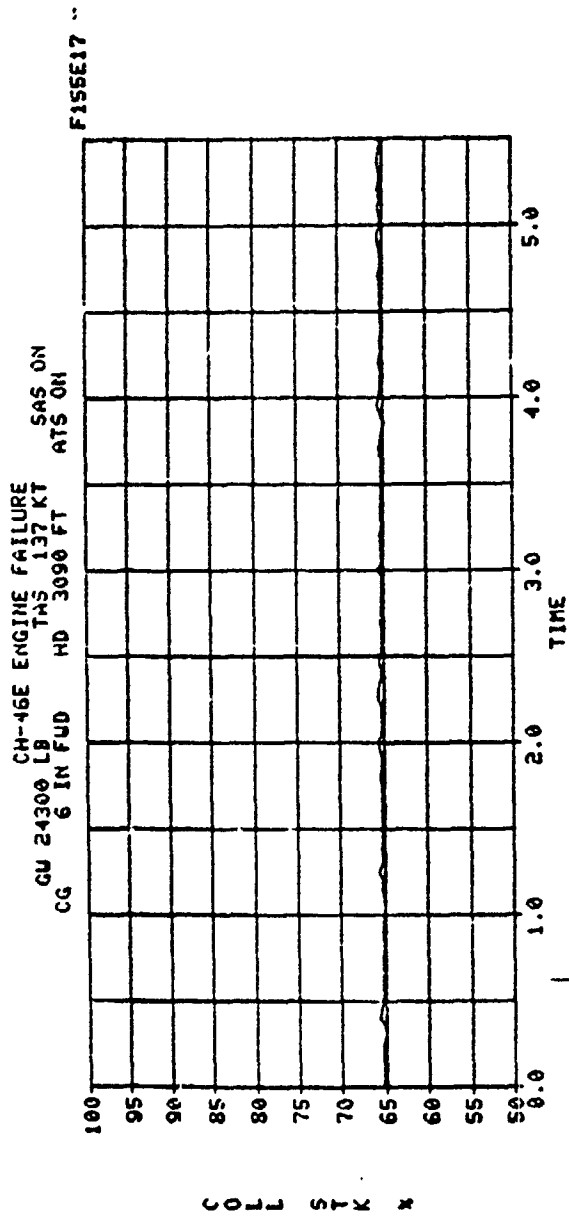


FIGURE 7-23

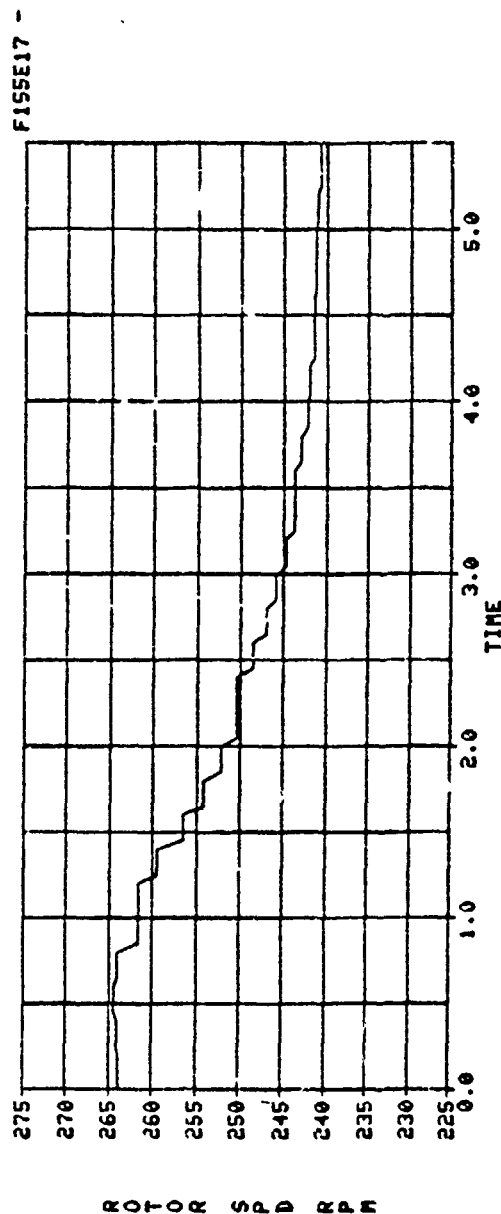
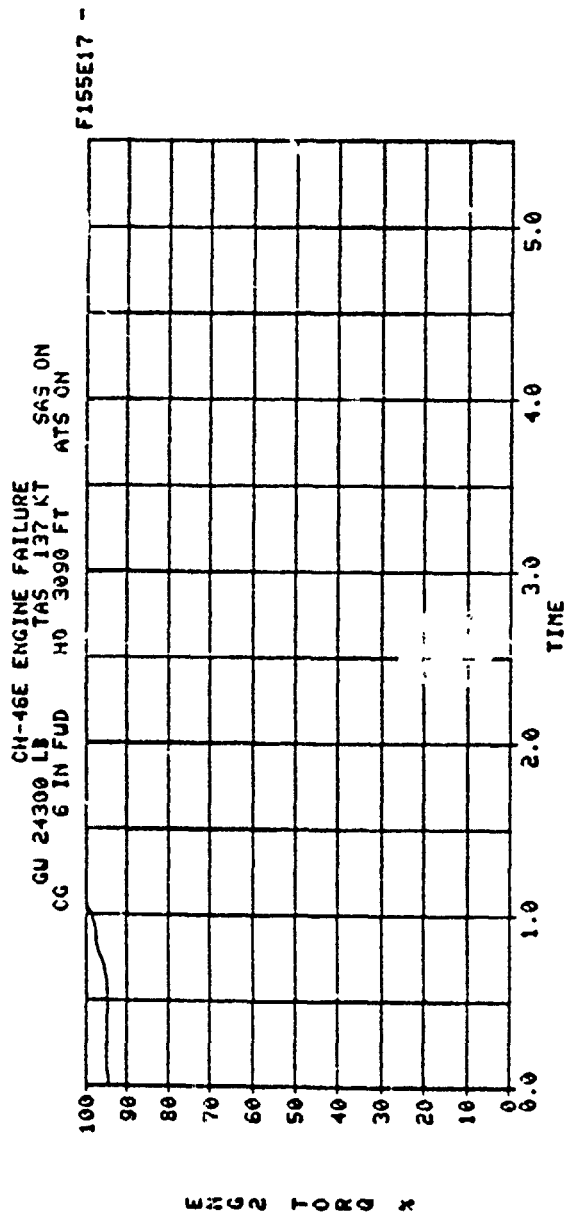


FIGURE 7-24

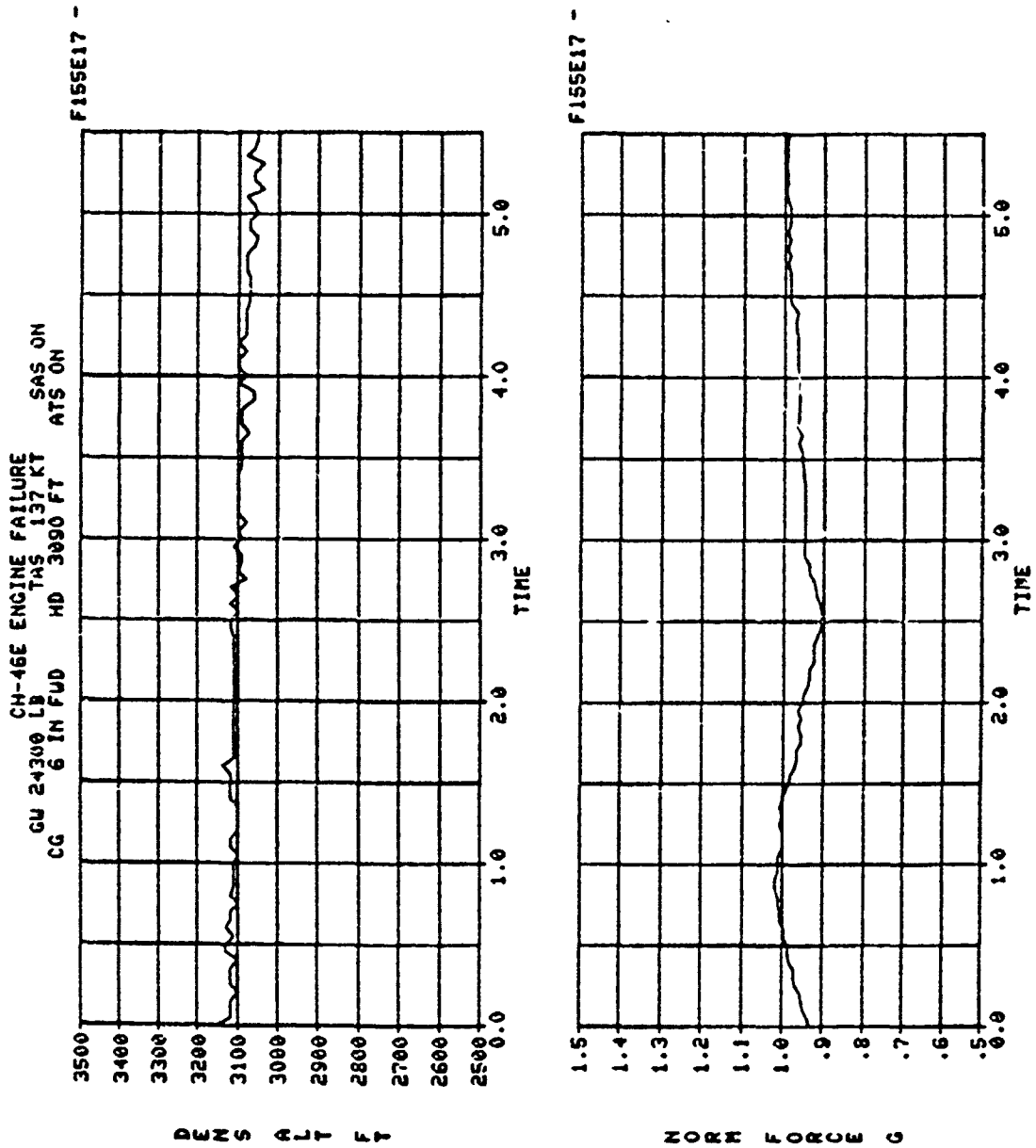


FIGURE 7-25

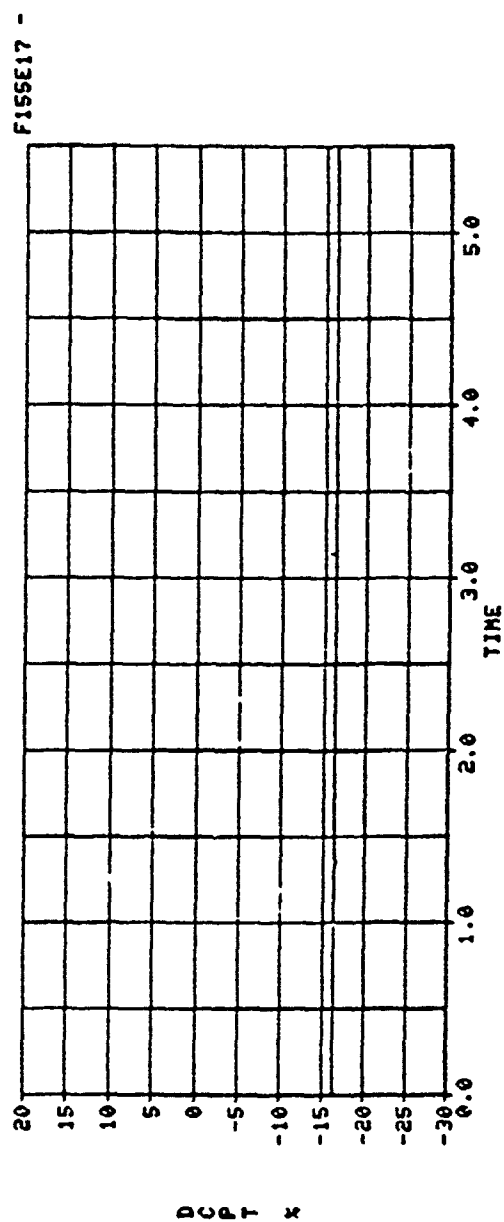
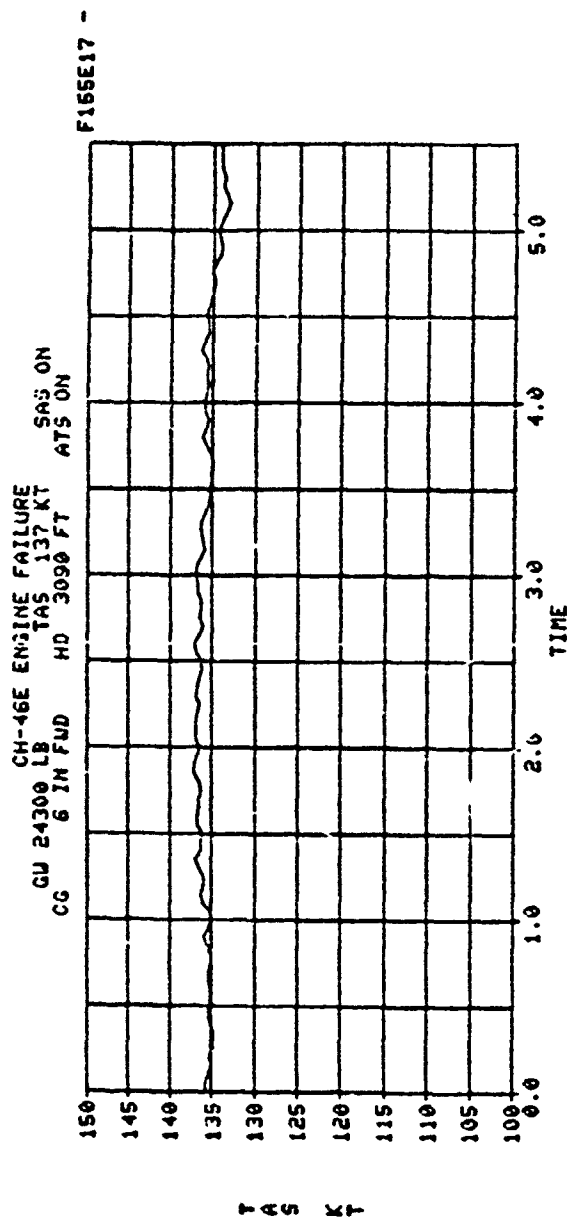


FIGURE 7-26

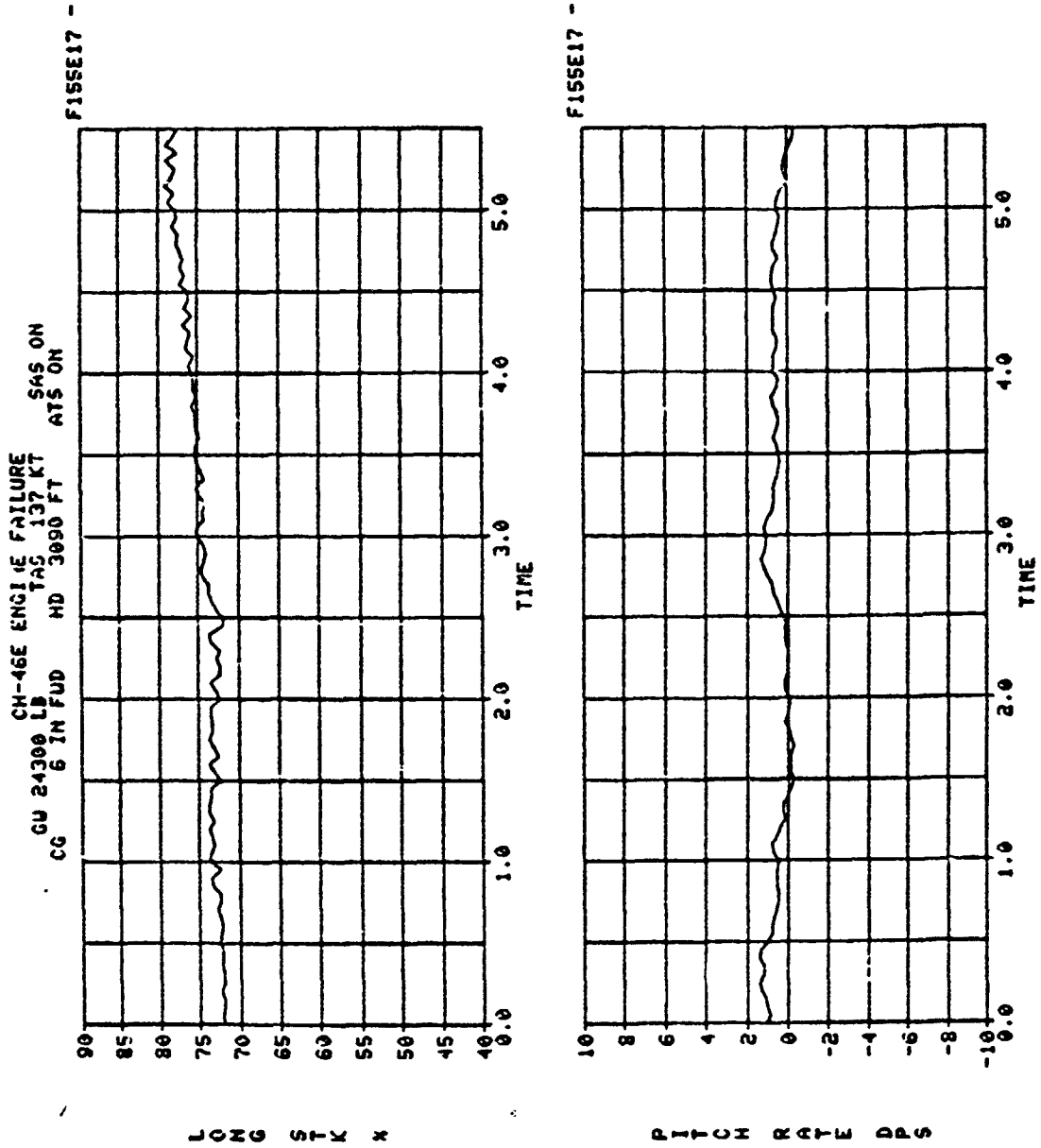


FIGURE 7-27

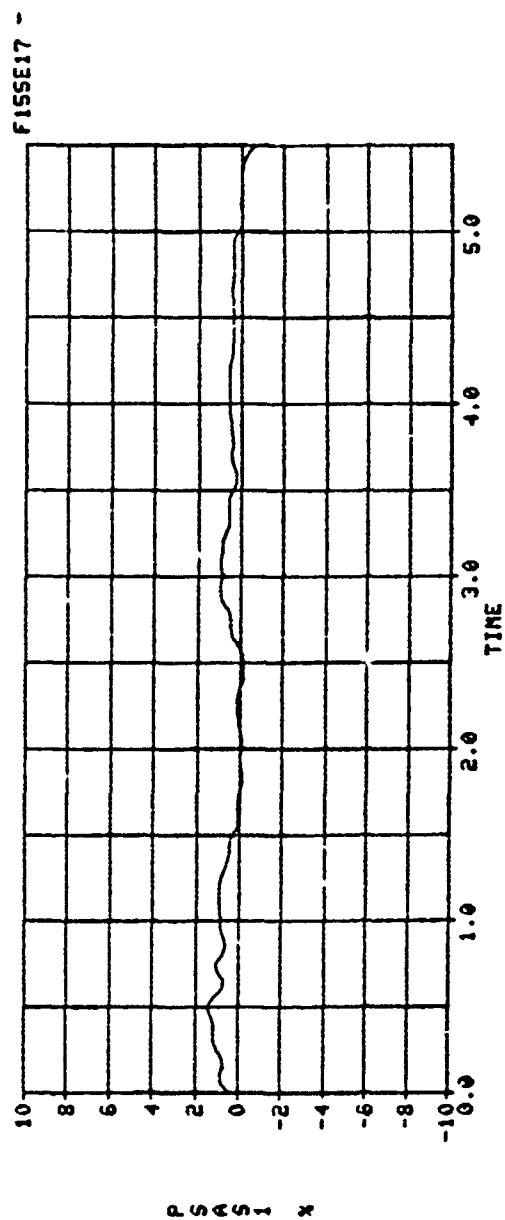
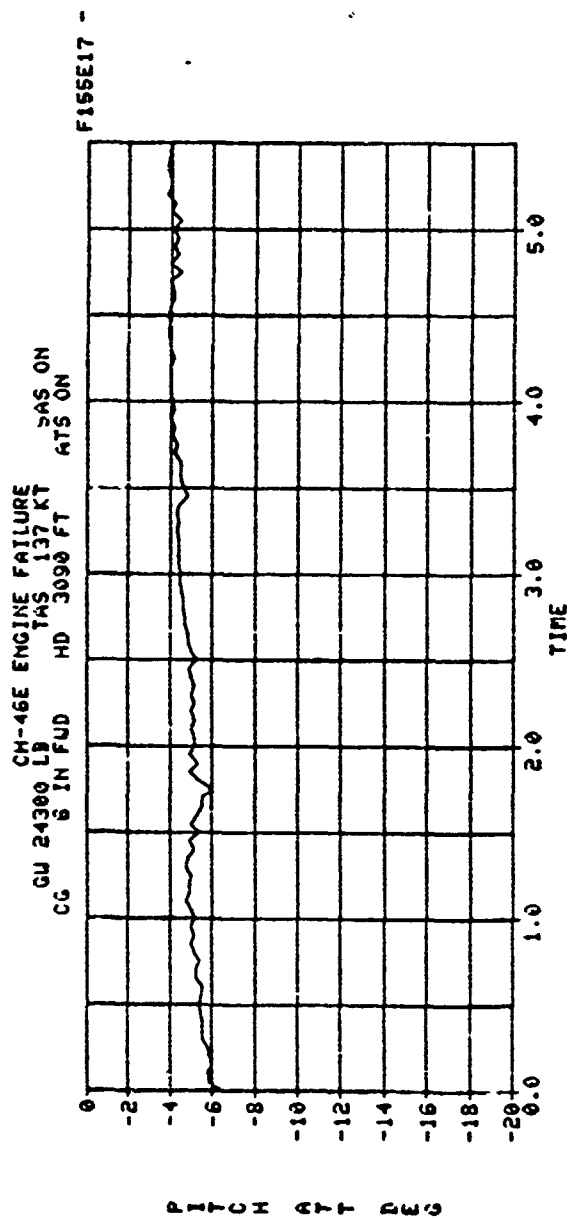


FIGURE 7-28

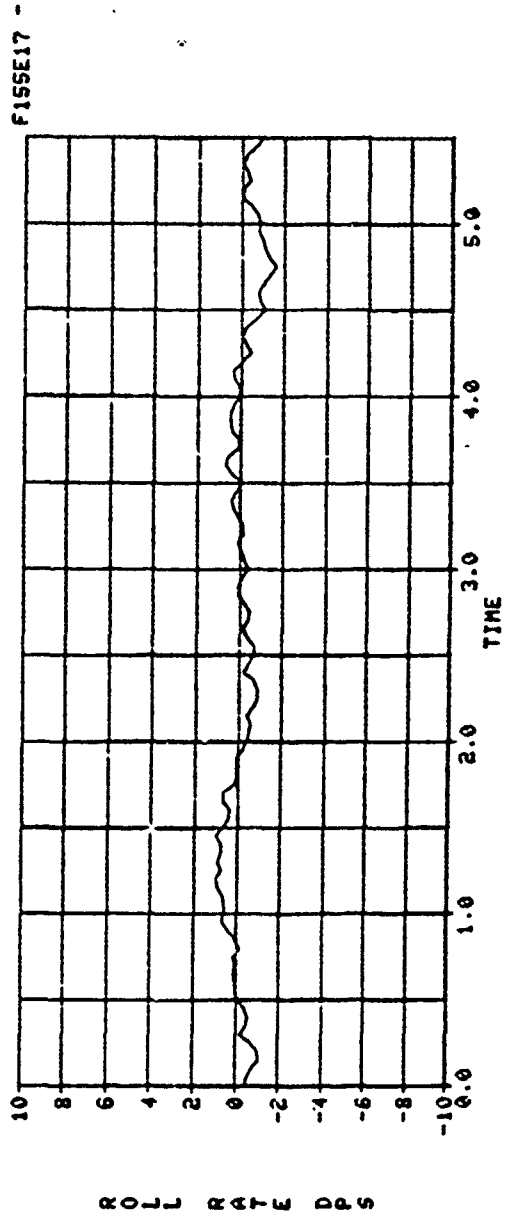
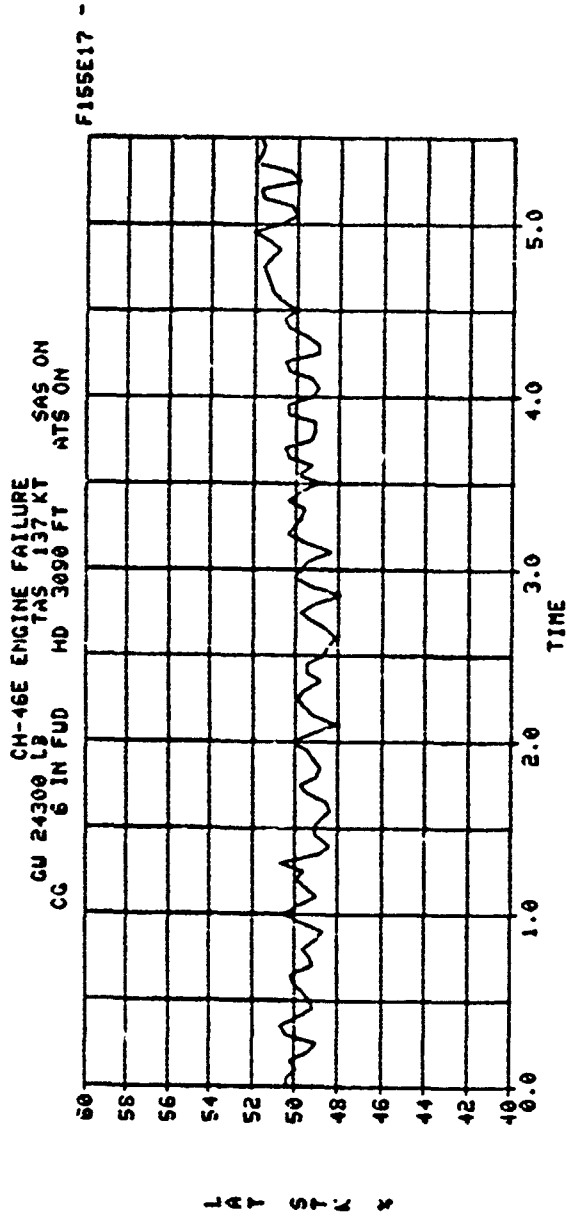


FIGURE 7-29

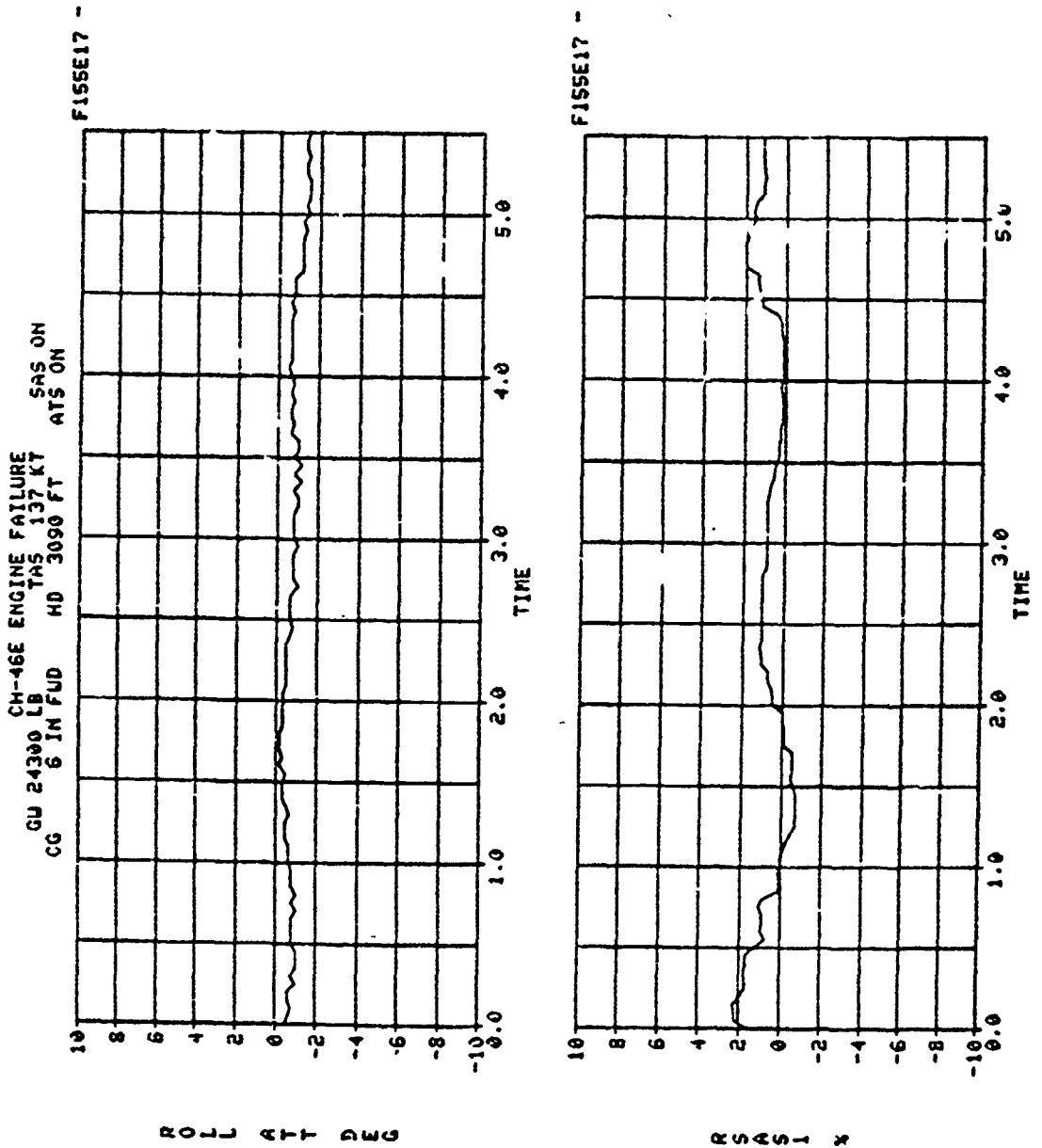


FIGURE 7-30

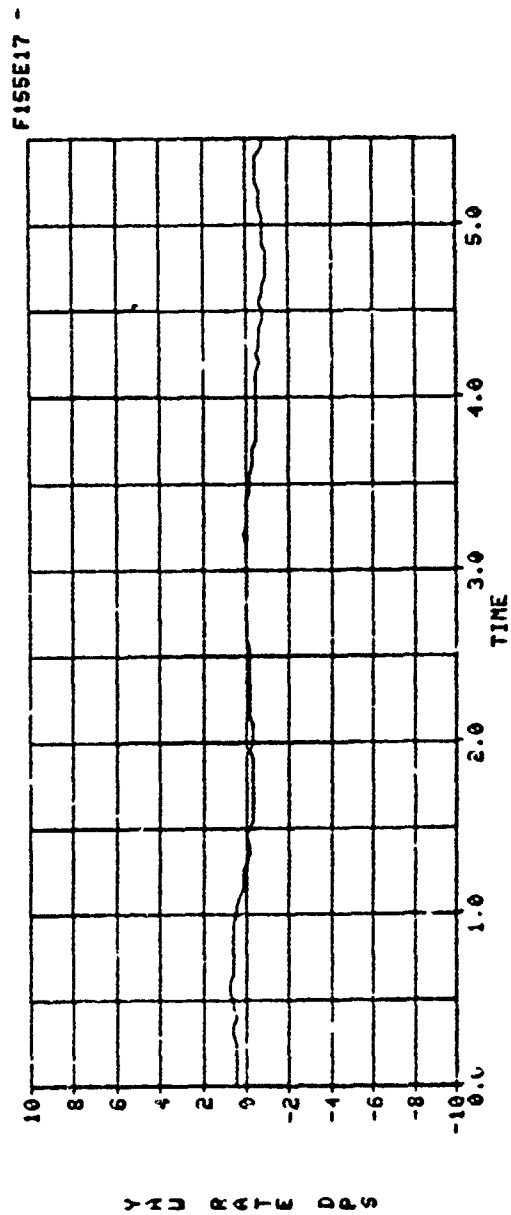
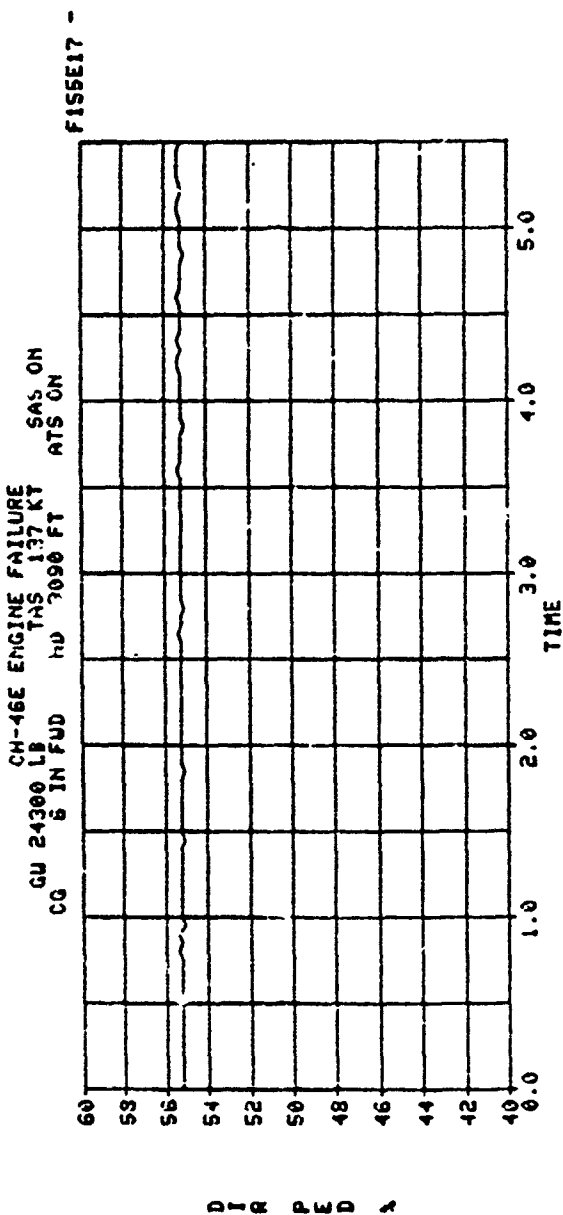


FIGURE 7-31

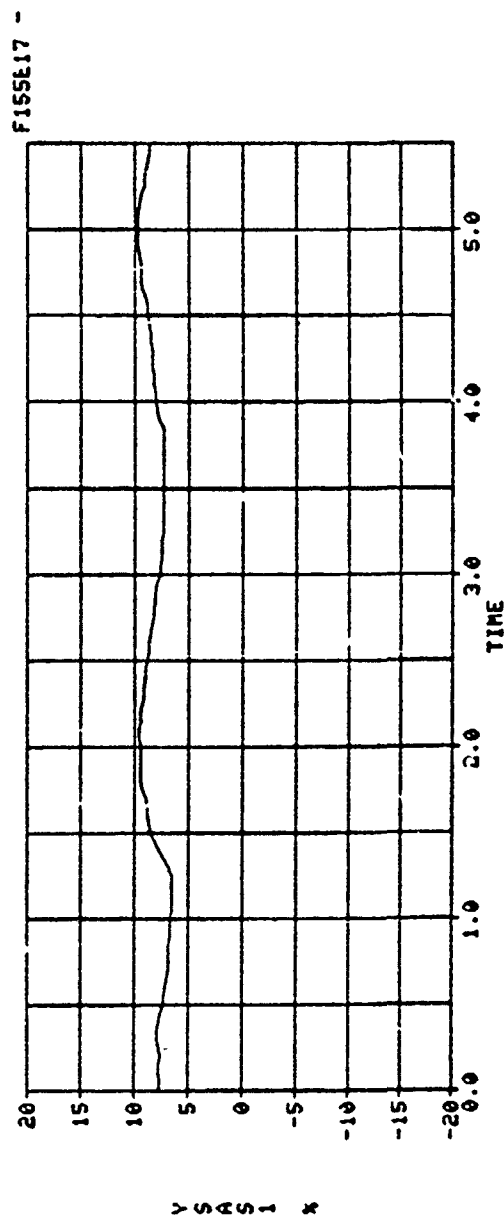
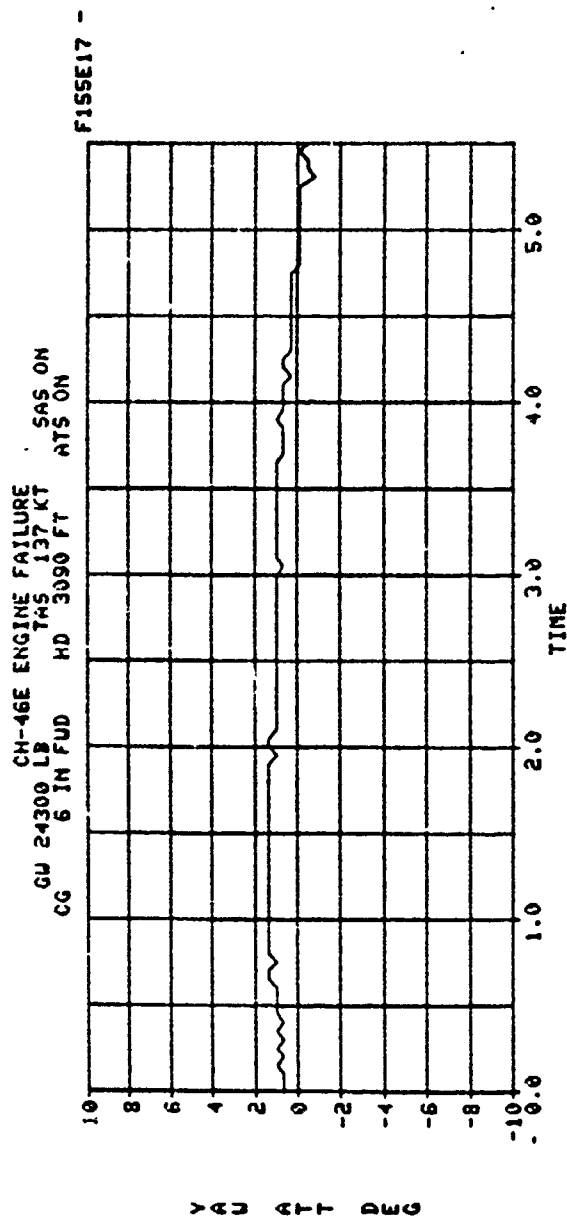


FIGURE 7-32

This Page Left Blank Intentionally .

## 8.0 TRIM AND STABILITY DATA

### 8.1 GENERAL TRIM AND STABILITY DATA

A complete set of trim and stability derivative data for the CH-46E is presented in Volume 4. The data were obtained from the Boeing Vertol Tandem Rotor Trim and Stability Analysis Program (A-97), and consist of a complete printout of all trim and stability derivative results available from the program, for the flight conditions summarized in Table 8-1. The trim and derivative output parameters are fully defined in Section 9.0, as well as in Volume 4.

### 8.2 THREE DEGREE APPROACH PATH DATA

Trim and stability data have also been obtained for the specific flight conditions listed in Table 8-2, which pertain specifically to a landing approach along a three degree glide slope.

The first case involves a steady shallow descent along a three degree glide slope at 80 knots. The second case is identical to the first, except that instead of steady flight, a 10 degree flare attitude is assumed. The third case is like the second, except the airspeed has decelerated to 60 knots while maintaining a three degree glide slope. The fourth case is like the third, except that instead of maintaining a three degree glide slope at 60 knots (319 ft/min. rate of descent), the 80 knot rate of descent is maintained at 60 knots, yielding a four degree glide slope.

The trim and stability data for these four cases appear immediately after Table 8-2. To interpret the output data, the output parameter definitions in Section 9.0 must be referred to.

TABLE 8-1

FLIGHT CONDITIONS FOR

CH-46E TRIM AND STABILITY DERIVATIVE ANALYSIS

GW = 24,300 lb      CG = 6 in. fwd			
<u>ALTITUDE</u>	<u>AIRSPEED</u>	<u>CLIMB RATE</u>	<u>SIDESLIP</u>
0 ft	-40 to 138 kt	0 ft/min	0 deg
8000	0 to 93	0	0
0	60 to 120	AUTO & MPC	0
0	50 to 130	0	± β max
0	-45 to 45	0	± 90
GW = 17,500 lb      CG = 20 in. aft			
<u>ALTITUDE</u>	<u>AIRSPEED</u>	<u>CLIMB RATE</u>	<u>SIDESLIP</u>
0 ft	-40 to 146 kt	0 ft/min	0 deg
14000	0 to 112	0	0
0	60 to 120	AUTO & MPC	0
0	50 to 140	0	± β max
0	-45 to 45	0	± 90
GW = 17,500 lb      CG = 40 in. fwd			
<u>ALTITUDE</u>	<u>AIRSPEED</u>	<u>CLIMB RATE</u>	<u>SIDESLIP</u>
0 ft	-40 to 146 kt	0 ft/min	0 deg
14000	0 to 112	0	0
0	60 to 120	AUTO & FPC	0
0	50 to 140	0	± β max
0	-45 to 45	0	0

TABLE 8-2

FLIGHT CONDITIONS FOR

CH-46E THREE DEGREE GLIDE SLOPE ANALYSIS

GW = 17,500 lb

CG = 11 in. aft

H<sub>D</sub> = 0 ft.

<u>CASE</u>	<u>AIRSPEED</u>	<u>CLIMB RATE</u>	<u>GLIDE SLOPE</u>	<u>FLARE ANGLE</u>
1	80 kt	-425 ft/min	3 deg	Trim
2	80	-425	3	10.0 deg
3	60	-319	3	10.0
4	60	-425	4	10.0

TRIM

V FE 8.000000D+01 4.400000D+01	RC ALPHA -4.250000D+02 4.053333D+00	GW ALFF 1.750000D+04 1.267219D+00	RHO THETA 2.378000D-03 1.139012D+00	XF LW LF LW 2.693290D+02 7.736861D+03
VTF VTR 7.050000D+02 7.050000D+02	CGF CGL -1.230042D+01 0.0	BETAF PHI 0.0 -2.988925D-01	PSI GAMMA -1.867500D-02 -3.005074D+00	XR LW LR LW 6.451588D+02 9.520173D+03
THEOF THEOR 1.194937D+01 1.337819D+01	AICF AICR 4.452052D-01 1.611750D-01	B1TF B1TR -8.000000D-01 -8.000000D-01	B1CF B1CR -3.000000D-01 -8.000000D-01	DFW LFFW 9.648978D+02 2.022532D+02
THETAC 1.266378D+01	DELTAB -3.058547D+00	DELTAS 9.765573D-02	DELTAR 1.237750D-01	DELTAC 4.390528D+00
TF TR 7.727494D+03 9.519379D+03	HF HR 4.662634D+02 6.567688D+02	YF YR 7.431038D+01 5.864444D+01	MHF MHR 1.269016D+03 2.250970D+03	LHF LHR 6.928324D+02 6.274585D+02
QF QR 7.581294D+03 1.009349D+04	LFZ DFX 2.699511D+02 9.481881D+02	YFY MF 8.631474D+01 -1.012455D+03	LF NF 1.069875D+02 5.734750D+02	RHPF RHPR 3.660116D+02 5.073731D+02
XR 1.027855D+02	L/DE 4.534296D+00	SHR :DT 9.733847D+02	WFF 9.743847D+02	NMLB 8.199019D-02
SIGOF SIGOR 5.841923D-02 5.841923D-02	CTSF CTSR 5.526191D-02 6.767919D-02	CPSF CPSR 2.024381D-03 2.806241D-03	AMTF AMTR 7.522877D-01 7.532478D-01	LAMDAF LAM DAR -2.749742D-02 -3.762568D-02
MUF MUR 1.907875D-01 1.913994D-01	VF VR 6.560632D+00 7.985364D+00	DFFR DFRF 1.767341D+00 7.157210D-38	DFF 9.032376D-01	AOF AOR 2.723316D+00 3.505123D+00
A1F A1R 3.036058D+00 3.657281D+00	B1F B1R 1.124993D+00 1.018830D+00	BETAOF BETAOR -4.560937D-01 -3.327517D-01	B18OF B18OR 5.622868D+00 6.988148D+00	A27OF A27OR 4.426137D+00 5.904249D+00
CAPVF CAPVR 1.351152D+02 1.362044D+02	ALPHAF ALPHAR -5.446667D+00 -7.823610D+00	BETAFW BETARW 3.600000D+02 3.600000D+02	ATIPF ATIPR -2.410610D+00 7.106136D-01	BPTPF BPTPR 3.237785D+00 3.796540D+00

FIGURE 8-1A A-97 OUTPUT - APPROACH CASE 1

TRIM

XFF	ZFF	MFF	TP
YFF	YFF	NFF	
0.0	0.0	0.0	0.0
0.0	0.0	0.0	
RMTF	CTFP	A90F	
RMTR	CTRP	A90RA	
5.090599D-01	5.485152D-02	4.766248D-01	
5.081030D-01	6.749455D-02	9.219776D-01	

NON UNIFORM DOWNWASH POWER CORRECTIONS

DELHPF	RHPF	SHPTOT	NMLB
DELHPR	RHPR	WFF	RP
1.238766D+01	3.783993D+02	1.001015D+03	7.983910D-02
1.524296D+01	5.226161D+02	1.002015D+03	1.397184D+03

FIGURE 8-1B A-97 OUTPUT - APPROACH CASE 1

HELICOPTER DERIVATIVES

ABILITY DERIVATIVES OUTPUT

MASS	IXX	IYY	IZZ
5.439174D+02	1.499900D+04	1.069780D+05	1.009310D+05
XU	XP	XDELB	XDELTA
XV	XQ	XDELS	XBETA
XW	XR	XDELR	XALPHA
-3.861263D-02	2.954044D-01	1.230621D-01	4.391151D-01
-1.561720D-03	1.340907D+00	-4.764747D-04	-2.105569D-01
5.546834D-02	-5.456742D-02	-3.373675D-02	7.478449D+00
ZU	ZP	ZDELB	ZDELTA
ZV	ZQ	ZDELS	ZBETA
ZW	ZR	ZDELR	ZALPHA
-2.460228D-02	-7.238605D-01	9.365059D-01	-8.457232D+00
4.353492D-03	-1.612155D+00	-9.115518D-03	5.869541D-01
-8.040293D-01	-7.341908D-01	4.559317D-02	-1.084022D+02
MU	MP	MDELB	MDELTA
MV	MQ	MDELS	MBETA
MW	MR	MDELR	MALPHA
-5.746592D-03	1.384781D-01	5.033517D-01	2.409871D-01
-4.732729D-04	-1.479138D+00	-3.501241D-03	-6.380843D-02
2.231113D-02	-2.359031D-01	1.418421D-03	3.008070D+00
YU	YP	YDELB	YDELTA
YV	YQ	YDELS	YBETA
YW	YR	YDELR	YALPHA
1.655303D-03	-1.626684D+00	7.435842D-02	1.658665D-02
-1.129075D-01	2.786969D-02	8.505429D-01	-1.522261D+01
6.600152D-03	-1.922217D-01	-1.394194D-01	8.898572D-01
LU	LP	LDELB	LDELTA
LV	LQ	LDELS	LBETA
LW	LR	LDELR	LALPHA
-7.072027D-04	-7.771617D-01	1.766123D-02	1.712637D-02
-6.161960D-03	5.368178D-02	3.546570D-01	-3.307787D-01
-4.020545D-04	-5.438124D-02	-1.543815D-01	-5.420649D-02
NU	NP	NDELB	NDELTA
NV	NQ	NDELS	NBETA
NW	NR	NDELR	NALPHA
4.097749D-04	-5.684675D-03	1.716945D-02	-3.233353D-03
-3.947109D-03	-1.105467D-01	1.106565D-02	-5.321641D-01
4.422849D-04	-3.366658D-02	1.229904D-01	5.963051D-02

FIGURE 8-1C A-97 OUTPUT - APPROACH CASE 1

COMPONENT DERIVATIVES

LONGITUDINAL

	U	MU	W	ALPHA	Q	THETAC
CTF	-0.718D-05	-0.506D-02	0.102D-03	0.138D-01	-0.165D-02	0.523D-01
CTR	0.102D-04	0.722D-02	0.658D-04	0.887D-02	0.206D-02	0.333D-01
CHF	0.554D-06	0.391D-03	0.729D-05	0.983D-03	-0.293D-03	0.451D-02
CHR	0.242D-05	0.170D-02	0.569D-05	0.767D-03	-0.338D-04	0.386D-02
AIF	0.226D-03	0.160D+00	0.621D-03	0.838D-01	-0.807D-01	0.570D+00
AIR	0.404D-03	0.285D+00	0.415D-03	0.560D-01	-0.617D-01	0.467D+00
VFR	-0.631D-01	-0.445D+02	0.207D+00	0.279D+02	-0.345D+01	0.106D+03
VRR	-0.355D-01	-0.250D+02	0.132D+00	0.178D+02	0.435D+01	0.645D+02
LF			0.312D+02	0.421D+04		
DF			-0.990D+00	-0.133D+03		
MF			0.229D+03	0.309D+05		

LATERAL-DIRECTIONAL

	V	BETA	P	R	AIC
CYF	-0.111D-05	-0.149D-03	-0.165D-03	-0.448D-04	0.331D-02
CYR	0.161D-05	0.217D-03	0.202D-03	-0.169D-05	0.405D-02
SIF	0.104D-03	0.140D-01	-0.670D-01	-0.134D-01	0.102D+01
BIR	-0.104D-03	-0.141D-01	0.714D-01	0.444D-03	0.103D+01
YF	-0.548D+02	-0.739D+04			
LF	-0.177D+02	-0.239D+04			
NF	-0.403D+03	-0.543D+05			
CTF					-0.137D-03
CTR					-0.131D-03

FORCE = 0.241446D+07

FIGURE 8-1D A-97 OUTPUT - APPROACH CASE 1

SUPPLEMENTARY DERIVATIVES

	BICF	BICR	MFGAF	MEGAR
X	0.938D+01	0.155D+02	0.0	0.0
Z	0.410D+02	0.631D+02	0.0	0.0
M	-0.829D+01	0.359D+01	0.0	0.0
Y	-0.614D+00	0.328D+00	0.0	0.0
L	-0.574D+00	0.299D+00	0.0	0.0
N	0.205D+00	-0.183D+00	0.0	0.0
CTF	-0.139D-01	-0.504D-07	0.0	0.0
CTR	0.504D-02	-0.139D-01	0.0	0.0
CHF	-0.427D-02	-0.104D-06	0.0	0.0
CHR	0.422D-03	-0.521D-02	0.0	0.0
AIF	-0.110D+01	-0.358D-04	0.0	0.0
AIR	0.285D-01	-0.111D+01	0.0	0.0
VFR	-0.282D+02	0.890D-02	0.0	0.0
VRR	0.106D+02	-0.277D+02	0.0	0.0
QF	0.553D+01	0.928D-03	0.0	0.0
QR	-0.186D+01	0.520D+01	0.0	0.0
	QFU	QFP	QFDELB	QFDELTAC
	QFV	QFQ	QFDELS	QFBETA
	QFW	QFR	QFDELR	QFALPHA
	0.719D-03	0.136D+00	0.216D+00	0.442D+00
	0.311D-03	0.294D+01	-0.765D-02	0.420D-01
	-0.408D-01	-0.143D+00	-0.110D-01	-0.550D+01
	QRU	QRP	QRDELB	QRDELTAC
	QRV	QRQ	QRDELS	QRBETA
	QRW	QRR	QRDELR	QRALPHA
	-0.766D-02	-0.209D-01	-0.266D+00	0.849D+00
	-0.138D-03	0.200D+01	0.742D-02	-0.187D-01
	-0.245D-01	0.230D+00	-0.150D-01	-0.331D+01

FIGURE 8-1E A-97 OUTPUT - APPROACH CASE 1

TRIM

V FE 8.000000D+01 4.400000D+01	RC ALPHA -4.250000D+02 1.300524D+01	GW ALFF 1.750000D+04 1.051726D+01	RHO THETA 2.378000D-03 1.000000D+01	XF LW LF LW -8.149312D+02 7.377796D+03
VTF VTR 7.050000D+02 7.050000D+02	CGF CGL -1.230042D+01 0.0	BETAF PHI 0.0 -3.022815D-01	PSI GAMMA -6.530246D-02 -3.005074D+00	XR LW LR LW -8.631673D+02 9.350730D+03
THEOF THEOR 9.436463D+00 1.074141D+01	AICF AICR 1.775413D-01 -1.078144D-01	BIYF BITR -8.000000D-01 -8.000000D-01	BICF BICR -8.000000D-01 -8.000000D-01	DFW LFFW 1.036329D+03 8.305797D+02
THETAC 1.008894D+01	DELTAB -2.961620D+00	DELTAS 7.831014D-02	DELTAR -2.297449D-03	DELTAC 2.394526D+00
TF TR 7.413818D+03 9.374986D+03	HF HR 3.623299D+02 5.392977D+02	YF YR 1.015936D+01 -1.033314D+01	MHF MHR 1.419614D+03 1.800202D+03	LHF LHR 4.090305D+02 4.126267D+02
QF QR 1.916994D+03 2.637011D+03	LFZ DFX 1.042490D+03 8.228324D+02	YFY MF 7.419029D+01 4.910258D+03	LF NF -1.810250D+02 6.640807D+02	RHPF RHPR 9.636224D+01 1.325556D+02
XR -2.332075D+03	L/DE 4.767135D+00	SHPTOT 3.289179D+02	WFF 3.299179D+02	NMLB 2.421512D-01
SIGOF SIGOR 5.841923D-02 5.841923D-02	CTSF CTSR 5.296724D-02 6.685366D-02	CPSF CPSR 5.329720D-04 7.331547D-04	AMTF AMTR 7.512575D-01 7.508840D-01	LAMDAF LAMDAR 2.728659D-03 -4.807179D-03
MUF MUR 1.912942D-01 1.906010D-01	VF VR 6.337207D+00 8.038563D+00	DFFR DFRF 1.496900D+00 4.391169D-38	DFF 8.299437D-01	AOF AOR 2.430525D+00 3.248411D+00
A1F A1R 2.305586D+00 2.924176D+00	B1F B1R 6.641391D-01 6.699786D-01	BETAOF BETAOR -2.989646D-02 1.388169D-01	B180F B180R 4.625251D+00 6.022968D+00	A270F A270R 3.163893D+00 4.659418D+00
CAPVF CAPVR 1.351152D+02 1.344541D+02	ALPHAF ALPHAR 3.505237D+00 1.981715D+00	BETAFW BETARW 3.600000D+02 3.600000D+02	ATIPF ATIPR 5.810823D+00 8.929413D+00	BPTPF BPTPR 2.399335D+00 2.999946D+00

FIGURE 8-2A A-97 OUTPUT - APPROACH CASE 2

TRIM

XFF LFF 0.0 0.0	ZFF YFF 0.0 0.0	MFF NFF 0.0 0.0	TP   2.450976D+03
RMTF RMTR 5.097309D-01 5.096741D-01	CTFP CTRP 5.230588D-02 6.629326D-02	A90F A90RA 4.697495D-02 4.506336D-01	

NON UNIFORM DOWNWASH POWER CORRECTIONS

DELHPF DELHPR 1.181276D+01 1.497167D+01	RHPF RHPR 1.081750D+02 1.475273D+02	SHPTOT WFF 3.557023D+02 3.567023D+02	NMLB RP 2.242767D-01 3.924842D+03
--	--	---	--

FIGURE 8-2B A-97 OUTPUT - APPROACH CASE 2

HELICOPTER DERIVATIVES

ABILITY DERIVATIVES OUTPUT

MASS	IXX	IYY	IZZ
5.439174D+02	1.499900D+04	1.069780D+05	1.009310D+05
XU	XP	XDELB	XDELTAC
XV	XQ	XDELS	XBETA
XW	XR	XDELR	XALPHA
-3.456823D-02	1.569987D-01	1.244992D-01	5.404067D-01
1.559036D-04	2.049026D+00	-8.071230D-04	2.053449D-02
6.681168D-02	-1.383506D-02	-4.019204D-02	8.799947D+00
ZU	ZP	ZDELB	ZDELTAC
ZV	ZQ	ZDELS	ZBETA
ZW	ZR	ZDELR	ZALPHA
-2.401503D-02	2.320783D+00	8.176813D-01	-8.609702D+00
-4.313569D-03	-1.158211D+00	-6.861803D-03	-5.681518D-01
-8.081783D-01	-6.153124D-01	3.382967D-02	-1.064473D+02
MU	MP	MDELB	MDELTAC
MV	MQ	MDELS	MBETA
MW	MR	MDELR	MALPHA
-6.113323D-03	3.709053D-01	4.943416D-01	2.218766D-01
-5.716609D-04	-1.493763D+00	-2.537444D-03	-7.529501D-02
2.316202D-02	-1.531245D-01	1.734755D-03	3.050733D+00
YU	YP	YDELB	YDELTAC
YV	YQ	YDELS	YBETA
YW	YR	YDELR	YALPHA
1.814148D-03	-2.304074D+00	2.634155D-02	1.158410D-02
-1.179110D-01	1.667779D-01	8.177529D-01	-1.553038D+01
-1.397450D-04	-2.389910D-01	-1.555010D-01	-1.840619D-02
LU	LP	LDELB	LDELTAC
LV	LQ	LDELS	LBETA
LW	LR	LDELR	LALPHA
-1.123241D-03	-9.159968D-01	2.908094D-02	1.882329D-02
1.194283D-03	2.366330D-02	3.462969D-01	1.573022D-01
2.215218D-03	-7.326862D-02	-1.541399D-01	2.917723D-01
NU	NP	NDELB	NDELTAC
NV	NQ	NDELS	NBETA
NW	NR	NDELR	NALPHA
7.887288D-04	-4.789763D-02	-8.602980D-03	-1.276346D-02
-4.899265D-03	-3.737240D-02	9.608319D-03	-6.452954D-01
-1.032412D-03	-2.655192D-02	1.182029D-01	-1.359818D-01

FIGURE 8-2C A-97 OUTPUT - APPROACH CASE 2

COMPONENT DERIVATIVES

LONGITUDINAL

	U	MU	W	ALPHA	Q	HETAC
CTF	-0.880D-05	-0.620D-02	0.103D-03	0.136D-01	-0.166D-02	0.523D-01
CTR	0.979D-05	0.690D-02	0.645D-04	0.849D-02	0.200D-02	0.351D-01
CHF	0.224D-06	0.158D-03	0.624D-05	0.822D-03	-0.355D-03	0.388D-02
CHR	0.196D-05	0.138D-02	0.505D-05	0.665D-03	-0.144D-03	0.358D-02
ALF	0.128D-03	0.903D-01	0.608D-03	0.801D-01	-0.798D-01	0.566D+00
AIR	0.315D-03	0.222D+00	0.394D-03	0.518D-01	-0.608D-01	0.470D+00
VFR	-0.650D-01	-0.458D+02	0.205D+00	0.270D+02	-0.341D+01	0.108D+03
VRR	-0.402D-01	-0.284D+02	0.127D+00	0.167D+02	0.418D+01	0.723D+02
LF			0.353D+02	0.465D+04		
DF			-0.320D+01	-0.422D+03		
MF			0.273D+03	0.360D+05		

LATERAL-DIRECTIONAL

	V	BETA	P	R	AIC
CYF	-0.781D-06	-0.103D-03	-0.239D-03	-0.466D-04	0.313D-02
CYR	0.125D-05	0.165D-03	0.280D-03	0.709D-05	0.396D-02
BIF	0.104D-03	0.137D-01	-0.661D-01	-0.118D-01	0.102D+01
BIR	-0.988D-04	-0.130D-01	0.679D-01	0.170D-02	0.102D+01
YF	-0.592D+02	-0.780D+04			
LF	0.741D+02	0.976D+04			
NF	-0.506D+03	-0.667D+05			
CTF					-0.111D-03
CTR					-0.999D-04

FORCE = 0.241446D+07

FIGURE 8-2D A-97 OUTPUT - APPROACH CASE 2

SUPPLEMENTARY DERIVATIVES

	BICF	BICR	OMEGAF	OMEGAR
X	0.797D+01	0.144D+02	0.0	0.0
Z	0.432D+02	0.622D+02	0.0	0.0
M	-0.803D+01	0.359D+01	0.0	0.0
Y	-0.488D-01	-0.132D+00	0.0	0.0
L	-0.713D+00	0.403D+00	0.0	0.0
N	0.533D+00	-0.415D+00	0.0	0.0
CTF	-0.139D-01	-0.129D-06	0.0	0.0
CTR	0.447D-02	-0.137D-01	0.0	0.0
CHF	-0.392D-02	-0.839D-07	0.0	0.0
CHR	0.337D-03	-0.495D-02	0.0	0.0
AIF	-0.110D+01	-0.217D-04	0.0	0.0
AIR	0.250D-01	-0.110D+01	0.0	0.0
VFR	-0.287D+02	0.599D-02	0.0	0.0
VRR	0.933D+01	-0.284D+02	0.0	0.0
QF	0.123D+02	0.650D-03	0.0	0.0
QR	-0.419D+01	0.128D+02	0.0	0.0
	QFU	QFP	QFDELB	QFDELTAC
	QFV	QFQ	QFDELS	QFBETA
	QFW	QFR	QFDELR	QFALPHA
	0.666D-02	-0.160D+00	-0.102D+00	-0.205D+00
	0.224D-03	0.356D+01	-0.741D-02	0.295D-01
	-0.914D-01	-0.120D+00	-0.105D-01	-0.120D+02
	QRU	QRP	QRDELB	QRDELTAC
	QRV	QRQ	QRDELS	QRBETA
	QRW	QRR	QRDELR	QRALPHA
	-0.123D-01	0.792D+00	0.182D+00	0.343D+00
	-0.154D-02	0.750D+00	0.643D-02	-0.203D+00
	-0.617D-01	0.110D+00	-0.150D-01	-0.813D+01

FIGURE 8-2E A-97 OUTPUT - APPROACH CASE 2

TRIM

V FE 6.000000D+01 4.400000D+01	RC ALPHA -3.190000D+02 1.300750D+01	GW ALFF 1.750000D+04 8.287001D+00	RHO THETA 2.378000D-03 1.000000D+01	XF LW LF LW -1.011811D+03 7.536793D+03
VTF VTR 7.050000D+02 7.050000D+02	CGF CGL -1.230042D+01 0.0	BETAF PHI 0.0 -1.952175D-01	PSI GAMMA -4.278212D-02 -3.007434D+00	XR LW LR LW -5.468625D+02 9.741597D+03
THEOF THEOR 9.781476D+00 1.186394D+01	AICF AICR 7.453882D-01 5.345089D-01	BITF BITR -2.500000D+00 -2.500000D+00	BICF BICR -2.500000D+00 -2.500000D+00	DFW LFFW 5.698550D+02 3.522203D+02
THETAC 1.082271D+01	DELTAB -2.990977D+00	DELTAS 7.923579D-02	DELTAR 2.586419D-01	DELTAC 2.963341D+00
TF TR 7.584577D+03 9.723868D+03	HF HR 5.488200D+02 8.026049D+02	YF YR 9.284338D+01 7.900466D+01	MHF MHR 2.338220D+03 2.719874D+03	LHF LHR 7.359100D+02 6.232107D+02
QF QR 2.552250D+03 5.898904D+03	LFZ DFX 4.714447D+02 4.759556D+02	YFY MF 4.650620D+01 1.898508D+03	LF NF -9.523682D+01 4.301121D+02	RHPF RHPR 1.282949D+02 2.965224D+02
WZ -2.827695D+03	L/DF 3.083000D+01	SHPTOT 5.248173D+02	WFF 5.058177D+02	NMLB 1.139509D-01
SIGOF SIGOR 5.841923D-02 5.841923D-02	CTSF CTSR 5.416233D-02 6.907377D-02	CPSF CPSR 7.095890D-04 1.640042D-03	AMTF AMTR 7.221989D-01 7.224548D-01	LAMDAR LAMDAR -3.465219D-03 -1.938573D-02
MUF MUR 1.434703D-01 1.429502D-01	VF VR 8.642676D+00 1.101828D+01	DFFR DFRF 1.533592D+00 3.247103D-38	DFF 8.572814D-01	AOF AOR 2.517450D+00 3.588323D+00
AIF AIR 3.799246D+00 4.420522D+00	BIF BIR 1.194951D+00 1.011932D+00	BETAOF BETAOR -1.369188D+00 -1.051378D+00	B180F B180R 6.254739D+00 7.906282D+00	A270F A270R 2.929988D+00 4.706539D+00
CAPVF CAPVR 1.013364D+02 1.008147D+02	ALPHAF ALPHAR 3.507503D+00 -1.505448D+00	BETAFW BETARW 3.600000D+02 3.600000D+02	ATIPF ATIPR 7.306749D+00 1.042802D+01	BPTPF BPTPR 3.982735D+00 4.534867D+00

FIGURE 8-3A A-97 OUTPUT - APPROACH CASE 3

TRIM

XFF	ZFF	MFF	TP
LFF	YFF	NFF	
0.0	0.0	0.0	2.479404D+03
0.0	0.0	0.0	
RMTF	CTFP	A90F	
RMTR	CTRP	A90RA	
5.402255D-01	5.343311D-02	3.771252D-01	
5.395952D-01	6.906437D-02	1.236216D+00	

NON UNIFORM DOWNWASH POWER CORRECTIONS

DELHPF	RHPF	SHPTOT	NMLB
DELHPR	RHPR	WFF	RP
5.654032D+00	1.339489D+02	5.377794D+02	1.113628D-01
7.308055D+00	3.038305D+02	5.387794D+02	1.948849D+03

FIGURE 8-3B A-97 OUTPUT - APPROACH CASE 3

HELICOPTER DERIVATIVES

ABILITY DERIVATIVES OUTPUT

MASS 5.439174D+02	IXX 1.499900D+04	IYY 1.069780D+05	IZZ 1.009310D+05
XU XV XW -2.633905D-02 -1.594795D-04 4.687121D-02	XP XQ XR 1.693763D-01 1.880257D+00 -4.248415D-02	XDELB XDELS XDELR 1.185453D-01 -8.566589D-04 -3.700814D-02	XDELTA XBETA XALPHA 3.367666D-01 -1.575985D-02 4.631837D+00
ZU ZV ZW -1.036403D-01 -1.303396D-02 -6.816325D-01	ZP ZQ ZR 3.604444D+00 -1.283881D+00 -6.767488D-01	ZDELB ZDELS ZDELR 9.704340D-01 -7.091272D-03 3.298979D-02	ZDELTA ZBETA ZALPHA -7.476043D+00 -1.288023D+00 -6.735928D+01
MU MV MW -7.240469D-03 -2.045234D-03 2.607924D-02	MP MQ MR 3.957446D-01 -1.444244D+00 -1.858585D-01	MDELB MDELS MDELR 4.672829D-01 -2.602585D-03 1.518782D-03	MDELTA MBETA MALPHA 2.379850D-01 -2.021110D-01 2.577164D+00
YU YV YW 5.176147D-04 -8.692668D-02 1.105230D-03	YP YQ YR -2.117798D+00 4.164459D-02 -2.055773D-01	YDELB YDELS YDELR 8.185236D-02 8.457078D-01 -1.713931D-01	YDELTA YBETA YALPHA 3.516282D-02 -8.590139D+00 1.092194D-01
LU LV LW -1.349513D-03 -1.763682D-03 2.419178D-03	LP LQ LR -8.872021D-01 2.120442D-02 -6.077223D-02	LDELB LDELS LDELR 3.040767D-02 3.545536D-01 -1.625016D-01	LDELTA LBETA LALPHA 1.956325D-02 -1.742879D-01 2.390644D-01
NU NV NW 7.829818D-04 -3.494650D-03 -7.579656D-04	NP NQ NR -3.353602D-02 -6.681462D-02 -2.467669D-02	NDELB NDELS NDELR 2.752585D-03 9.394024D-03 1.221948D-01	NDELTA NBETA NALPHA -1.130268D-02 -3.453431D-01 -7.490255D-02

FIGURE 8-3C A-97 OUTPUT - APPROACH CASE 3

COMPONENT DERIVATIVES

LONGITUDINAL

	U	MU	W	ALPHA	Q	THETAC
CTF	-0.190D-05	-0.134D-02	0.967D-04	0.955D-02	-0.160D-02	0.477D-01
CTR	0.219D-04	0.154D-01	0.467D-04	0.461D-02	0.196D-02	0.277D-01
CHF	0.696D-06	0.491D-03	0.795D-05	0.785D-03	-0.374D-03	0.443D-02
CHR	0.350D-05	0.247D-02	0.450D-05	0.455D-03	-0.811D-04	0.341D-02
AlF	0.197D-03	0.179D+00	0.437D-03	0.432D-01	-0.769D-01	0.406D+00
AlR	0.403D-03	0.284D+00	0.230D-03	0.227D-01	-0.646D-01	0.327D+00
VFR	-0.912D-01	-0.643D+02	0.253D+00	0.250D+02	-0.445D+01	0.131D+03
VRR	-0.454D-01	-0.320D+02	0.120D+00	0.118D+02	0.561D+01	0.722D+02
LF			0.243D+02	0.240D+04		
DF			-0.319D+01	-0.316D+03		
MF			0.182D+03	0.180D+05		

LATERAL-DIRECTIONAL

	V	BETA	P	R	AIC
CYF	-0.859D-06	-0.849D-04	-0.233D-03	-0.446D-04	0.322D-02
CYR	0.151D-05	0.149D-03	0.244D-03	0.131D-05	0.412D-02
BIF	0.439D-03	0.434D-01	-0.680D-01	-0.111D-01	0.102D+01
BIR	-0.431D-03	-0.426D-01	0.690D-01	-0.121D-04	0.102D+01
YF	-0.416D+02	-0.411D+04			
LF	0.404D+02	1.399D+04			
NF	-0.377D+03	-0.373D+05			
CTF					-0.1.7J-93
CTR					-0.9.1D-04

FORCE = 0.241446D+07

FIGURE 8-3D A 97 OUTPUT - APPROACH CASE 3

SUPPLEMENTARY DERIVATIVES

	BICF	BICR	OMEGAF	OMEGAR
X	0.109D+02	0.170D+02	0.0	0.0
Z	0.270D+02	0.444D+02	0.0	0.0
M	-0.618D+01	0.213D+01	0.0	0.0
Y	-0.611D+00	0.133D+00	0.0	0.0
L	-0.572D+00	0.272D+00	0.0	0.0
N	0.318D+00	-0.230D+00	0.0	0.0
CTF	-0.934D-02	-0.106D-05	0.0	0.0
CTR	0.397D-02	-0.959D-02	0.0	0.0
CHF	-0.398D-02	-0.325D-06	0.0	0.0
CHR	0.374D-03	-0.503D-02	0.0	0.0
AIF	-0.106D+01	-0.730D-04	0.0	0.0
AIR	0.163D-01	-0.106D+01	0.0	0.0
VFR	-0.264D+02	0.243D-01	0.0	0.0
VRR	0.113D+02	-0.258D+02	0.0	0.0
QF	0.780D+01	0.290D-02	0.0	0.0
QR	-0.271D+01	0.656D+01	0.0	0.0
	QFU	QFP	QFDELB	QFDELTAC
	QFV	QFQ	QFDELS	QFBETA
	QFW	QFR	QFDELR	QFALPHA
	0.361D-03	0.228D+00	0.104D-01	0.231D-01
	0.928D-03	0.383D+01	-0.536D-02	0.917D-01
	-0.771D-01	-0.420D-01	-0.788D-02	-0.762D+01
	QRU	QRP	QRDELB	QRDELTAC
	QRV	QRQ	QRDELS	QRBETA
	QRW	QRR	QRDELR	QRALPHA
	-0.177D-01	0.433D+00	-0.563D-01	0.717D+00
	-0.296D-02	0.170D+01	0.540D-02	-0.293D+00
	-0.331D-01	0.104D+00	-0.125D-01	-0.327D+01

FIGURE 8-3E A-97 OUTPUT - APPROACH CASE 3

TRIM

V FE 6.000000D+01 4.400000D+01	RC ALPHA -4.250000D+02 1.400826D+01	GW ALFF 1.750000D+04 9.338628D+00	RHO THETA 2.378000D-03 1.000000D+01	XF LW LF LW -1.135871D+03 7.509490D+03
VTF VTR 7.050000D+02 7.050000D+02	CGF CGL -1.230042D+01 0.0	BETAF PHI 0.0 -1.837418D-01	PSI GAMMA -4.336775D-02 -4.008198D+00	XR LW LR LW -7.548397D+02 9.728193D+03
THEOF THEOR 9.574103D+00 1.161388D+01	AICF AICR 6.926457D-01 4.959343D-01	BITF BITR -2.500000D+00 -2.500000D+00	BICF BICR -2.500000D+00 -2.500000D+00	DFW LFFW 5.773187D+02 3.915653D+02
THETAC 1.059399D+01	DELTAB -2.957576D+00	DELTAS 7.414146D-02	DELTAR 2.401066D-01	DELTAC 2.786042D+00
TF TR 7.575539D+03 9.725141D+03	HF HR 5.420894D+02 7.931839D+02	YF YR 8.429133D+01 7.096399D+01	MHF MHR 2.308296D+03 2.685490D+03	LHF LHR 6.987916D+02 6.012422D+02
QF QR 2.098544D+03 5.145992D+03	LFZ DFX 5.196673D+02 4.653667D+02	YFY MF 4.345067D+01 2.269408D+03	LF NF -9.864690D+01 4.084892D+02	RHPF RHPR 1.054883D+02 2.586756D+02
XR -3.109718D+03	L/DE 3.108927D+00	SHPTOT 4.641639D+02	WFF 4.651639D+02	NMLB 1.286713D-01
SIGOF SIGOR 5.841923D-02 5.841923D-02	CTSF CTSR 5.407561D-02 6.911320D-02	CPSF CPSR 5.834476D-04 1.430714D-03	AMTF AMTR 7.219574D-01 7.220769D-01	LAMDAR LAMDAR -9.642372D-04 -1.626616D-02
MUF MUR 1.432948D-01 1.426656D-01	VF VR 8.645125D+00 1.107113D+01	DFFR DFRF 1.476070D+00 2.200698D-38	DFF 8.480960D-01	AOF AOR 2.495153D+00 3.562573D+00
AIF AIR 3.750555D+00 4.364528D+00	BIF BIR 1.134670D+00 9.762570D-01	BETAOF BETAOR -1.339071D+00 -1.012346D+00	B18OF B18OR 6.185366D+00 7.827228D+00	A27OF A27OR 2.832691D+00 4.594960D+00
CAPVF CAPVR 1.013364D+02 1.005801D+02	ALPHAF ALPHAR 4.508264D+00 -2.258694D-01	BETAFW BETARW 3.600000D+02 3.600000D+02	ATIPF ATIPR 8.258819D+00 1.137279D+01	BPTPF BPTPR 3.918435D+00 4.472380D+00

FIGURE 8-4A A-97 OUTPUT - APPROACH CASE 4

TRIM

XFF LFF 0.0 0.0	ZFF YFF 0.0 0.0	MFF NFF 0.0 0.0	TP 2.463801D+03
RMTF RMTR 5.404720D-01 5.399220D-01	CTFP CTRP 5.323955D-02 6.896934D-02	A90F A90RA 3.352790D-01 1.180492D+00	

NON UNIFORM DOWNWASH POWER CORRECTIONS

DELHPF DELHPR 5.633549D+00 7.297999D+00	RHPF RHPR 1.111219D+02 2.659736D+02	SHPTOT WFF 4.770954D+02 4.780954D+02	NMLB RP 1.254980D-01 2.196214D+03
--	--	---	--

FIGURE 8-4B A-97 OUTPUT - APPROACH CASE 4

HELICOPTER DERIVATIVES

ABILITY DERIVATIVES OUTPUT

MASS 5.439174D+02	IXX 1.499900D+04	IYY 1.069780D+05	IZZ 1.009310D+05
XU XV XW -2.587095D-02 2.802699D-04 4.680820D-02	XP XQ XR 1.681653D-01 1.947242D+00 -3.944151D-02	XDELB XDELS XDELR 1.185994D-01 -8.391979D-04 -3.760638D-02	XDELTAC XBETA XALPHA 3.466112D-01 2.758064D-02 4.606275D+00
ZU ZV ZW -1.033939D-01 -1.372217D-02 -6.910619D-01	ZP ZQ ZR 3.582747D+00 -1.161837D+00 -6.563566D-01	ZDELB ZDELS ZDELR 9.349019D-01 -7.641687D-03 3.275651D-02	ZDELTAC ZBETA ZALPHA -7.525340D+00 -1.350363D+00 -6.800563D+01
MU MV MW -7.208364D-03 -2.25202D-03 2.557971D-02	MP MQ MR 3.940601D-01 -1.440235D+00 -1.782781D-01	MDELB MDELS MDELR 4.644646D-01 -2.567156D-03 1.577199D-03	MDELTAC MBETA MALPHA 2.331229D-01 -1.992949D-01 2.517234D+00
YU YV YW 5.305050D-04 -8.834893D-02 1.348926D-03	YP YQ YR -2.190564D+00 5.766033D-02 -2.076407D-01	YDELB YDELS YDELR 7.616603D-02 8.445319D-01 -1.724082D-01	YDELTAC YBETA YALPHA 3.045652D-02 -8.694192D+00 1.327443D-01
LU LV LW -1.359085D-03 -1.248875D-03 2.458147D-03	LP LQ LR -9.042250D-01 2.003294D-02 -6.151558D-02	LDELB LDELS LDELR 3.066232D-02 3.542539D-01 -1.625987D-01	LDELTAC LBETA LALPHA 1.958793D-02 -1.228986D-01 2.419000D-01
NU NV NW 8.196420D-04 -3.453308D-03 -8.685522D-04	NP NQ NR -3.669956D-02 -6.057090D-02 -2.430370D-02	NDELB NDELS NDELR 6.936079D-04 9.316147D-03 1.220256D-01	NDELTAC NBETA NALPHA -1.194349D-02 -3.398312D-01 -8.547200D-02

FIGURE 8-4C A-97 OUTPUT - APPROACH CASE 4

COMPONENT DERIVATIVES

LONGITUDINAL

	U	MU	W	ALPHA	Q	THETAC
CTF	-0.198D-05	-0.140D-02	0.968D-04	0.952D-02	-0.160D-02	0.477D-01
CTR	0.217D-04	0.153D-01	0.484D-04	0.477D-02	0.193D-02	0.285D-01
CHF	0.664D-06	0.468D-03	0.789D-05	0.777D-03	-0.380D-03	0.439D-02
CHR	0.345D-05	0.243D-02	0.473D-05	0.466D-03	-0.937D-04	0.344D-02
AIF	0.190D-03	0.134D+00	0.436D-03	0.429D-01	-0.768D-01	0.405D+00
AIR	0.396D-03	0.279D+00	0.235D-03	0.232D-01	-0.646D-01	0.328D+00
VFR	-0.914D-01	-0.645D+02	0.252D+00	0.248D+02	-0.444D+01	0.131D+03
VRR	-0.482D-01	-0.340D+02	0.124D+00	0.122D+02	0.554D+01	0.748D+02
LF			0.249D+02	0.245D+04		
DF			-0.279D+01	-0.274D+03		
MF			0.189D+03	0.186D+05		

LATERAL-DIRECTIONAL

	V	BETA	P	R	AIC
CYF	-0.834D-06	-0.821D-04	-0.240D-03	-0.446D-04	0.321D-02
CYR	0.148D-05	0.146D-03	0.253D-03	0.228D-05	0.412D-02
BIF	0.440D-03	0.433D-01	-0.679D-01	-0.110D-01	0.102D+01
BIR	-0.432D-03	-0.425D-01	0.689D-01	0.880D-04	0.102D+01
YF	-0.425D+02	-0.418D+04			
LF	0.466D+02	0.458D+04			
NF	-0.374D+03	-0.368D+05			
CTF					-0.108D-03
CTR					-0.947D-04

FORCE = 0.241446D+07

FIGURE 8-4D A-97 OUTPUT - APPROACH CASE 4

SUPPLEMENTARY DERIVATIVES

	BICF	BICR	OMEGAF	OMEGAR
X	0.108D+02	0.170D+02	0.0	0.0
Z	0.275D+02	0.442D+02	0.0	0.0
M	-0.613D+01	0.212D+01	0.0	0.0
Y	-0.537D+00	0.998D-01	0.0	0.0
L	-0.571D+00	0.272D+00	0.0	0.0
N	0.339D+00	-0.244D+00	0.0	0.0
CTF	-0.961D-02	-0.107D-05	0.0	0.0
CTR	0.383D-02	-0.954D-02	0.0	0.0
CHF	-0.396D-02	-0.321D-06	0.0	0.0
CHR	0.359D-03	-0.501D-02	0.0	0.0
AIF	-0.106D+01	-0.705D-04	0.0	0.0
AIR	0.157D-01	-0.106D+01	0.0	0.0
VFR	-0.264D+02	0.238D-01	0.0	0.0
VRR	0.109D+02	-0.259D+02	0.0	0.0
QR	0.819D+01	0.288D-02	0.0	0.0
QF	-0.283D+01	0.708D+01	0.0	0.0
	QFU	QFP	QFDELB	QFDELTA
	QFV	QFQ	QFDELS	QFBETA
	QFW	QFR	QFDELR	QFALPHA
	0.573D-03	0.194D+00	-0.132D-01	-0.260D-01
	0.906D-03	0.389D+01	-0.538D-02	0.891D-01
	-0.812D-01	-0.448D-01	-0.778D-02	-0.799D+01
	QRU	QRP	QRDELB	QRDELTA
	QRV	QRQ	QRDELS	QRBETA
	QRW	QRR	QRDELR	QRALPHA
	-0.188D-01	0.503D+00	-0.187D-01	0.670D+00
	-0.328D-02	0.159D+01	0.521D-02	-0.323D+00
	-0.371D-01	0.958D-01	-0.124D-01	-0.365D+01

FIGURE 8-4E A-07 OUTPUT - APPROACH CASE 4

## 9.0 TRIM AND STABILITY ANALYSIS PROGRAM (A-97)

### 9.1 DESCRIPTION OF PROGRAM

The Boeing Vertol Tandem Rotor Trim and Stability Analysis Program (A-97) is a digital program which provides a simultaneous solution of the six degree-of-freedom inelastic airframe equations of motion and the three degree-of-freedom inelastic rotor equations of motion. Non-linear fuselage characteristics are incorporated by table look-up. Rotor stall, compressibility and reverse flow are accounted for using a numerical blade element approach, with a two-dimensional airfoil table look-up for sectional lift and drag.

Helicopter trim is obtained through an iterative solution to the six steady-state equations of motion developed by a force and moment balance along and about a body-fixed axis system. Non-linear fuselage force and moment characteristics are accounted for by a two dimensional table look-up for lift, drag, pitch moment, side force, roll moment and yaw moment as functions of fuselage angle of attack and sideslip, modified to account for the local effects of rotor downwash.

Within the main iteration loop of the program, rotor iteration loops are incorporated which apply a numerical technique to the solution of the rotor flapping and force equations. In this rotor subroutine, a blade element approach applies a two-dimensional table look-up procedure to determine local  $C_L$  and  $C_D$  as functions of local blade angle of attack and Mach No., thereby accounting for blade stall, reverse flow and compressibility effects on the rotors. The effects of rotor mutual interference are accounted for by a series of internal equations which adjust the computed inflow to each rotor by an empirical factor applied to the induced velocity

generated by the other rotor. This empirical factor is a function of rotor system airspeed, angle of attack, rotor gap (vertical separation) and overlap.

The main limitations of the program arise from the following simplifying assumptions:

- Induced velocity distribution is assumed uniform.
- Blade lag and all elastic degrees of freedom are neglected.
- Non-steady aerodynamic and spanwise flow effects are neglected.

Twelve stability derivatives and control powers are obtained numerically by evaluating the changes in the helicopter forces and moments from trim, caused by small perturbations in twelve independent parameters. These derivatives are quasi-static; i.e. the helicopter is assumed to reach a new steady state condition after the perturbation is applied.

## 9.2 INPUT SHEET

Figure 9-1 shows an A-97 input sheet, with input locations filled out to represent the CH-46E at 24,300 lb., 20 in. aft CG, in level flight at 120 kt at sea level.

## 9.3 FUSELAGE DATA TABLE

The fuselage data table SKD represents the CH-46D, E and F fuselage aerodynamic characteristics. A listing is enclosed at the end of this Section. The table consists of a small preliminary set of data, followed by six main sets which represent respectively the lift, drag, sideforce, pitch moment, roll moment and yaw moment characteristics of the fuselage.

The first line of the preliminary set gives the number of sideslip values (33) and angle of attack values (8) which constitute the dimensions of each of the six main data sets. The next seven lines specify the 33 sideslip angles, and the following two lines specify the 8 angles of attack. There then follows a set of 8 groups of data with 33 entries each. These entries define the values of fuselage lift ( $L/q$ ) at the 33 sideslip angles and 8 angles of attack specified above. After the set of lift data comes a similar set of drag ( $D/q$ ) data, sideforce ( $Y/q$ ) data, pitch moment ( $M/q$ ) data, roll moment ( $R/q$ ) data, and yaw moment ( $N/q$ ) data.

#### 9.4 AIRFOIL DATA TABLES

Airfoil data tables 529 and 530 represent the CH-46E airfoil lift and drag characteristics. Both tables represent the V23010-1.58 airfoil section, the former being used at inboard blade stations where two-dimensional flow prevails, while the latter, which includes some three-dimensional relief, is used at the blade tip station. A listing of each airfoil table is included at the end of this section, following the fuselage data listing.

##### 9.4.1 Format of Airfoil Tables

The aerodynamic characteristics of an airfoil are input as two separate arrays of values:

- o The lift coefficient,  $C_L$ , is input at constant Mach Numbers at angles of attack from  $-20^\circ$  to  $20^\circ$ , for a maximum of up to 15 Mach Numbers and up to 26 angles of attack, where a minimum of four angles of attack is required.

- o The drag coefficient,  $C_D$ , is input at constant angles of attack for up to 15 Mach Numbers. The angle of attack range is not fixed and it has to be specified in the input. (A range  $-10^\circ$  to  $16^\circ$  is generally acceptable.)

A description of the airfoil tables is presented next. Enough detail is provided to assist both in the interpretation of existing tables or in the preparation of new ones.

#### 9.4.2 Lift Coefficient

##### Card

- a. Title Card (FORMAT (6X, I3, 17A4), with
  - o Table number to go in columns 7, 8, 9.
  - o Table number and table description starting in Column 11.
  
- b. Definition of positive and negative angle of attack range.
  - o Maximum positive angle of attack, set at  $180^\circ$ .
  - o Maximum negative angle of attack, set at  $-180^\circ$ .
  
- c. Constants used in equations to define the lift coefficient for angles of attack between  $20^\circ$  and  $340^\circ$ , as described in Section 4 of Reference 5.
  - o Lift coefficient for angle of attack at  $180^\circ$ , normally set at  $C_L = 0.0$
  - o Constant K1, for lift at  $20^\circ$  to  $90^\circ$ .
  - o Constant K2, for lift at  $90^\circ$  to  $160^\circ$  and  $160^\circ$  to  $180^\circ$  (separate equations).

- o Constant K3, for lift at  $180^\circ$  to  $200^\circ$  and  $200^\circ$  to  $270^\circ$  (separate equations).
- o Constant K4, for lift at  $270^\circ$  to  $340^\circ$ .

The constants K1, K2, K3 and K4 are normally set to 1.0. The equations and plots in Section 4 (Reference 5) show how the lift level at high angles of attack can be altered by using different K constants.

- d. Number of Mach Numbers in the lift table. The number of Mach Numbers used for the table is located in Columns 4 and 5. The maximum number allowed is 15.
- e. Mach Number data card(s). List Mach Numbers in ascending order starting with  $M = 0.0$  and finishing with  $M = 1.0$ .
- f. Case quantity card. This card determines the number of angle of attack and lift coefficient entries (26 maximum) for each Mach Number. The number of entries used is located in Columns 4 and 5.
- g. Angle of attack data card(s). List angles of attack, in degrees, in ascending order starting from  $0^\circ$ . The angle of attack values must be defined within the intervals  $0^\circ$  to  $20^\circ$  and  $340^\circ$  to  $360^\circ$ .
- h. Lift coefficient data card(s). Values of the lift coefficient corresponding to the angles of attack above, are listed in the same order as the angle of attack inputs.

Steps f, g and h are repeated for each Mach Number shown in card(s) e.

### 9.4.3 Drag Coefficient

#### Card

- a. Maximum positive and negative angles of attack in drag table. The angles are in degrees between  $0^\circ$  and  $360^\circ$ .
- b. Number of angles of attack in the drag table. The number of angles of attack is located in columns 4 and 5. A maximum of 26 angles of attack is allowed.
- c. Angle of attack data card(s). List angles of attack starting with  $0^\circ$  through  $360^\circ$  covering the ranges  $0^\circ$  to max. positive, and max. negative to  $360^\circ$ .
- d. Case quantity card. This card determines the number of Mach Number and drag coefficient entries (15 maximum) for each angle of attack. The number of entries is located in Columns 4 and 5.
- e. Mach Number data card(s). List Mach Numbers in ascending order starting with  $M = 0.0$  and finishing with  $M = 1.0$ . Seven Mach Numbers per card up to a maximum total of fifteen.
- f. Drag coefficient data card(s). Values of the drag coefficient corresponding to the Mach Numbers above are listed in the same order as the Mach Number inputs.

## 9.5 OUTPUT DATA

An example of A-97 output data is given in Figure 9-2, which presents a full set of trim and derivative output. These data are for the same flight conditions as entered in Section 9.2. Definitions for all output parameters are listed in Tables 9-1 and 9-2.

TABLE 9-1A

A97 TRIM ANALYSIS OUTPUT DEFINITION

(In order of appearance)

V	True airspeed along flight path	knots
FE	Equivalent drag area of fuselage	ft <sup>2</sup>
RC	Rate of climb	ft./min.
ALPHA	Fuselage angle of attack w.r.t. remote airstream	deg.
GW	Helicopter gross weight	lb.
ALFF	Fuselage angle of attack w.r.t. local airstream	deg.
RHO	Atmospheric density	sl./ft <sup>3</sup>
THETA	Fuselage pitch attitude (Euler angle)	deg.
XFLW	Forward rotor propulsive force parallel to local airstream	lb.
LFLW	Forward rotor lift force force perpendicular to local airstream	lb.
VTF(R)	Forward (aft) rotor tip speed	ft./sec
CGF	C.G. location ahead of reference station (approx.)	in.
CGL	Lateral c.g. offset from butt line 0	in.
BETAF	Fuselage sideslip angle	deg.
PHI	Fuselage roll altitude (Euler angle)	deg.
PSI	Fuselage yaw attitude (Euler angle)	deg.
GAMMA	Flight path climb angle	deg.
XR LW	Aft rotor propulsive force parallel to local airstream	lb.
LR LW	Aft rotor lift force perpendicular to local airstream	lb.
THEOF(R)	Forward (aft) rotor root collective pitch at CL of rotor	deg.

TABLE 9-1B

AlCF(R)	Forward (aft) rotor lateral cyclic pitch (positive tilts TPP toward advancing side)	deg.
BlTF(R)	Forward (aft) rotor longitudinal trim cyclic pitch (positive tilts TPP forward)	deg.
BlCF(R)	Forward (aft) rotor total longitudinal cyclic pitch (positive tilts TPP forward)	deg.
DFW	Fuselage drag parallel to local airstream	lb.
LFFW	Fuselage lift perpendicular to local airstream	lb.
THETAC	Mean rotor root collective pitch	deg.
DELTAB	Longitudinal stick position (all trim systems neutral)	in.
DELTAS	Lateral stick position (all trim system neutral)	in.
DELTAR	Directional pedal position (all trim systems neutral)	in.
DELTAC	Collective stick position	in.
TF(R)	Forward (aft) rotor thrust parallel to shaft axis	lb.
HF(R)	Forward (aft) rotor downstream force perpendicular to shaft axis	lb.
YF(R)	Forward (aft) rotor side force perpendicular to shaft axis toward advancing side	lb.
MHF(R)	Forward (aft) rotor nose-up hub moment	lb.-ft.
LHF(R)	Forward (aft) rotor roll hub moment toward advancing side	lb.-ft.
QF(R)	Forward rotor torque required	lb.-ft.
LFZ	Fuselage lift in fuselage axis system	lb.
DFX	Fuselage drag in fuselage axis system	lb.
YFY	Fuselage side force to right side	lb.

TABLE 9-1C

MF	Fuselage nose-up pitch moment	lb.-ft.
LF	Fuselage right roll moment	lb.-ft.
NF	Fuselage right yaw moment	lb.-ft.
RHPF(R)	Forward (aft) rotor power required	HP
XR	Total rotor propulsive force along flight path	lb.
L/DE	Equivalent lift/drag ratio of helicopter	-
SHPTOT	Total power required by helicopter	HP
WFF	Dummy parameter	-
NMLB	Dummy parameter	-
SIGOF(R)	Forward (aft) rotor solidity ratio	-
CTSF(R)	Forward (aft) rotor thrust coefficient	-
CPSF(R)	Forward (aft) rotor power coefficient	-
AMTF(R)	Forward (aft) rotor advancing tip Mach No.	-
LAMDAF(R)	Forward (aft) rotor inflow ratio	-
MUF(R)	Forward (aft) rotor advance ratio	-
VF(R)	Forward (aft) rotor induced velocity	ft./sec.
DFFR	Interference factor for forward rotor on aft rotor	-
DFRF	Interference factor for aft rotor on forward rotor	-
DFF	Interference factor for both rotors on fuselage	-
AOF(R)	Forward (aft) rotor coning angle	deg.
AlF(R)	Forward (aft) rotor longitudinal flapping angle (positive for aft TPP tilt)	deg.
BlF(R)	Forward (aft) rotor lateral flapping angle (positive for TPP tilt to advancing side)	deg.

TABLE 9-1D

FETAOF(R)	Forward (aft) rotor blade flap angle at downwind azimuth ( $\psi = 0^\circ$ )	deg.
B180F(R)	Forward (aft) rotor blade flap angle at upwind azimuth ( $\psi = 180^\circ$ )	deg.
A270F(R)	Forward (aft) rotor blade tip angle of attack on retreating side ( $\psi = 270^\circ$ )	deg.
CAPVF(R)	Forward (aft) rotor velocity in local airstream	ft./sec.
ALPHAF(R)	Forward (aft) rotor disc angle of attack w.r.t. local airstream	deg.
BETAF(R)W	Forward (aft) rotor disc sideslip angle w.r.t. local airstream	deg.
ATIPF(R)	Forward (aft) rotor TPP angle of attack w.r.t. remote airstream	deg.
BPTPF(R)	Forward (aft) rotor total flapping amplitude (lateral and longitudinal)	deg.
XFF, LFF ZFF, YFF MFF, NFF	Force and moment components of external force applied to the helicopter (e.g. auxiliary propulsion, tow cable force, etc.)	lb. & lb.-ft.
TP	Magnitude of external force on helicopter	lb.
RMTF(R)	Forward (aft) rotor retreating blade tip Mach No.	-
CTF(R)P	Thrust coefficient format for LF(R) LW	-
A90F(R)	Forward (aft) rotor blade tip angle of attack on advancing side ( $\psi = 90^\circ$ )	deg.
DELHPF(R)	Additional power computed for forward (aft) rotor by nonuniform downwash power correction	HP
RHPF(R)	Forward (aft) rotor power required, revised by nonuniform downwash power correction	HP
SHPTOT	Total power required by helicopter, revised by nonuniform downwash power correction	HP

TABLE 9-1E

WFF	Dummy parameter	-
NMLB	Dummy parameter	-
RP	Dummy parameter	-

TABLE 9-2A

A97 STABILITY DERIVATIVE OUTPUT DEFINITION

Helicopter Derivative Parameters

(In order of appearance)

X	Non-dimensionalized force component along helicopter longitudinal axis, positive forward	ft./sec <sup>2</sup>
Z	Non-dimensionalized force component along helicopter vertical axis, positive down	ft./sec <sup>2</sup>
M	Non-dimensionalized pitch moment about helicopter lateral axis, positive nose up	rad/sec <sup>2</sup>
Y	Non-dimensionalized force component along helicopter lateral axis, positive right	ft./sec <sup>2</sup>
L	Non-dimensionalized roll moment about helicopter longitudinal axis, positive roll right	rad/sec <sup>2</sup>
N	Non-dimensionalized yaw moment about helicopter vertical axis, positive nose right	rad/sec <sup>2</sup>
U	Velocity perturbation along helicopter longitudinal axis, positive forward	ft./sec.
V	Velocity perturbation along helicopter lateral axis, positive right	ft./sec.
W	Velocity perturbation along helicopter vertical axis, positive down	ft./sec.
P	Angular rate perturbation about helicopter longitudinal axis, positive roll right	rad/sec.
Q	Angular rate perturbation about helicopter lateral axis, positive nose up	rad/sec.
R	Angular rate perturbation about helicopter vertical axis, positive nose right	rad/sec.
DELB	Pitch control perturbation about helicopter lateral axis, positive nose up	in.

TABLE 9-2B

DELS	Roll control perturbation about helicopter longitudinal axis, positive roll right	in.
DELR	Yaw control perturbation about helicopter vertical axis, positive nose right	in.
DELTAC	Collective control perturbation along helicopter vertical axis, positive up	in.
ALPHA	Aerodynamic angle of attack perturbation, ( $\tan^{-1} W/U$ )	rad
BETA	Aerodynamic sideslip angle perturbation, ( $\tan^{-1} V/U$ )	rad

Component Derivative Parameters

(In alphabetical order)

ALPHA	Aerodynamic angle of attack perturbation	rad
AIC	Rotor lateral cyclic pitch perturbation (positive tilts TPP toward advancing side)	rad
ALF(R)	Forward (aft) rotor longitudinal flapping angle (positive for aft TPP tilt)	rad
BETA	Aerodynamic sideslip angle perturbation	rad
BLF(R)	Forward (aft) rotor lateral flapping angle (positive for TPP tilt to advancing side)	rad
CHF(R)	Forward (aft) rotor downstream force coefficient, perpendicular to shaft axis	-
CTF(R)	Forward (aft) rotor thrust coefficient, parallel to shaft axis	-
CYF(R)	Forward (aft) rotor sideforce coefficient, perpendicular to shaft toward advancing side	-
DF	Fuselage drag in fuselage axis system	lb.
LF	Fuselage lift in fuselage axis system	lb.
LF	Fuselage right roll moment	lb.-ft.

TABLE 9-2C

MF	Fuselage nose up pitch moment	lb.-ft.
MU	Rotor advance ratio perturbation	-
NF	Fuselage nose right yaw moment	lb.-ft.
P	Angular rate perturbation about helicopter longitudinal axis, positive roll right	rad/sec.
Q	Angular rate perturbation about helicopter lateral axis, positive nose up	rad/sec.
R	Angular rate perturbation about helicopter vertical axis, positive nose right	rad/sec.
THETAC	Rotor collective pitch perturbation	rad
U	Velocity perturbation along helicopter longitudinal axis, positive forward	ft./sec.
V	Velocity perturbation along helicopter lateral axis, positive to right	ft./sec.
VF(R)R	Forward (aft) rotor induced velocity	ft./sec.
W	Velocity perturbation along helicopter vertical axis, positive down	ft./sec.
YF	Fuselage side force to right side	lb.

Supplementary Derivative Parameters

(In alphabetical order)

B1CF(R)	Forward (aft) rotor longitudinal cyclic pitch perturbation (positive tilts TPP forward)	rad
OMEGAF(R)	Forward (aft) rotor RPM perturbation (not computed for synchronized rotors)	rad/sec.
QF(R)	Non-dimensionalized forward (aft) rotor torque required	rad/sec <sup>2</sup>

All other parameters are as defined above for "Helicopter Derivative Parameters" and "Component Derivative Parameters".

RETURN TO:		TRIM AND STABILITY ANALYSIS FOR TANDEM HELICOPTERS	AIRFOIL DATA			
PROGRAM A-97			TABLE 1	TABLE 2	TABLE 3	TABLE 4
HELICOPTER MODEL SKD			529	530		

INPUT			CASE NO.	INPUT			CASE NO.	INPUT			CASE NO.
NO	SYM	UNIT		NO	SYM	UNIT		NO	SYM	UNIT	
1	V	AMOTS	120.	49	b <sub>0</sub>	—	3	97	δ <sub>ACCF</sub>	DEG	0
2	R/C	FT/MIN	0	50	c <sub>0</sub>	FT	.425	98	δ <sub>ACCB</sub>	DEG.	0.
3	G.W.	LOS	24300	51	F <sub>10</sub>	—	0.	99	δ <sub>ACCB</sub>	DEG	0
4	H <sub>p</sub>	FT	0.	52	θ <sub>TWR</sub>	DEG	-8.5	100	N <sub>TANES</sub>	—	3
5	T	°	59.	53	λ <sub>CR</sub>	—	.219	101	λ <sub>TAB1</sub>	—	.219
6	β <sub>F</sub>	DEG	0.	54	k <sub>RR</sub>	—	0.	102	λ <sub>TAB2</sub>	—	.85
7	α <sub>FF</sub>	LOS/HR	1.	55	l <sub>0</sub>	DEG	7.0	103	λ <sub>TAB3</sub>	—	1.00
8	β <sub>FF</sub>	LOS/HR SHIP	1.	56	V <sub>DR</sub>	FT/SEC	705.	104	λ <sub>TAB4</sub>	—	
9	K <sub>FF</sub>	—	1.	57	I <sub>0</sub>	SLUGS -FT <sup>2</sup>	1120	105	λ <sub>TAB5</sub>	—	
10	N <sub>FF</sub>	—	1.	58	M <sub>DR</sub>	FT-LOS	2330	108	θ <sub>TW</sub>	—	4.
11	η <sub>F</sub>	—	1.	59	B <sub>ITR</sub>	DEG	4.0	107	N <sub>Z</sub>	—	
12	η <sub>R</sub>	—	1.	60	B <sub>ICR</sub>	DEG/IN	0.	108	X <sub>1</sub>	—	
13	B <sub>IP</sub>	ACC HP	100.	61	A <sub>ICR</sub>	DEG/IN	-1.37	109	X <sub>2</sub>	—	
14	V <sub>HR</sub>	AMOTS	0.	62	A <sub>ICR</sub>	DEG/IN	2.44	110	X <sub>3</sub>	—	
15	f <sub>e</sub>	FT <sup>2</sup>	44	63	θ <sub>TW</sub>	DEG	5.29	111	X <sub>4</sub>	—	
16	Δu	FT/SEC	5	64	θ <sub>0</sub>	DEG/IN	-639	112	X <sub>5</sub>	—	
17	Δv	FT/SEC	5.	65	l <sub>0</sub>	FT	15.8	113	σ <sub>0</sub>	—	
18	Δw	FT/SEC	5	66	h <sub>0</sub>	FT	10.7	114	σ <sub>1</sub>	—	
19	Δp	DEG/SEC	5	67	d <sub>0</sub>	FT	0	115	X <sub>6</sub>	—	
20	Δq	DEG/SEC	5.	68	l <sub>c</sub>	FT	-1.2	116	X <sub>6</sub>	—	
21	Δr	DEG/SEC	5.	69	h <sub>c</sub>	FT	-0.1	117	σ <sub>1</sub>	—	
22	Δδ <sub>c</sub>	DEG.	1	70	d <sub>c</sub>	FT	0.	118	σ <sub>2</sub>	—	
23	Δδ <sub>0</sub>	IN.	1.	71	INT	—	5.	119	σ <sub>3</sub>	—	
24	Δδ <sub>L</sub>	IN.	1.	72	DER	—	0.	120	σ <sub>4</sub>	—	
25	Δδ <sub>R</sub>	IN.	1.	73	F	LOS	0	121	σ <sub>5</sub>	—	
26	R <sub>F</sub>	FT.	25.5	74	X <sub>FF</sub>	FT	0	122	σ <sub>6</sub>	—	
27	C <sub>F</sub>	FT	1.56	75	Y <sub>FF</sub>	FT.	0	123	σ <sub>7</sub>	—	
28	b <sub>F</sub>	—	3.	76	Z <sub>FF</sub>	FT	0	124	σ <sub>8</sub>	—	
29	e <sub>F</sub>	FT.	.425	77	W <sub>FF</sub>	DEG.	0.	125	σ <sub>9</sub>	—	
30	f <sub>IF</sub>	—	0.	78	θ <sub>FF</sub>	DEG	0.	128	θ <sub>TW1</sub>	DEG.	
31	θ <sub>TWR</sub>	DEG	-8.5	79	I <sub>XX</sub>	SLUGS -FT <sup>2</sup>	17735.	127	θ <sub>TW2</sub>	DEG.	
32	X <sub>CR</sub>	—	.219	80	I <sub>YY</sub>	SLUGS -FT <sup>2</sup>	115701.	128	θ <sub>TW3</sub>	DEG.	
33	k <sub>RR</sub>	—	0	81	I <sub>ZZ</sub>	SLUGS -FT <sup>2</sup>	106769.	129	θ <sub>TW4</sub>	DEG.	
34	l <sub>0</sub>	DEG.	9.5	82	I <sub>ZZ</sub>	SLUGS -FT <sup>2</sup>	10012.	130	θ <sub>TW5</sub>	DEG.	
35	V <sub>TR</sub>	FT/SEC	705.	83	T <sub>CHAR</sub>	—	0	131	θ <sub>TW6</sub>	DEG.	
36	I <sub>0</sub>	LOS -FT <sup>2</sup>	1120.	84	—	—	0 0	132	θ <sub>TW7</sub>	DEG.	
37	M <sub>DR</sub>	FT-LOS	2330.	85	θ	DEG	0.	133	θ <sub>TW8</sub>	DEG.	
38	B <sub>ITR</sub>	DEG	2.8	86	T <sub>0</sub>	—	0.	134	θ <sub>TW9</sub>	DEG.	
39	B <sub>ICR</sub>	DEG/IN	0.	87	T <sub>L0</sub>	—	0	135	N <sub>UD</sub>		1
40	A <sub>ICR</sub>	DEG/IN	1.64	88	T <sub>T</sub>	LOS.	0	136	K <sub>F</sub>		1.56
41	A <sub>ICR</sub>	DEG/IN	2.44	89	θ <sub>T</sub>	DEG.	0	137	ΔZ		1.56
42	θ <sub>TW</sub>	DEG.	8.71	90	W <sub>T</sub>	DEG.	0				
43	l <sub>0</sub>	DEG/IN	.639	91	Y <sub>T</sub>	FT	0	119	AW	RPS	0.
44	l <sub>0</sub>	FT	17.2	92	Y <sub>T</sub>	FT.	0.	120	AW	RPS	0.
45	h <sub>0</sub>	FT	6.1	93	Z <sub>T</sub>	FT.	0	171	ABUSE	RAD	0.1
46	d <sub>0</sub>	FT	0	94	σ <sub>0</sub>	DEG/IN	1.29	171	ABUSE	RAD	0.1
47	h <sub>c</sub>	FT	35.5	95	σ <sub>0</sub>	DEG/IN	1.29				
48	l <sub>c</sub>	FT	1.56	96	β <sub>ACCF</sub>	DEG	0.				

Figure 9-1 A-97 INPUT SHEET (Typical)

TRIM

V FE 1.200000D+02 4.400000D+01	RC ALPHA 0.0 3.950123D-01	GW ALFF 2.430000D+04 -1.583609D+00	RHO THETA 2.378000D-03 4.402904D-01	XF LW LF LW 1.260445D+03 1.219621D+04
VTF VTR 7.050000D+02 7.050000D+02	CGF CGL 6.239495D+00 0.0	BETAF PHI 0.0 -4.304547D-01	PSI GAMMA -2.897783D-03 0.0	XR LW LR LW 1.589627D+03 1.194967D+04
THEOF THEOR 1.652549D+01 1.716219D+01	AICF AICR -2.660313D-01 -3.559054D-01	B1TF B1TR 2.800000D+00 4.000000D+00	B1CF B1CR 2.800000D+00 4.000000D+00	DFW LFFW 2.157337D+03 8.479755D+01
THETAC 1.684384D+01	DELTAB -3.174262D+00	DELTAS 1.029000D-02	DELTAR -1.516481D-01	DELTAC 7.630884D+00
TF TR 1.224200D+04 1.204642D+04	HF HR 6.854137D+02 4.533266D+02	YF YR 5.864929D+01 5.790984D+01	MHF MHR 1.864533D+03 1.268156D+03	LHF LHR 8.867044D+02 9.289536D+02
QF QR 1.847454D+04 2.104082D+04	LFZ DFX 9.966867D+01 2.156701D+03	YFY MF 1.861127D+02 -3.869964D+03	LF NF 7.586383D+02 6.991866D+02	RHPF RHPR 9.286669D+02 1.057667D+03
XR 2.195750D+03	L/DE 7.010955D+00	SHPTOT 2.086334D+03	WFF 2.087334D+03	NMLB 5.748961D-02
SIGOF SIGOR 5.841923D-02 5.841923D-02	CTSF CTSR 8.676783D-02 8.564260D-02	CPSF CPSR 5.136384D-03 5.849871D-03	AMTF AMTR 8.107789D-01 8.113728D-01	LAMDAF LAMDAR -5.532464D-02 -5.856792D-02
MUF MUR 2.838569D-01 2.855711D-01	VF VR 6.932082D+00 6.759314D+00	DFFR DFRF 1.618399D+00 2.715417D-01	DFF 9.191692D-01	AOF AOR 4.676605D+00 4.598625D+00
A1F A1R 3.028768D+00 2.059491D+00	B1F B1R 1.439853D+00 1.508474D+00	BETAOF BETAOR 1.132310D+00 2.038444D+00	B18OF B18OR 7.258837D+00 6.199418D+00	A27OF A27OR 1.077835D+01 1.096130D+01
CAPVF CAPVR 2.026728D+02 2.042675D+02	ALPHAF ALPHAR -9.104988D+00 -9.732481D+00	BETAFW BETARW 3.600000D+02 3.600000D+02	ATIPF ATIPR -6.076220D+00 -4.545497D+00	BPTPF BPTPR 3.353597D+00 2.552841D+00

FIGURE 9-2A A-97 OUTPUT DATA (TYPICAL)

TRIM

XFF	ZFF	MFF	TP
LFF	YFF	NFF	
0.0	0.0	0.0	0.0
0.0	0.0	0.0	
RMTF	CTFP	A90F	
RMTR	CTRP	A90RA	
4.475526D-01	8.646668D-02	7.513619D-01	
4.466828D-01	8.471883D-02	7.403006D-01	

3

NON UNIFORM DOWNWASH POWER CORRECTIONS

DELHPF	RHPF	SHPTOT	NMLB
DELHPR	RHPR	WFF	RP
6.116725D+01	9.898342D+02	2.207432D+03	5.433720D-02
5.993081D+01	1.117598D+03	2.208432D+03	1.320394D+03

FIGURE 9-2B A-97 OUTPUT DATA (TYPICAL)

HELICOPTER DERIVATIVES

STABILITY DERIVATIVES OUTPUT

MASS 7.552682D+02	IXX 1.773500D+04	IYY 1.157010D+05	IZZ 1.067690D+05
XU XV XW -4.639774D-02 -7.295587D-04 4.534633D-02	XP XQ XR 8.190768D-02 1.232392D+00 -3.501802D-02	XDELB XDELS XDELR 2.995072D-02 -1.424371D-03 -3.933992D-02	XDELTA XBETA XALPHA 3.880805D-01 -1.478873D-01 9.192062D+00
ZU ZV ZW 1.828268D-02 5.161436D-03 -6.890382D-01	ZP ZQ ZR -8.565600D-01 -2.111599D+00 -5.364988D-01	ZDELB ZDELS ZDELR 4.419884D-01 -6.128484D-03 8.998662D-02	ZDELTA ZBETA ZALPHA -7.310245D+00 1.046264D+00 -1.396735D+02
MU MV MW -2.817400D-03 8.529271D-04 1.012176D-02	MP MQ MR 2.110222D-01 -1.369130D+00 -3.561702D-01	MDELB MDELS MDELR 4.955564D-01 -7.879279D-03 1.518260D-03	MDELTA MBETA MALPHA 1.271578D-01 1.728951D-01 2.051761D+00
YU YV YW 2.280255D-03 -1.290233D-01 -3.806622D-03	YP YQ YR -1.044760D+00 -5.803616D-03 -1.652531D-01	YDELB YDELS YDELR 7.739074D-03 8.726928D-01 9.023258D-03	YDELTA YBETA YALPHA -9.370916D-04 -2.615405D+01 -7.716324D-01
LU LV LW 2.141228D-04 -1.637886D-02 -5.234853D-04	LP LQ LR -6.164785D-01 6.529759D-02 -2.376264D-02	LDELB LDELS LDELR -2.586552D-02 4.113135D-01 -1.360597D-01	LDELTA LBETA LALPHA -9.759720D-03 -3.320125D+00 -1.061146D-01
NU NV NW 1.763654D-04 -3.698349D-03 -4.120916D-04	NP NQ NR -4.439538D-02 -1.545054D-01 -8.277363D-02	NDELB NDELS NDELR 5.373065D-02 1.568339D-02 1.659887D-01	NDELTA NBETA NALPHA -2.867393D-03 -7.496847D-01 -8.353424D-02

FIGURE 9-2C A-97 OUTPUT DATA (TYPICAL)

COMPONENT DERIVATIVES

LONGITUDINAL

	U	MU	W	ALPHA	Q	THETAC
CTF	-0.967D-05	-0.682D-02	0.107D-03	0.218D-01	-0.145D-02	0.581D-01
CTR	0.139D-05	0.982D-03	0.879D-04	0.178D-01	0.218D-02	0.447D-01
CHF	0.167D-05	0.117D-02	0.908D-05	0.184D-02	-0.321D-03	0.572D-02
CHR	0.269D-05	0.189D-02	0.584D-05	0.118D-02	-0.436D-04	0.399D-02
A1F	0.392D-03	0.276D+00	0.102D-02	0.206D+00	-0.889D-01	0.899D+00
A1R	0.511D-03	0.360D+00	0.843D-03	0.171D+00	-0.590D-01	0.788D+00
VFR	-0.468D-01	-0.330D+02	0.147D+00	0.297D+02	-0.208D+01	0.788D+02
VRR	-0.303D-01	-0.214D+02	0.120D+00	0.243D+02	0.299D+01	0.593D+02
LF			0.490D+02	0.993D+04		
DF			-0.124D+01	-0.252D+03		
MF			0.258D+03	0.524D+05		

LATERAL-DIRECTIONAL

	V	BETA	P	R	A1C
CYF	-0.274D-05	-0.555D-03	-0.167D-03	-0.692D-04	0.523D-02
CYR	0.275D-05	0.557D-03	0.160D-03	-0.174D-04	0.516D-02
B1F	-0.250D-03	-0.506D-01	-0.658D-01	-0.169D-01	0.103D+01
B1R	0.352D-03	0.713D-01	0.722D-01	0.416D-03	0.103D+01
YF	-0.842D+02	-0.171D+05			
LF	-0.143D+03	-0.289D+05			
NF	-0.381D+03	-0.772D+05			
CTF					-0.385D-03
CTR					-0.320D-03

FORCE = 0.241446D+07

FIGURE 9-2D A-97 OUTPUT DATA (TYPICAL)

SUPLEMENTARY DERIVATIVES

	BICF	BICR	OMEGAF	OMEGAR
X	0.105D+02	0.114D+02	0.0	0.0
Z	0.550D+02	0.711D+02	0.0	0.0
M	-0.106D+02	0.631D+01	0.0	0.0
Y	0.183D+00	-0.231D+00	0.0	0.0
L	-0.104D+00	-0.212D-01	0.0	0.0
N	-0.129D+00	0.236D+00	0.0	0.0
CTF	-0.218D-01	0.380D-06	0.0	0.0
CTR	0.512D-02	-0.220D-01	0.0	0.0
CHF	-0.666D-02	0.854D-07	0.0	0.0
CHR	0.315D-03	-0.629D-02	0.0	0.0
AIF	-0.122D+01	0.154D-04	0.0	0.0
AIR	0.456D-01	-0.122D+01	0.0	0.0
VFR	-0.295D+02	-0.599D-02	0.0	0.0
VRR	0.722D+01	-0.295D+02	0.0	0.0
QF	-0.407D+01	-0.441D-03	0.0	0.0
QR	0.721D+00	-0.671D+01	0.0	0.0
	QFU	QFP	QFDELB	QFDELTAC
	QFV	QFQ	QFDELS	QFBETA
	QFW	QFR	QFDELR	QFALPHA
	-0.591D-02	-0.518D+00	0.762D+00	0.176D+01
	-0.178D-03	0.243D+01	-0.144D-01	-0.361D-01
	-0.655D-02	-0.739D+00	-0.224D-01	-0.133D+01
	QRU	QRP	QRDELB	QRDELTAC
	QRV	QRQ	QRDELS	QRBETA
	QRW	QRR	QRDELR	QRALPHA
	-0.720D-02	0.451D+00	-0.936D+00	0.186D+01
	-0.298D-03	0.199D+01	0.168D-01	-0.604D-01
	0.979D-02	0.824D+00	-0.293D-01	0.198D+01

FIGURE 9-2E A-97 OUTPUT DATA (TYPICAL)

EGSKD000

-90.	-30.	-70.	-60.	-55.	0001
-50.	-45.	-40.	-30.	-25.	0002
-20.	-15.	-12.	-9.	-6.	0003
-3.	0.	3.	6.	9.	0004
12.	15.	20.	25.	30.	0005
40.	45.	50.	55.	60.	0006
70.	80.	90.			0007
					0008

SIDESLIP ANGLES

-90.0	-14.8	-4.5	0.4	5.3	0009
10.2	20.2	90.			0010

ANGLE OF ATTACK  
VALUES

-330.	-330.	-330.	-330.	-330.	0011
-330.	-330.	-330.	-330.	-330.	0012
-330.	-330.	-330.	-330.	-330.	0013
-330.	-330.	-330.	-330.	-330.	0014
-330.	-330.	-330.	-330.	-330.	0015
-330.	-330.	-330.	-330.	-330.	0016
-330.	-330.	-330.	-330.	-330.	0017
-317.	-330.	-322.	-301.	-287.	0018
-291.	-267.	-221.	-104.	-70.5	0019
-96.9	-52.6	-53.8	-55.3	-56.3	0020
-55.5	-55.4	-55.3	-54.9	-54.9	0021
-53.1	-50.6	-55.	-55.	-46.	0022
-188.	-231.	-249.	-255.	-283.	0023
-318.	-333.	-317.			0024
-320.	-312.	-296.	-263.	-245.	0025
-221.	-204.	-172.	-63.9	-36.0	0026
-11.3	-4.2	-7.9	-9.4	-8.7	0027
-7.8	-9.2	-10.1	-10.3	-9.7	0028
-8.0	-8.1	-11.5	-27.1	-34.0	0029
-155.	-179.	-195.	-223.	-238.	0030
-276.	-307.	-309.			0031
-314.	-303.	-278.	-239.	-214.	0032
-189.	-173.	-142.	-52.1	-22.7	0033
-1.3	9.7	13.4	11.0	8.9	0034
9.6	9.0	8.5	7.0	9.8	0035
11.1	7.9	0.2	-17.0	-23.7	0036
-142.	-155.	-173.	-198.	-227.	0037
-260.	-303.	-313.			0038
-321.	-301.	-264.	-204.	-177.	0039
-159.	-146.	-116.	-34.5	-5.4	0040
14.1	26.3	29.0	28.9	24.6	0041
26.3	26.8	25.8	24.1	27.5	0042
27.1	24.2	13.7	-6.7	-35.4	0043
-125.	-137.	-151.	-163.	-199.	0044
-255.	-297.	-313.			0045
-315.	-283.	-245.	-197.	-154	0046
-131.	-114.	-79.3	-7.4	17.3	0047
34.4	44.0	48.5	47.4	42.3	0048
45.4	46.7	44.5	42.8	45.6	0049
45.3	43.6	32.8	17.4	-19.7	0050
-88.3	-109.	-131.	-145.	-177	0051
-242.	-294.	-112.			0052
-317.	-265.	-712.	-123.	-92.9	0053
-86.8	-70.8	-15.1	53.6	69.7	0054
80.3	82.3	86.2	85.4	83.0	0055
84.9	85.5	83.0	79.4	81.1	0056
83.5	79.4	70.5	52.0	17.0	0057
-30.6	-82.8	-94.1	-97.0	-112.	0058
-211	-252.	-310.2			0059
330.	330.	330.	330.	330.	0060
330.	330.	330.	330.	330.	0061
330.	330.	330.	330.	330.	0062
330.	330.	330.	330.	330.	0063
330.	330.	330.	330.	330.	0064
330.	330.	330.	330.	330.	0065
330.	331.	330.			0066

LIFT L/q  
(FT<sup>2</sup>)

CH-46 FUSELAGE CHARACTERISTICS

0.0	0.0	0.0	0.0	0.0	0067
0.0	0.0	0.0	0.0	0.0	0068
0.0	0.0	0.0	0.0	0.0	0069
0.0	0.0	0.0	0.0	0.0	0070
0.0	0.0	0.0	0.0	0.0	0071
0.0	0.0	0.0	0.0	0.0	0072
0.0	0.0	0.0	0.0	0.0	0073
-22.84	-25.26	-20.60	-7.24	-5.35	0074
8.50	14.89	15.64	21.86	33.04	0075
19.77	21.23	22.43	22.79	23.03	0076
23.50	24.87	24.58	23.91	22.85	0077
22.40	20.78	19.55	14.85	10.63	0078
2.32	2.87	-4.90	-15.68	-14.33	0079
-23.41	-26.43	-31.23			0080
-24.91	-19.11	-4.23	0.	0.80	0081
-0.59	6.83	23.21	24.48	25.79	0082
27.81	29.29	29.23	29.15	28.35	0083
28.27	28.32	28.28	27.70	27.98	0084
27.61	27.26	25.23	22.14	18.07	0085
13.69	-4.58	-17.23	-6.52	-4.31	0086
-19.30	-23.98	-28.79			0087
-24.63	-17.32	-6.12	-1.84	-5.77	0088
-3.96	11.01	15.55	24.23	26.25	0089
29.47	30.88	29.09	28.03	28.11	0090
28.07	28.13	28.29	28.19	29.03	0091
29.67	29.39	28.96	24.22	20.08	0092
15.11	-2.21	-7.48	-4.40	3.19	0093
-11.12	-24.60	29.24			0094
-2.08	-16.26	-3.54	3.68	-7.01	0095
-5.53	10.10	14.90	23.01	25.09	0096
28.30	29.07	27.52	27.78	23.35	0097
26.00	26.84	26.95	26.18	29.02	0098
29.20	28.57	27.55	24.40	21.37	0099
17.64	-2.46	-7.73	-8.14	3.50	0100
-12.65	-23.22	-31.04			0101
-27.13	-19.52	-5.65	10.07	-6.48	0102
-9.27	6.52	8.80	17.39	20.81	0103
24.17	26.76	27.14	26.40	23.53	0104
23.61	23.23	23.55	23.33	26.93	0105
26.68	26.47	25.29	22.47	19.33	0106
10.14	-9.43	-13.61	-11.70	0.70	0107
-13.85	-22.59	-30.69			0108
-26.44	-16.28	-14.56	-0.62	3.90	0109
12.62	17.39	0.17	4.18	7.45	0110
13.61	16.94	18.72	18.32	16.81	0111
17.20	17.93	17.26	17.62	19.41	0112
18.19	17.80	15.81	12.01	14.48	0113
5.01	19.38	16.81	4.29	-5.42	0114
-12.06	-19.89	-29.40			0115
0.0	0.0	0.0	0.0	0.0	0116
0.0	0.0	0.0	0.0	0.0	0117
0.0	0.0	0.0	0.0	0.0	0118
0.0	0.0	0.0	0.0	0.0	0119
0.0	0.0	0.0	0.0	0.0	0120
0.0	0.0	0.0	0.0	0.0	0121
0.0	0.0	0.0	0.0	0.0	0122

DRAG D/q  
(FT<sup>2</sup>)

CH-46 FUSELAGE CHARACTERISTICS

346.	344.	333.	326.	350.	0123
360.	314.	260.	194.	154.	0124
147.	109.	90.2	67.7	47.2	0125
24.2	0.0	-15.8	-38.1	-59.1	0126
-85.2	-105.	-134.	-168.	-195.	0127
-271.	-316.	-356.	-349.	-332.	0128
-341.	-337.	-343.			0129
346.	344.	333.	326.	350.	0130
360.	314.	260.	194.	154.	0131
147.	109.	90.2	67.7	47.2	0132
24.2	5.1	-15.8	-38.1	-59.1	0133
-85.2	-105.	-134.	-168.	-195.	0134
-271.	-316.	-356.	-349.	-332.	0135
-341.	-337.	-343.			0136
338.	354.	341.	355.	371.	0137
406.	359.	283.	195.	160.	0138
128.	101.	79.8	61.7	44.8	0139
23.5	5.0	-12.8	-32.2	-51.6	0140
-69.7	-87.3	-119.	-150.	-187.	0141
-270.	-345.	-392.	-359.	-339.	0142
-342.	-341.	-334.			0143
327.	344.	357.	360.	386	0144
424	364.	296.	201	154	0145
119.	88.3	73.2	57.6	39.5	0146
22.2	3.6	-13.3	-32.4	-48.7	0147
-63.2	-79.4	-110.	-149	-192.	0148
-283	-358.	-402.	-375.	-342	0149
-344	-348	-333.			0150
334.	349.	345	367.	407.	0151
435.	375.	307.	206.	164	0152
121.	84.2	66.6	50.7	39.2	0153
19.6	4.8	-13.1	-32.1	-42.5	0154
-58.5	-78.0	-112.	-155.	-199	0155
-293.	-367.	-416.	-399.	-373.	0156
-349.	-348.	-330.			0157
328.	350.	366.	398.	423.	0158
444.	388.	329	222.	177.	0159
111	86.1	67.7	49.2	39.6	0160
20.5	3.5	-15.4	-33.9	-43.0	0161
-60.7	-80.0	-119.	-167.	-217.	0162
-315	-385.	-435.	-423.	-410.	0163
-360	-343.	-327.			0164
377.	353.	386.	430	428.	0165
405.	374.	349.	254.	211.	0166
15.	106.	81.6	64.2	49.6	0167
23.9	2.9	-22.1	-46.1	-61.1	0168
-81.2	-105.	-153.	-204.	-250.	0169
-334	-374.	-400.	-431.	-449.	0170
-381.	-351.	-327.			0171
327	353.	386	430.	428.	0172
405.	374.	349.	254.	211	0173
15.	106.	81.6	64.2	49.6	0174
23.9	0.0	-22.1	-46.1	-61.1	0175
-81.2	-105.	-153.	-204	-250.	0176
-334	-374.	-400.	-431.	-449	0177
-381	-341	-327			0178

SIDE FORCE

Y/q

(FT<sup>2</sup>)

CH-46 FUSELAGE CHARACTERISTICS

0 0	0 0	0 0	0 0	0 0	0179
0.0	0.0	0.0	0.0	0.0	0180
0.0	0.0	0.0	0.0	0.0	0181
0.0	0.0	0.0	0.0	0.0	0182
0.0	0.0	0.0	0.0	0.0	0183
0.0	0.0	0.0	0.0	0.0	0184
0.0	0.0	0.0	0.0	0.0	0185
-773.	-851.	-1106.	-1332.	-1567.	0186
-1462.	-1337.	-1050.	-615.	-429.	0187
-957.	-510.	-478.	-464.	-452.	0188
-436.	-429.	-434.	-451.	-459.	0189
-506.	-541.	-555.	-659.	-814.	0190
-1267.	-1549.	-1677.	-1663.	-1364.	0191
-1069.	-846.	-579.			019.
-762.	-802.	-750.	-1234.	-1318.	0193
-1591.	-1281.	-872.	-447.	-361.	0194
-267.	-198.	-168.	-173.	-185.	0195
-172.	-158.	-149.	-172.	-179.	0196
-178.	-198.	-256.	-370.	-501.	0197
-904.	-1491.	-1709.	-1241.	-958.	0198
-821.	-729.	-551.			0199
-699.	-808.	-624.	-1074.	-1293	0200
-1700.	-1310	-797.	-366.	-235	0201
-137.	-67.8	-65.8	-42.2	-54.9	0202
-53.2	-34.4	-45.7	-63.0	-46.9	0203
-33.3	-79.5	-116.	-239	-407	0204
-815.	-1443.	-1603.	-1163.	-776.	0205
-712.	-719.	-590.			0206
-743.	-774.	-522.	-915.	-1400.	0207
-1580.	-1228.	-706.	-284.	-151.	0208
-33.9	56.2	102	123.	81.5	0209
96.7	104.5	97.5	74.4	112.5	0210
93.9	49.4	-19.8	-151.	-288.	0211
-721.	-1373.	-1617.	-1245.	-863.	0212
-651.	-656.	-621.			0213
-700.	-643.	-590.	-987.	-1314.	0214
-1558.	-1164.	-792.	-265.	-111.	0215
46.3	168.	223.	251	215	0216
225.	244.	234.	209.	234.	0217
217.	176.1	93.4	-46.0	-187.	0218
-710.	-1348.	-1641.	-1450.	-1381.	0219
-983.	-563.	-535.			0220
-562.	-556.	-635.	-800.	-950	0221
-848.	-740.	-798.	-251.	-2.4	0222
248.	393.	473	529.	527	0223
544.	553.	562.	525.	526	0224
492.	404.	276.	132.	-38.2	0225
-626.	-779.	-996.	-894.	-786	0226
-610.	-502.	-514.			0227
0 0	0 0	0 0	0 0	0 0	0228
0.0	0.0	0.0	0.0	0.0	0229
0.0	0.0	0.0	0.0	0.0	0230
0.0	0.0	0.0	0.0	0.0	0231
0.0	0.0	0.0	0.0	0.0	0232
0.0	0.0	0.0	0.0	0.0	0233
0.0	0.0	0.0	0.0	0.0	0234

PITCH MOMENT

M/q

(FT<sup>3</sup>)

CH-46 FUSELAGE CHARACTERISTICS

0.0	0.0	0.0	0.0	0.0	0235
0.0	0.0	0.0	0.0	0.0	0236
0.0	0.0	0.0	0.0	0.0	0237
0.0	0.0	0.0	0.0	0.0	0238
0.0	0.0	0.0	0.0	0.0	0239
0.0	0.0	0.0	0.0	0.0	0240
0.0	0.0	0.0	0.0	0.0	0241
-16.2	0.7	50.	54.	73.	0242
188.	146.	148.	294.	322.	0243
352.	281.	234.	187.	135.	0244
66.8	21.5	-39.9	-97.2	-206.	0245
-195.	-257.	-289.	-358.	-362.	0246
-276.	-232.	-241.	-42.2	15.8	0247
31.9	16.9	-23.2			0248
47.4	23.9	55.4	48.7	13.4	0249
144.	153.	174.	246.	248.	0250
252.	237.	185.	163.3	109.8	0251
49.4	18.3	-7.9	-62.0	-129.	0252
-174.	-216.	-222.	-222.	-206.	0253
-124.	-227.	-131.	19.5	25.8	0254
39.7	-13.3	-65.2			0255
13.8	-6.8	12.7	53.7	-9.6	0256
138.	159	146.	140.	154.	0257
156.	151.	136.	96.2	72.1	0258
52.0	11.9	-16.4	-43.3	-83.8	0259
-135.	-153.	-141.	-121.	-107	0260
-56.3	-143.	-42.4	97.9	96.4	0261
93.9	14.2	-20.4			0262
4.9	-27.0	1.9	38.6	72.0	0263
121.	109.	97.9	58.4	81.3	0264
88.6	100.	92.8	63.4	29.5	0265
6.0	-2.4	-11.8	-17.3	-65.3	0266
-96.4	-100.0	-74.2	-48.2	0.2	0267
6.7	-90.7	19.2	104.	122.	0268
119.	46.1	6.8			0269
-25.8	-45.5	-30.2	-46.5	15.5	0270
105.	38.5	37.2	21.1	15.8	0271
28.5	45.7	45.7	40.5	9.0	0272
1.5	-5.4	11.0	12.2	-26.7	0273
-37.2	-33.2	11.9	64.	104.2	0274
86.1	15.5	17.5	131.	149.	0275
146.	52.0	45.9			0276
-45.1	-83.2	-58.6	-111	-94.4	0277
-118.0	-114.2	32.2	24.5	-14.3	0278
-15.7	-12.7	-7.5	-1.9	-10.3	0279
13.3	-4.2	-3.5	36.7	29.4	0280
19.6	35.5	110	178.	172.	0281
149	177	212.	228.	271.	0282
183.	128.	114.			0283
0.0	0.0	0.0	0.0	0.0	0284
0.0	0.0	0.0	0.0	0.0	0285
0.0	0.0	0.0	0.0	0.0	0286
0.0	0.0	0.0	0.0	0.0	0287
0.0	0.0	0.0	0.0	0.0	0288
0.0	0.0	0.0	0.0	0.0	0289
0.0	0.0	0.0	0.0	0.0	0290

ROLL MOMEN

L/q

(FT<sup>3</sup>)

CH-46 FUSELAGE CHARACTERISTICS

0.0	0.0	0.0	0.0	0.0	0291
0.0	0.0	0.0	0.0	0.0	0292
0.0	0.0	0.0	0.0	0.0	0293
0.0	0.0	0.0	0.0	0.0	0294
0.0	0.0	0.0	0.0	0.0	0295
0.0	0.0	0.0	0.0	0.0	0296
0.0	0.0	0.0	0.0	0.0	0297
-347.	39.3	329.	473.	400.	0298
335.	290.	258.	133.	144.	0299
-65.0	-49.9	-17.1	10.8	9.2	0300
-6.6	-20.8	7.7	-20.9	6.0	0301
93.	112.	62.	107.	54.	0302
-47.	-92.	-260.	-435.	-614.	0303
-396.	-26.	389.			0304
-310.	111.	610.	907.	855.	0305
810.	765.	732.	521.	386.	0306
191.	23.5	54.3	83.5	97.2	0307
78.1	19.1	-61.6	-84.4	-78.5	0308
-45.6	-43.2	-121.	-307.	-452.	0309
-694.	-725.	-785.	-850.	-948.	0310
-673	-107.	356.			0311
-257.	138.	788.	1073.	1060.	0312
1035	995.	961.	712.	600.	0313
414.	213.	110.	152.	157.	0314
86.4	21.3	-118.	-194.	-154.	0315
-147.	-234.	-337.	-557.	-667.	0316
-995.	-1005.	-1025.	-1065.	-1168	0317
-792.	-168.	304			0318
-221.	168	939.	1265.	1225	0319
1150.	1160.	1116.	865.	696	0320
520	315.	219	164.	243.	0321
166.3	37.5	-152.	-288.	-195.	0322
-233	-337.	-546.	-698.	-836.	0323
-1175.	-1195.	-1235.	-1285.	-1316.	0324
-881.	-204.	286.			0325
-246.	169.	1055.	1600.	1485.	0326
1340.	1265.	1115.	916.	764.	0327
567	381.	241.	204.	317.	0328
17.5	32.1	-158.	-325.	-239.	0329
289	-400.	-610.	-809.	-1007.	0330
-1185.	-1300.	-1390.	-1515.	-1642.	0331
-902.	-222.	244.			0332
-703.	207.	1250.	1808	1690.	0333
1550.	1370.	1182	963	759.	0334
527.	331.	222.	184.	208.	0335
73.1	-13.9	-104.	-259.	-263.	0336
-272.	-375.	-411.	390.	-1143.	0337
-1409.	-1625.	-1787.	-1910.	-1992.	0338
-1014.	-305.	262.			0339
0.0	0.0	0.0	0.0	0.0	0340
0.0	0.0	0.0	0.0	0.0	0341
0.0	0.0	0.0	0.0	0.0	0342
0.0	0.0	0.0	0.0	0.0	0343
0.0	0.0	0.0	0.0	0.0	0344
0.0	0.0	0.0	0.0	0.0	0345
0.0	0.0	0.0	0.0	0.0	0346

YAW MOMENT

N/q

(FT<sup>3</sup>)

CH-46 FUSELAGE CHARACTERISTICS

EGCLD529	529							
180.0	120.0							00001000
0.0	1.0	1.0	1.0	1.0				00002000
0.11								00003000
0.21	.3	.4	.5	.6	.7	.74		00004000
0.4	.86	.9	1					00005000
0.0	20.0	340.	360.0					00006000
-1.1	2.106	-2.306	-1					00007000
0.1	20.	340.	360.					00008000
-1.1	2.106	-2.306	-1					00009000
0.1	20.	340.	360.					00010000
-1.115	2.297	-2.527	-115					00011000
0.1	20.	340.	360.					00012000
-1.115	2.475	-2.705	-115					00013000
0.1	20.	340.	360.					00014000
-1.12	2.626	-2.866	-12					00015000
0.1	20.	340.	360.					00016000
-1.16	3.268	-3.588	-16					00017000
0.1	20.	340.	360.					00018000
-1.14	3.46	-3.74	-14					00019000
0.1	20.	340.	360.					00020000
-1.2	5.8	-6.2	-2					00021000
0.1	20.	340.	360.					00022000
-1.26	8.14	-8.66	-26					00023000
0.1	20.	340.	360.					00024000
-1.03	2.845	-2.905	-1.03					00025000
0.1	20.	340.	360.					00026000
-1.16	3.26	-2.58	-1.16					00027000
15.0	350.0							00028000
0.0	1.0	2.0	4.0	6.0	8.0	10.0		00029000
11.0	12.0	15.0	350.0	357.0	358.0	359.0		00030000
15.0								00031000
0.0	0.50	0.750	0.825	0.855	0.885	1.0		00032000
0.0107	0.00766	0.01195	0.01585	0.018	0.03115	0.0871		00033000
0.0	0.6	0.725	0.79	0.825	0.85	0.9		00034000
1.0								00035000
0.0137	.0075	0.102	.013	.0178	.0235	.0405		00036000
.0881								00037000
0.0	0.65	0.76	0.8	0.85	.93	1.		00038000
0.0107	.00745	.014	0.185	.031	.0586	.0961		00039000
0.0	0.5	0.65	0.7	0.75	0.8	1.0		00040000
0.0107	0.00766	0.009	0.0185	0.03745	0.0663	0.2111		00041000
0.0	0.3	0.4	0.5	0.55	0.6	0.675		00042000
0.7	1.0							00043000
0.1	.0085	.0078	0.077	.0107	.0175	.045		00044000
.055	.2606							00045000
0.0	0.4	0.5	0.54	0.575	0.65	1.0		00046000
0.0112	0.0085	0.01016	0.0156	0.02603	0.06045	0.2811		00047000
0.0	0.15	0.3	0.4	0.475	0.525	1.0		00048000
0.0142	0.0142	0.0098	0.0110	0.0187	0.0296	0.3111		00049000
0.0	0.15	0.3	0.35	0.4	0.8	1.0		00050000
0.0157	0.0157	0.0119	0.0137	0.015	0.2603	0.3611		00051000
0.0	0.15	0.3	0.32	0.34	0.4	1.0		00052000
0.0177	0.0177	0.015	0.01685	0.0181	0.022	0.4411		00053000
0.0	0.1	0.125	0.15	0.175	0.3	1.0		00054000
0.0297	0.0297	0.0307	0.0322	0.043	0.1195	0.5661		00055000
0.0	0.2	0.35	0.485	0.61	0.75	1.0		00056000
0.0687	0.0755	0.0872	0.0987	0.1135	0.18235	0.3051		00057000
0.0	0.25	0.5	0.69	0.85	0.9	1.0		00058000
0.0122	0.0097	0.02765	0.0379	0.0587	0.0671	0.1261		00059000
0.0	0.3	0.45	0.625	0.75	0.9	1.0		00060000
0.0117	0.0095	0.0098	0.0235	0.02735	0.0531	0.1011		00061000
0.0	0.5	0.65	0.8	0.825	0.9	1.0		00062000
0.0117	0.00865	0.01445	0.0198	0.02275	0.0461	0.0911		00063000
0.0	.5	.75	.825	.855	.885	1.0		00064000
0.0107	.0077	.012	.0159	.018	.0311	.0871		00065000
END								00066000
								00067000
								00068000
								00069000
								00070000
								00071000
								00072000
								00073000
								00074000
								00075000
								00076000
								00077000
								00078000
								00079000
								00080000
								00081000
								00082000
								00083000
								00084000
								00085000
								00086000
								00087000
								00088000
								00089000
								00090000
								00091000
								00092000
								00093000
								00094000
								00095000

EGCL0530	530	530	530	530	530	530	530
180.0	180.0	1.0	1.0	1.0			
0.0	1.0						
.11	.3	.4	.5	.6	.7	.74	
.81	.86	.9	1.				
0.	20.	340.	360.				
-.1	2.106	-2.306	-1				
0.	20.	340.	360.				
-.1	2.106	-2.306	-1				
0.	20.	340.	360.				
-.115	2.297	-2.527	-1.115				
0.	20.	340.	360.				
-.115	2.475	-2.705	-1.115				
0.	20.	340.	360.				
-.12	2.626	-2.866	-1.2				
0.	20.	340.	360.				
-.16	3.268	-3.588	-1.16				
0.	20.	340.	360.				
-.115	2.922	-3.152	-1.115				
0.	20.	340.	360.				
-.09	2.36	-2.54	-0.9				
0.	20.	340.	360.				
-.065	1.935	-2.065	-0.65				
0.	20.	340.	360.				
-.07	1.61	-1.75	-0.7				
0.	20.	340.	360.				
-.04	.76	-.84	-.04				
15.0	350.0						
0.0	1.0	2.0	4.0	6.0	8.0	10.0	
11.0	12.0	15.0	350.0	357.0	358.0	359.0	
360.9							
0.0	0.50	0.750	0.825	0.855	0.885	1.0	
0.0107	0.00766	0.01195	0.01585	0.018	0.03115	0.0871	
0.0	0.6	0.725	0.79	0.825	0.85	0.9	
1.0							
.0107	.0075	.0102	.013	.0178	.0235	.0405	
.8881							
0.0	0.65	0.76	0.8	0.85	.93	1.	
.0107	.00745	.014	.0185	.031	.0586	.0961	
0.0	0.5	0.65	0.7	0.75	0.8	1.0	
0.0107	0.00766	0.009	0.0185	0.03745	0.0663	0.2111	
0.0	0.3	0.4	0.5	0.55	0.6	0.675	
0.7	1.0						
.01	.0885	.0078	.0077	.0107	.0175	.043	
.055	.2606						
0.0	0.4	0.5	0.54	0.575	0.65	1.0	
0.0112	0.0085	0.01016	0.0156	0.02603	0.06045	0.2811	
0.0	0.15	0.3	0.4	0.475	0.525	1.0	
0.0142	0.0142	0.0098	0.0110	0.0187	0.0296	0.3111	
0.0	0.15	0.3	0.35	0.4	0.8	1.0	
0.0157	0.0157	0.0119	0.0137	0.015	0.2603	0.3611	
0.0	0.15	0.3	0.32	0.34	0.4	1.0	
0.0177	0.0177	0.015	0.01685	0.0181	0.022	0.4411	
0.0	0.1	0.125	0.15	0.175	0.3	1.0	
0.0297	0.0297	0.0307	0.0322	0.043	0.1195	0.5661	
0.0	0.2	0.35	0.465	0.61	0.75	1.0	
0.0687	0.0755	0.0872	0.0987	0.1135	0.18235	0.3051	
0.0	0.35	0.5	0.69	0.85	0.9	1.0	
0.0122	0.0097	0.02765	0.0379	0.0587	0.0671	0.1261	
0.0	0.3	0.45	0.625	0.75	0.9	1.0	
0.0117	0.0095	0.0098	0.0235	0.02735	0.0531	0.1011	
0.0	0.5	0.65	0.8	0.825	0.9	1.0	
0.0117	0.00865	0.01445	0.0198	0.02275	0.0461	0.0911	
0.	.5	.75	.825	.85	.885	1.0	
.0107	.0077	.012	.0159	.018	.0311	.0871	
END							

00001000  
00002000  
00003000  
00004000  
00005000  
00006000  
00007000  
00008000  
00009000  
00010000  
00011000  
00012000  
00013000  
00014000  
00015000  
00016000  
00017000  
00018000  
00019000  
00020000  
00021000  
00022000  
00023000  
00024000  
00025000  
00026000  
00027000  
00028000  
00029000  
00030000  
00031000  
00032000  
00033000  
00034000  
00035000  
00036000  
00037000  
00038000  
00039000  
00040000  
00041000  
00042000  
00043000  
00044000  
00045000  
00046000  
00047000  
00048000  
00049000  
00050000  
00051000  
00052000  
00053000  
00054000  
00055000  
00056000  
00057000  
00058000  
00059000  
00060000  
00061000  
00062000  
00063000  
00064000  
00065000  
00066000  
00067000  
00068000  
00069000  
00070000  
00071000  
00072000  
00073000  
00074000  
00075000  
00076000  
00077000  
00078000  
00079000  
00080000  
00081000  
00082000  
00083000  
00084000  
00085000  
00086000  
00087000  
00088000  
00089000  
00090000  
00091000  
00092000  
00093000  
00094000  
00095000

CH-46 AIRFOIL TABLES

This Page Left Blank Intentionally

10. REFERENCES

1. Boeing Vertol Company: "CH-46 Composite Rotor Blade Vehicle Technology Flight Test Report," D210-11168-4, May 1979.
2. Naval Air Systems Command: "NATOPS Flight Manual, Navy Model CH-46E Helicopters," NAVAIR 01-250HDC-1 (Change 1), August 1981.
3. Boeing Vertol Company: "Tandem Rotor Helicopter Trim and Stability Analysis, IBM Program A-81 and A-97," Aero. Inv. III-264, March 1965; Revised, December 1965.
4. Military Specification: "Helicopter Flying and Ground Handling Qualities, General Requirements for," MIL-H-8501A, Amended April 1962.
5. Boeing Vertol Company: "Updated Airfoil Characteristics for Rotor Performance Calculations (1972)," D210-10529-1, September 1972.

NADC-81118-60

DISTRIBUTION LIST

AIRTASK NO. A030-320D/001B/2F41-4000-000

	<u>No. of Copies</u>
NAVAIR (AIR-954) . . . . .	5
(2 for retention)	
(1 for AIR-320D)	
(1 for AIR-5301)	
(1 for AIR-5115H)	
DTIC, Alexandria, VA . . . . .	12
NAVAIRDEVCON, Warminster, PA . . . . .	12
(2 for 60011)	
(1 for 605)	
(6 for 6053)	
(3 for 813)	
AVRADCOM, Moffett Field, CA . . . . .	1
(1 for D. Key)	
ARVIN/Cal Span Technology Center, Buffalo, NY . . . . .	1
(1 for C. Chalk)	
Systems Technology Inc. . . . .	1
(1 for W. Clement)	
NAVAIRTESTCON, Patuxent River, MD . . . . .	2
(1 for COM M. Hollis)	
(1 for H. Kolwey)	